Analysis of a Model for Dirac Leptogenesis with Left–Right Symmetry in Extra Dimensions

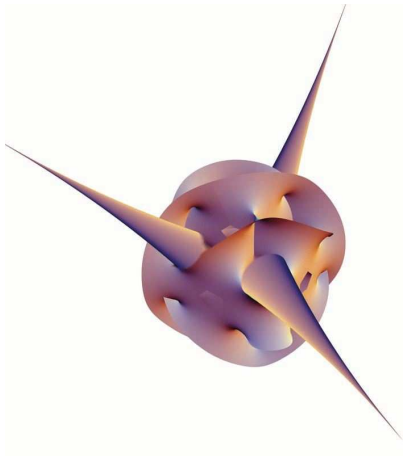

Diploma Thesis

by

Andreas Bechinger

Revised Version: December 8th, 2007
(Original Version: September 4th, 2007)

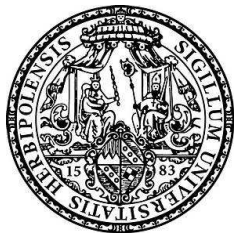

Julius–Maximilians–Universität Würzburg
Institut für Theoretische Physik und Astrophysik
Lehrstuhl für Theoretische Physik II
Prof. Dr. Reinhold Rückl

Abstract

Dirac leptogenesis offers the possibility to explain the baryon asymmetry of the Universe in the presence of Dirac neutrinos with small masses. In this thesis, we discuss a left–right symmetric Dirac leptogenesis scenario that is embedded in an extra–dimensional geometry with three five–dimensional throats. The baryon asymmetry is generated by the decay of heavy Kaluza–Klein resonances that have a relative mass splitting of the order $\sim 10^{-14}$. We calculate the resulting resonant enhancement of the baryon asymmetry and study the gauge symmetry breaking in the bulk. We thus find a baryon asymmetry $\eta_B \approx 10^{-10}$ which is in perfect agreement with observation.

Kurzfassung

Dirac–Leptogenese bietet in Gegenwart von Dirac–Neutrinos mit kleinen Massen eine Möglichkeit die Baryonasymmetrie des Universums zu erklären. In dieser Diplomarbeit diskutieren wir ein links–rechts symmetrisches Dirac–Leptogenese Szenario, welches eingebettet ist in eine extradimensionale Geometrie mit drei fünfdimensionalen "throats". Die Baryonasymmetrie wird durch den Zerfall schwerer Kaluza–Klein Resonanzen erzeugt, die einen relativen Massenunterschied der Grössenordnung $\sim 10^{-14}$ aufweisen. Wir berechnen die resultierende resonante Verstärkung der Baryonasymmetrie und studieren die Brechung der Eichgruppe im Bulk. Wir finden dabei eine Baryonasymmetrie $\eta_B \approx 10^{-10}$, die sich in perfekter Übereinstimmung mit der Beobachtung befindet.

Contents

Chapter 1

Introduction

It seems to be an inherent characteristic of mankind to wonder about the existence of matter. As far back as thousands of years, prophets and philosophers first raised the question for being. In our Western tradition, one of the first pre–Socratic philosophers who asked for the origin of matter at the dawn of the Axial Age, *i.e.*, around 600 BC, was Anaximander from Miletus. He postulated the "apeiron" ("infinite" or "limitless") as the first principle. The apeiron is an endless, unlimited primordial mass from which perpetually everything is derived and to which all things are returning. This abstract principle has been understood as some sort of chaos from which the Universe originates in the separation of opposites in the primordial matter.

These fundamental questions and ideas have influenced our perception of the world and its origin for centuries. Although we have to make a clear cut between these ancient ideas and our scientific concepts of Nature today, the basic question why there is something and not nothing still awaits its answer.

From our present understanding of the Big Bang, we expect particles and antiparticles to be generated by the same amount and we intuitively assume that the laws of Nature are symmetric for particles and antiparticles. However, we know that there is no significant amount of antimatter on earth. Furthermore, solar rays and planetary probes show the pure matter content of our solar system. When we turn our attention to larger scales, cosmic rays indicate a small level of antiprotons. This amount of antiprotons can consistently be explained as a secondary product of collisions between cosmic rays and the interstellar medium. Consequently, our whole galaxy seems to be built up by matter. If a matter–antimatter symmetry is constituted at the level of galaxy clusters, we would expect a strong γ–ray signal, due to intracluster gas which would lead to a nucleon–antinucleon annihilation. We know from X–ray emissions about the existence of intracluster gas, but have not seen any evidence of a significant baryon–antibaryon annihilation. Therefore, if there is a considerable amount of antimatter in the Universe, it must have been isolated from matter on scales of at least 10^{12} to 10^{14} $M_\odot$. In a locally baryon–symmetric Universe, an unknown mechanism must have caused a segregation of antimatter at temperatures greater than 38 MeV. However, at that time, the horizon of the Universe only contained 10^{-7} $M_\odot$. Thus,

all evidence indicates a fundamental asymmetry between baryons and antibaryons.

The baryon asymmetry of the Universe is defined as the ratio of the total baryon number density Δn_B to photon density n_γ[1]:

$$\eta_B = \frac{n_B - n_{\overline{B}}}{n_\gamma} = \frac{\Delta n_B}{n_\gamma}. \tag{1.1}$$

Unfortunately, there is no accurate way of measuring η_B directly. Thus, we have to use indirect methods.

One way to estimate η_B is offered by Big-Bang-Nucleosynthesis (BBN). The abundance of the light elements D, ^{3}He, ^{4}He, and ^{7}Li, produced at a temperature scale of 1 MeV is sensitive to the ratio n_B/n_γ. Our observations are in good agreement with the theoretical prediction [1]

$$3.4 \cdot 10^{-10} < \eta_B < 6.9 \cdot 10^{-10}. \tag{1.2}$$

A second independent probe consists of the analysis of the small temperature anisotropies of the Cosmic Microwave Background (CMB). The CMB anisotropies give information about the acoustic oscillations of the baryon/photon fluid around the last scattering of photons. Combining both methods, one finds [2]

$$\eta_B = (6.14 \pm 0.25) \cdot 10^{-10}. \tag{1.3}$$

The conditions to enable the evolution of a baryon asymmetry in the Universe have been formulated by Sakharov [3], *i.e.*, violation of baryon number (B), CP–violation, and out–of–equilibrium processes. These conditions are commonly accounted for in terms of leptogenesis [4] (see also [5–7]), where the out–of–equilibrium decay of heavy Majorana neutrinos generates a lepton asymmetry due to a violation of lepton number (L). This L asymmetry is later on transferred to the baryonic sector by non–perturbative sphaleron processes [8, 9]. This scenario has the attractive feature of explaining not only the baryon asymmetry η_B but also accounts for the smallness of the neutrino masses ($\sim 10^{-2}$ eV) via the (type–I) seesaw mechanism [10–13].

Although, the seesaw mechanism predicts Majorana neutrinos, we do not know experimentally whether the neutrinos are Majorana or Dirac particles. The seesaw mechanism has the advantage that it could be tested in planned neutrinoless double beta decay experiments [14–21]. However, if no signal for neutrinoless double beta decay is found, there will always be the possibility that neutrinos are Dirac particles like all the other known fermions. From this point of view, it is therefore interesting to consider Dirac neutrinos.

[1] The number density of photons increases with time due to heavy particle annihilation processes, while the number density of baryons is not affected by these reactions. Thus, it is convenient to use the entropy density s instead of n_γ with $s = 7.04\, n_\gamma$ in the present Universe. The observed values of η_B are given for n_γ, while for our calculations we use s in this thesis.

In the Standard Model (SM) of elementary particle physics, based on the gauge group

$$G_{\rm SM} = SU(3)_c \times SU(2)_L \times U(1)_Y, \tag{1.4}$$

the active left–handed (LH) neutrinos would be massless. But Dirac neutrinos can be simply obtained by introducing right–handed (RH) neutrinos that are singlets under $G_{\rm SM}$. A more unified framework for Dirac neutrinos is offered by left–right (LR) symmetric theories [22–24], which have the gauge group

$$G_{LR} = SU(3)_c \times SU(2)_L \times SU(2)_R \times U(1)_{B-L} \supset G_{\rm SM}, \tag{1.5}$$

and restore, with respect to the SM, a parity symmetry. In terms of Grand Unified Theories (GUTs), G_{LR} can be embedded into the Pati–Salam group [25]

$$G(224) = SU(4) \times SU(2)_L \times SU(2)_R \supset G_{LR}. \tag{1.6}$$

Coming from an $SO(10)$ GUT, *e.g.*, there are two primary descendants that lead to the SM: one via $SU(5)$ and the other via $G(224)$ [26] (see Fig. 1.1).

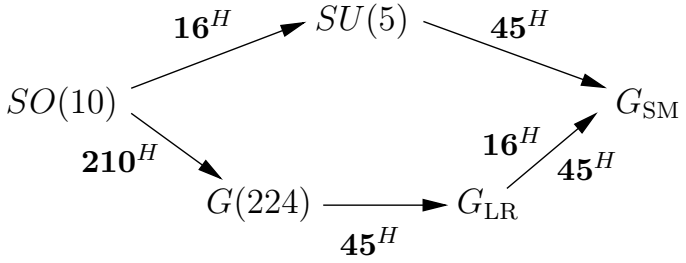

Figure 1.1: Primary descendants of $SO(10)$ symmetry breaking, where $\mathbf{16}^H$, $\mathbf{45}^H$, and $\mathbf{210}^H$, denote the representations of the Higgs fields responsible for spontaneously breaking the respective symmetries.

In Fig. 1.1, the symmetry breaking $SO(10) \to SU(5)$ allows to implement easily the seesaw mechanism, and would therefore lead to Majorana neutrinos. Going, instead, via $SO(10) \to G(224)$, leads to the LR–symmetric model, and is, hence, compatible with Dirac neutrinos. In a unified model, such as $SO(10)$, we might thus have either Majorana or Dirac neutrinos, depending on the detailed pattern of symmetry breaking.

In the case of Dirac neutrinos, we can, without the seesaw mechanism, no longer make use of the usual (Majorana) leptogenesis, but need Dirac leptogenesis [27] to generate the observed baryon asymmetry η_B. In Dirac leptogenesis, heavy copies of the SM Higgs doublet decay into LH lepton doublets and RH neutrinos, and the smallness of the Dirac neutrino Yukawa couplings of the order $\sim 10^{-12}$ prevents the generated asymmetry from being washed out. The original version of Dirac leptogenesis, however, suffers from two major drawbacks. First, it lacks of providing an attractive origin of the heavy scalars. Second, it does not offer any connection between low–energy observables and the parameters relevant for leptogenesis. Third, and most

importantly, the original Dirac leptogenesis model requires GUT scale baryogenesis to produce a realistic baryon asymmetry, which is plagued with several problems connected with inflation and gravitino overproduction. Thus, it would be desirable to consider models for Dirac leptogenesis which resolve these shortcomings.

In this thesis, we discuss Dirac leptogenesis for a LR–symmetric model in extra dimensions. Here, going to LR symmetry in extra dimensions serves the following purposes:

- LR symmetry accounts for the Dirac nature of the neutrinos and the
- extra dimensions provide the heavy scalar resonances with suitable properties.

Since this model has many scalars charged under $G_{\rm SM}$ in the effective low–energy theory, one has to make sure that the usual electroweak symmetry breaking (EWSB) can take place. Moreover, the model establishes a close connection between the low–energy observables (Dirac neutrino Yukawa couplings) and the high–energy parameters entering leptogenesis. This requires to resort to resonant leptogenesis in order to obtain sufficient baryon asymmetry. To enable resonant leptogenesis, the model is formulated in an extra dimensional space consisting of so–called throats [28] (in the flat limit) which are known to arise naturally in flux compactifications [29,30]. The major technical motivation for working with throats is to keep the mass splitting between the resonating scalars under control.

This thesis is organized as follows: First, in Chapter 2, we start with a short review of the theory of neutrino masses and mixing. Then, in Chapter 3, we will discuss the basic aspects of baryogenesis and leptogenesis. The main features and consequences of LR–symmetric models and extra dimensions are highlighted in Chapter 4. We study in Chapter 5 the generation of an L asymmetry between LH and RH leptons due the decay of the heavy scalars. Then, we consider the minimization of the potential of a single scalar bi–doublet that propagates in a compact extra dimension in Chapter 6. Next, in Chapter 7, we introduce the model for Dirac leptogenesis on three throats. The resulting amount of baryon asymmetry in this model will be determined in Chapter 8. Finally, we present our summary and conclusions in Chapter 9. In the Appendix, we collect detailed calculations for the $1 \to 2$ decay rate of a particle, the minimization of the scalar potential and a brief summary of the procedure of chemical potentials.

Chapter 2

Neutrino Masses and Mixing

In this Chapter, we will start with a discussion of neutrino masses and mixing. First, we give a brief summary of the SM. Then, we will discuss neutrino masses and mixing. Special emphasis will be put on exemplary models for small neutrino masses.

2.1 The Standard Model

Over the last decades, the Standard Model has shown excellent accuracy in describing experimental data. Here, we give a concise account of the SM as a fundamental for all further discussions in this work.

In this Chapter, and throughout this thesis, we will work in "God-given" units, *i.e.*, $\hbar = c = 1$.

2.1.1 Particle Content

The SM is based on the symmetry group $G_{\rm SM} = SU(3)_c \times SU(2)_L \times U(1)_Y$, where $SU(3)_c$ refers to the strong interaction, described by quantum chromodynamics (QCD), while the electroweak (EW) interaction, described by the Glashow-Weinberg-Salam model, is embedded into $SU(2)_L \times U(1)_Y$. The SM has the important property to be a renormalizable gauge theory. The symmetry group $U(1)_Q$ of quantum electrodynamics (QED) results from spontaneous symmetry breaking (SSB) of the EW symmetry

$$SU(2)_L \times U(1)_Y \xrightarrow{\rm SSB} U(1)_Q, \tag{2.1}$$

induced by the Higgs mechanism. The electric charge Q of a particle is generated by the hypercharge Y of $U(1)_Y$ and the third component of weak isospin T_3, following the Gell-Mann-Nishijima relation

$$Q = T_3 + \frac{Y}{2}. \tag{2.2}$$

	Leptons			Quarks		
	$\begin{pmatrix} \nu_e \\ e \end{pmatrix}_L$	$\begin{pmatrix} \nu_\mu \\ \mu \end{pmatrix}_L$	$\begin{pmatrix} \nu_\tau \\ \tau \end{pmatrix}_L$	$\begin{pmatrix} u \\ d \end{pmatrix}_L$	$\begin{pmatrix} c \\ s \end{pmatrix}_L$	$\begin{pmatrix} t \\ b \end{pmatrix}_L$
	e_R	μ_R	τ_R	$\begin{matrix} u_R \\ d_R \end{matrix}$	$\begin{matrix} c_R \\ s_R \end{matrix}$	$\begin{matrix} t_R \\ b_R \end{matrix}$
observed	yes	yes	yes	yes	yes	yes
	Gauge Bosons			Higgs Scalar		
	G^a_μ	A^a_μ	B_μ	$\begin{pmatrix} \phi^+ \\ \phi^0 \end{pmatrix}$		
observed	yes	yes	yes	no		

Table 2.1: Particle content of the Standard Model.

The most general renormalizable Lagrangian for the particle content of the SM, as summarized in Tab. 2.1, is

$$\begin{aligned}\mathcal{L}_{\rm SM} &= -\frac{1}{4g_1^2}B_{\mu\nu}B^{\mu\nu} - \frac{1}{4g_2^2}A^a_{\mu\nu}A^{\mu\nu a} - \frac{1}{4g_3^2}G^a_{\mu\nu}G^{\mu\nu a} \\ &\quad + \overline{Q}_{Li}\mathrm{i}\not{D}Q_{Li} + \overline{u}_{Ri}\mathrm{i}\not{D}u_{Ri} + \overline{d}_{Ri}\mathrm{i}\not{D}d_{Ri} + \overline{\psi}_{Li}\mathrm{i}\not{D}\psi_{Li} + \overline{e}_{Ri}\mathrm{i}\not{D}e_{Ri} \\ &\quad + |D_\mu\Phi|^2 + Y_u^{ij}\overline{Q}_{Li}u_j\widetilde{\Phi} + Y_d^{ij}\overline{Q}_{Li}d_j\Phi + Y_e^{ij}\overline{\psi}_{Li}e_j\Phi \\ &\quad - \lambda(\Phi\Phi^\dagger)^2 + \lambda v^2\Phi\Phi^\dagger + \frac{\theta}{64\pi^2}\varepsilon^{\mu\nu\rho\sigma}G^a_{\mu\nu}G^a_{\rho\sigma},\end{aligned} \tag{2.3}$$

where $B_{\mu\nu} = \partial_\mu B_\nu - \partial_\nu B_\mu$, $A^a_{\mu\nu} = \partial_\mu A^a_\nu - \partial_\nu A^a_\mu + g_2 f^{abc}A^b_\mu A^c_\nu$, and $G^a_{\mu\nu} = \partial_\mu G^a_\nu - \partial_\nu G^a_\mu + g_3 f^{abc}G^b_\mu G^c_\nu$ (f^{abc} is the structure constant and $a, b, c = 1, 2, 3$) are the gauge field strength tensors for the gauge fields B_μ, A^a_μ, and G^a_μ. Furthermore, g_1, g_2 and g_3 denote the coupling strengths of the gauge bosons B_μ, A^a_μ, and G^a_μ to the fermionic current $j^\mu = \overline{\psi}\gamma^\mu\psi$. In Eq. (2.3), the angle $\theta < 10^{-10}$ denotes the CP–violation in QCD. The covariant derivative D_μ is

$$D_\mu = \partial_\mu - \mathrm{i}g_2\frac{\sigma_a}{2}A^a_\mu - \mathrm{i}\frac{g_1}{2}YB_\mu. \tag{2.4}$$

The particles of the SM can be classified by multiplets according to their transformations under $G_{\rm SM}$, *i.e.*, $(SU(3)_c, SU(2)_L, U(1)_Y)$. For the fermionic content, we have

$$(\mathbf{1}, \overset{\psi_L}{\mathbf{2}}, -1) \oplus (\mathbf{1}, \overset{e_R}{\mathbf{1}}, 2) \oplus (\mathbf{3}, \overset{Q_L}{\mathbf{2}}, 1/3) \oplus (\mathbf{3}, \overset{u_R}{\mathbf{1}}, +4/3) \oplus (\mathbf{3}, \overset{d_R}{\mathbf{1}}, -2/3). \tag{2.5}$$

Note that the SM does not contain RH (SM singlet) neutrinos $\nu_R \sim (\mathbf{1}, \mathbf{1}, 0)$. The representations for the gauge bosons are given by

$$\overset{G^a_\mu}{(\mathbf{8}, \mathbf{1}, 0)} \oplus \overset{A^a_\mu}{(\mathbf{1}, \mathbf{3}, 0)} \oplus \overset{B_\mu}{(\mathbf{1}, \mathbf{1}, 0)}. \tag{2.6}$$

The masses of the fermions and gauge bosons in the SM are generated by interactions with the Higgs scalar Φ $(\mathbf{1}, \mathbf{2}, -1)$, which is responsible for EWSB.

2.1.2 Electroweak Symmetry Breaking

In the SM, EWSB is achieved via a complex Higgs scalar doublet

$$\Phi = \begin{pmatrix} \phi^+ \\ \phi^0 \end{pmatrix}. \tag{2.7}$$

The scalar Lagrangian is given by

$$\mathcal{L}_{\text{scalar}} = D_\mu \Phi^\dagger D^\mu \Phi - V(\Phi), \tag{2.8}$$

where the potential $V(\Phi)$ has the form

$$V(\Phi) = -\mu^2 \Phi^\dagger \Phi + \lambda (\Phi^\dagger \Phi)^2, \tag{2.9}$$

in which $\mu^2 \sim 100\,\text{GeV}$ and $\lambda > 0$ is some dimensionless parameter. Due to the gauge freedom, we can rotate the vacuum expectation value (VEV) $\langle \Phi \rangle$ of Φ in such way that it becomes

$$\langle \Phi \rangle = \frac{1}{\sqrt{2}} \begin{pmatrix} 0 \\ v \end{pmatrix}, \tag{2.10}$$

where $v = (\mu^2/\lambda)^{1/2}$ is real. Since

$$\frac{g_2}{2\sqrt{2}} = \left(\frac{m_W^2 G_F}{\sqrt{2}} \right)^{1/2}, \tag{2.11}$$

we get a VEV of the order $v = (\sqrt{2} G_F)^{1/2} \simeq 246\,\text{GeV}$, where $m_W = g_2 v/2 = 80.403 \pm 0.029\,\text{GeV}$ is the mass of the $W^\pm$ gauge bosons and $G_F = 1.166 \times 10^{-5}\text{GeV}$ denotes the Fermi coupling constant. We can expand the Higgs potential $V(\Phi)$ around its VEV as

$$V(\Phi) = V(\langle \Phi \rangle) + \frac{1}{2} \frac{\partial^2 V}{|\partial \Phi|^2} \Big|_{\langle \Phi \rangle} (\Phi - \langle \Phi \rangle)^2 + \ldots, \tag{2.12}$$

where the mass matrix is given by

$$M_\Phi^2 = \frac{\partial^2 V}{\partial |\Phi^2|} \Big|_{\langle \Phi \rangle}, \tag{2.13}$$

which gives a massive Higgs scalar H with mass $m_H = (2\mu^2)^{1/2}$.

Gauge Boson Masses

The kinetic term of the scalar Lagrangian in Eq. (2.3) leads via SSB to two charged massive gauge bosons $W^{\pm}$ with mass $m_W = g_2 v/2$, where θ_W [$\sin^2\theta_W = 0.23152(14)$] is the Weinberg angle defined by $\tan\theta_W = g_1/g_2$. The magnitude of the electric charge of the positron is $e = g_1 g_2/(g_1+g_2)^{1/2}$. Furthermore, we have the gauge boson mass terms

$$\begin{aligned}\mathcal{L}^{A^3_\mu - B_\mu} &= \frac{v^2}{2}\left|\left(g_2\frac{\sigma_3}{2}A^3_\mu + \frac{g_1}{2}YB_\mu\right)\begin{pmatrix}0\\1\end{pmatrix}\right|^2 \\ &= \frac{v^2}{8}\left[\begin{pmatrix}B_\mu & A^3_\mu\end{pmatrix}\begin{pmatrix}g_1^2 & -g_1g_2\\ -g_1g_2 & g_2^2\end{pmatrix}\begin{pmatrix}B^\mu\\ A^{3\mu}\end{pmatrix}\right]. \end{aligned} \tag{2.14}$$

Diagonalizing this matrix by a rotation through θ_W, we find the two mass eigenvalues for the photon and the neutral Z boson:

$$m_\gamma = 0 \quad \text{and} \quad m_Z = \frac{(g_2^2+g_1^2)}{4}v^2, \tag{2.15}$$

where

$$m_Z = \frac{g_2 v}{2\cos\theta_W} = \frac{m_W}{\cos\theta_W} = 91.1876 \pm 0.0021\,\text{GeV}. \tag{2.16}$$

The interplay of massive and massless gauge bosons in the presence of broken symmetries is described by the Goldstone theorem:

Goldstone Theorem. *Every spontaneously broken generator of a continuous, global symmetry generates a massless particle, a Goldstone boson. If the symmetry is not only broken spontaneously but also explicitly, we find massive pseudo–Nambu–Goldstone bosons.*

Fermion Masses

A gauge–invariant mass term for SM leptons as well as Dirac neutrinos, and in an analogous way for quarks, can be written in terms of Yukawa couplings as

$$\begin{aligned}\mathcal{L}_Y &= -Y_e\overline{\psi}_L\Phi e_R - Y_\nu\overline{\psi}_L\widetilde{\Phi}\nu_R + \text{h.c.} \\ &= -Y_e\frac{v+H}{\sqrt{2}}\overline{\psi}_L\begin{pmatrix}0\\1\end{pmatrix}e_R - Y_\nu\frac{v+H}{\sqrt{2}}\overline{\psi}_L\begin{pmatrix}1\\0\end{pmatrix}\nu_R + \text{h.c.} \\ &= -\frac{Y_e v}{\sqrt{2}}\overline{e}e - \frac{Y_e}{\sqrt{2}}\overline{e}eH - \frac{Y_\nu v}{\sqrt{2}}\overline{\nu}\nu - \frac{Y_\nu}{\sqrt{2}}\overline{\nu}\nu H, \end{aligned} \tag{2.17}$$

where $\widetilde{\Phi} = \mathrm{i}\sigma_2\Phi^*$ and σ_i $(i = 1,2,3)$ denotes the Pauli matrices. Thus, we see that the leptons acquire the Dirac masses

$$m_e = \frac{Y_e v}{\sqrt{2}} \quad \text{and} \quad m_\nu = \frac{Y_\nu v}{\sqrt{2}}, \tag{2.18}$$

while the Yukawa coupling strengths are given by

$$Y_{\overline{e}He} = \frac{m_e}{v} \quad \text{and} \quad Y_{\overline{\nu}H\nu} = \frac{m_\nu}{v}. \tag{2.19}$$

2.2 Neutrino Masses

In the SM, neutrinos are massless. In recent years, however, we have learned from solar [31,32], atmospheric [33], reactor [34,35], and accelerator [36] neutrino oscillation experiments that neutrinos exhibit nonzero (even large in contrast to the quark sector) mixing (for a summary of current neutrino oscillation data, see Tab. 2.2.2). The smallness of neutrino masses and the large neutrino mixing angles open the door to physics beyond the SM.

2.2.1 Dirac versus Majorana Neutrinos

Since neutrinos carry no electric charge, they could be Majorana or Dirac particles like all other fermions in the SM. To discuss the differences between Dirac and Majorana particles, we can use the Weyl representation of spinors.

Any Dirac spinor $\Psi_{\rm D}$ can be decomposed into chiral states as

$$\Psi_{\rm D} = P_L \Psi_{\rm D} + P_R \Psi_{\rm D} = \Psi_{{\rm D}L} + \Psi_{{\rm D}R}, \tag{2.20}$$

where $P_{L,R} = \frac{1}{2}(1 \pm \gamma_5)$. The Dirac spinor $\Psi_{\rm D}$ consists of four components and can be decomposed into two two–component Weyl spinors ξ_α and $\overline{\eta}^{\dot\alpha}$ as

$$\Psi_{\rm D} = P_L \Psi_{\rm D} + P_R \Psi_{\rm D} = \begin{pmatrix} \xi_\alpha \\ 0 \end{pmatrix} + \begin{pmatrix} 0 \\ \overline{\eta}^{\dot\alpha} \end{pmatrix} = \begin{pmatrix} \xi_\alpha \\ \overline{\eta}^{\dot\alpha} \end{pmatrix}, \tag{2.21}$$

where $\alpha, \dot\alpha = 1, 2$ [37]. In this notation, Weyl spinors with undotted upper indices and with dotted lower indices are defined as the LH and RH projections, respectively. Charge conjugation $\Psi^c_{\rm D}$ of $\Psi_{\rm D}$, *i.e.*,

$$\Psi^c_{\rm D} = C \overline{\Psi}^T_{\rm D}, \tag{2.22}$$

leads to

$$\Psi_{\rm D} = \begin{pmatrix} \xi_\alpha \\ \overline{\eta}^{\dot\alpha} \end{pmatrix} \xrightarrow{C} \begin{pmatrix} \eta_\alpha \\ \overline{\xi}^{\dot\alpha} \end{pmatrix} = \Psi^c_{\rm D}. \tag{2.23}$$

A Majorana spinor $\Psi_{\rm M}$, on the other hand, consists of only two independent components:

$$\Psi_{\rm M} = \begin{pmatrix} \xi_\alpha \\ \overline{\xi}^{\dot\alpha} \end{pmatrix}. \tag{2.24}$$

Thus, we see that

$$\Psi^c_{\rm M} = \Psi_{\rm M}, \tag{2.25}$$

i.e., Majorana particles are their own antiparticles. Every Dirac spinor can be represented by a sum of two Majorana spinors:

$$\Psi_{\rm D} = \Psi_{\rm M1} + {\rm i}\Psi_{\rm M2}, \tag{2.26}$$

where the Majorana spinors $\Psi_{\mathrm{M}i}$ $(i = 1, 2)$ are given by

$$\Psi_{\mathrm{M1}} = \frac{1}{2}(\Psi_{\mathrm{D}} + \Psi_{\mathrm{D}}^c) \quad \text{and} \quad \Psi_{\mathrm{M2}} = \frac{1}{2\mathrm{i}}(\Psi_{\mathrm{D}} - \Psi_{\mathrm{D}}^c). \tag{2.27}$$

Taking this into account, we can, *e.g.*, write a Dirac neutrino ν in the Weyl basis as

$$\nu = \begin{pmatrix} \xi_\alpha \\ \overline{\eta}^{\dot{\alpha}} \end{pmatrix}, \tag{2.28}$$

where ν, ξ_α, and $\overline{\eta}^{\dot{\alpha}}$ denote column–vectors consisting of three flavors, *e.g.*, $\nu = (\nu_e, \nu_\mu, \nu_\tau)^T$. We find

$$\nu_L = \xi_\alpha, \quad \nu_L^c = \overline{\xi}^{\dot{\alpha}}, \quad \nu_R = \overline{\eta}^{\dot{\alpha}}, \quad \text{and} \quad \nu_R^c = \eta_\alpha, \tag{2.29}$$

where the notation here is defined by

$$\overline{\nu}_{L,R} \equiv \overline{(\nu_{L,R})}, \quad \nu_{L,R}^c \equiv (\nu_{L,R})^c, \quad \text{and} \quad \overline{\nu}_{L,R}^c \equiv \overline{(\nu_{L,R})^c}. \tag{2.30}$$

The most general mass terms for the neutrinos therefore take the form

$$-\mathcal{L}_{\mathrm{mass}} = -(\mathcal{L}_{\mathrm{mass}}^D + \mathcal{L}_{\mathrm{mass}}^M) = \overline{\nu}_L M_D \nu_R + \frac{1}{2}(\overline{\nu}_L^c M_L \nu_L + \overline{\nu}_R^c M_R \nu_R) + \mathrm{h.c.} \tag{2.31}$$

Note that we cannot assign a well–defined lepton number L to Majorana neutrinos, since they are a linear combination of two Dirac neutrinos with $L = +1$ and $L = -1$ [see Eq. (2.27)]. Consequently, every Majorana mass term violates L by $\Delta L = \pm 2$. We furthermore see that $B - L$ is always violated by Majorana mass terms.

2.2.2 Neutrino mixing

In Eq. (2.31) Dirac neutrino mass matrix M_D is a general complex 3×3 matrix, whereas the Majorana mass matrices $M_{L,R}$ are general complex symmetric 3×3 matrices. These mass matrices can be diagonalized by the following transformations:

$$M_D^{\mathrm{diag}} = U_D^\dagger M_D U_D', \quad M_L^{\mathrm{diag}} = U_L^T M_L U_L, \quad \text{and} \quad M_R^{\mathrm{diag}} = {U_R'}^T M_R U_R', \tag{2.32}$$

Parameter	Best–fit $\pm 1\sigma$	1σ acc.	2σ range	3σ range
$\Delta m_{21}^2 [10^-5\mathrm{eV}^2]$	7.9 ± 0.3	4%	$7.3 - 8.5$	$7.1 - 8.9$
$\lvert\Delta m_{31}^2\rvert [10^-5\mathrm{eV}^2]$	$2.5^{+0.20}_{-0.25}$	10%	$2.1 - 3.0$	$1.9 - 3.2$
$\sin^2\theta_{12}$	$0.30^{+0.02}_{-0.03}$	9%	$0.26 - 0.36$	$0.24 - 0.40$
$\sin^2\theta_{23}$	$0.50^{+0.08}_{-0.07}$	16%	$0.38 - 0.64$	$0.34 - 0.68$
$\sin^2\theta_{13}$	–	–	≤ 0.025	≤ 0.041

Table 2.2: Current best–fit values for three–flavor neutrino oscillation parameters [38]. Shown are the values with 1σ errors, the relative accuracies at 1σ, as well as the allowed ranges for 2σ and 3σ.

where the unitary mixing matrices U_x ($x \in \{D, L, R\}$) act on the LH neutrinos ν_L, while U'_x transforms the RH neutrinos ν_R. In order to parametrize U_x and U'_x, we can use the fact that a general unitary 3×3 matrix U can always be written as

$$U = D\widehat{U}K = \mathrm{diag}(e^{\mathrm{i}\varphi_1}, e^{\mathrm{i}\varphi_2}, e^{\mathrm{i}\varphi_3}) \cdot \widehat{U} \cdot \mathrm{diag}(e^{\mathrm{i}\alpha_1}, e^{\mathrm{i}\alpha_2}, 1), \tag{2.33}$$

where $\varphi_1, \varphi_2, \varphi_3, \alpha_1, \alpha_2 \in [0, 2\pi)$ and

$$\widehat{U} = \begin{pmatrix} c_{12}c_{13} & s_{12}c_{13} & s_{13}e^{-\mathrm{i}\widehat{\delta}} \\ -s_{12}c_{23} - c_{12}s_{23}s_{13}e^{\mathrm{i}\widehat{\delta}} & c_{12}c_{23} - s_{12}s_{23}s_{13}e^{\mathrm{i}\widehat{\delta}} & s_{23}c_{13} \\ s_{12}s_{23} - c_{12}c_{23}s_{13}e^{\mathrm{i}\widehat{\delta}} & -c_{12}s_{23} - s_{12}c_{23}s_{13}e^{\mathrm{i}\widehat{\delta}} & c_{23}c_{13} \end{pmatrix}. \tag{2.34}$$

The matrix $\widehat{U}$ in Eq. (2.34) is given in the standard parametrization with $s_{ij} = \sin\widehat{\theta}_{ij}$, $c_{ij} = \cos\widehat{\theta}_{ij}$, where $\widehat{\theta}_{ij} \in \{\widehat{\theta}_{12}, \widehat{\theta}_{13}, \widehat{\theta}_{23}\}$, $\widehat{\theta}_{ij} \in [0, \frac{\pi}{2}]$, and $\widehat{\delta} \in [0, 2\pi)$.

2.2.3 Neutrino Masses at Tree–Level

The smallness of the observed neutrino masses surprises. Thus, different scenarios for the generation of small neutrino masses have been suggested in order to avoid a fine tuning of neutrino masses.

Considering the SM as an effective field theory, obtained by integrating out heavy degrees of freedom [39, 40], we can employ higher dimension operators as the origin of small neutrino masses. Weinberg [41] has suggested a dimension–5 mass operator (*cf.* Fig. 2.1)

$$\mathcal{L}_{\mathrm{mass}} = Y_{abmn}\overline{\psi}^c_{iaL}\phi_{jb}\phi_{km}\psi_{lnL}\epsilon_{ij}\epsilon_{kl} + \mathrm{h.c.}, \tag{2.35}$$

where a and b are generation indices, m and n number the Higgs doublets and i, j, k and l are $SU(2)$ indices. The coupling constant is of the order $Y_{abmn} \simeq 1/M_{\mathrm{Pl}}$ on dimensional grounds. In the one–generation–case, *i.e.*, for $a = b$ and $m = n$, the neutrino mass is

$$m_\nu \simeq \frac{v^2}{M_{\mathrm{Pl}}} \simeq 10^{-5}\mathrm{eV}, \tag{2.36}$$

where $v \simeq 10^2\mathrm{GeV}$ and $M_{\mathrm{Pl}} \simeq 10^{18}\mathrm{GeV}$. But this value for the neutrino mass is by a factor of $10^3 - 10^5$ too small to be in agreement with current neutrino data.

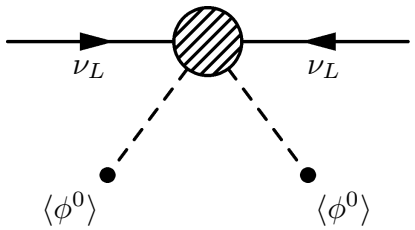

Figure 2.1: Dimension–5 operator generating neutrino masses.

Weinberg's dimension–5 operator can, *e.g.*, be ultraviolet completed in the type–I seesaw mechanism [10–12]. For $\nu \equiv (\nu_L,\, \nu_R^c)^T$, we can rewrite Eq. (2.31) as $-\mathcal{L}_{\rm mass} = \frac{1}{2}\overline{\nu}^c \mathcal{M} \nu + \text{h.c.}$ In this equation, $\mathcal{M}$ denotes the 6×6 Majorana neutrino mass matrix

$$\mathcal{M} = \begin{pmatrix} 0 & M_D \\ M_D^T & M_R \end{pmatrix}, \tag{2.37}$$

in which "0" is a 3×3 mass matrix with zero entries only, while M_D and M_R are 3×3 matrices with entries of the order v and $M_{B-L} \simeq 10^{14}\,\text{GeV}$ (the $B - L$ breaking scale), respectively. We can transform $\mathcal{M}$ to a block-diagonal matrix by

$$\mathcal{M}^{\rm diag} = V^T \mathcal{M} V = \begin{pmatrix} M_1 & 0 \\ 0 & M_2 \end{pmatrix}, \tag{2.38}$$

where V is a unitary 6×6 matrix of the form

$$V = \begin{pmatrix} C_1 & S_2^\dagger \\ -S_1 & C_2^\dagger \end{pmatrix}. \tag{2.39}$$

Here, the entries of S_i $(i = 1, 2)$ are of the order v/M_{B-L} whereas C_i has entries of order unity. Using the unitarity conditions for V and neglecting quartic terms of S_i that do not appear in combination with M_R, we find

$$S_1 \simeq M_R^{-1} M_D^T C_1 \quad \text{and} \quad S_2 \simeq C_2 M_R^{-1} M_D^T. \tag{2.40}$$

In the limit $M_D \to 0$, the matrices M_1 and M_2 are to lowest order in $1/M_{B-L}$ given by

$$M_1 \simeq -M_D M_R^{-1} M_D^T \quad \text{and} \quad M_2 \simeq M_{B-L}. \tag{2.41}$$

In the one–generation case, these become $m_1 \simeq v^2/M_{B-L}$ and $m_2 \simeq m_R \simeq M_{B-L}$. This leads to light neutrino masses of the order

$$m_\nu \simeq \frac{v^2}{M_{B-L}} \simeq 10^{-1}\text{eV}, \tag{2.42}$$

which is in agreement with solar and atmospheric neutrino data. Apart from the type–I seesaw mechanism, there exist also type–II [42–44], and type–III [45] seesaw mechanisms. For a classification of effective neutrino mass operators see also Ref. [46].

2.2.4 Neutrino Masses via Radiative Corrections

Besides these tree–level scenarios, neutrino mass models with an extended Higgs sector have been suggested. The neutrino masses are generated by radiative corrections. In this context, we can distinguish models by the types of the additional Higgs scalars. We will consider the cases of a singly charged singlet, a doubly charged singlet, or a Higgs triplet.

Following Zee [47], we can extend the scalar sector of the SM by a charged $SU(2)$ singlet h^+, *i.e.*,

$$-\mathcal{L} = Y_{hij}\overline{\psi}^c_{ikL}\psi_{jlL}\epsilon_{kl}h^+ + \text{h.c.}, \tag{2.43}$$

where i, j are generation indices, k, l denote $SU(2)$ indices and Y_{hij} is a Yukawa coupling matrix. Due to Fermi statistics, we have $Y_{ij} = -Y_{ji}$. We can assign a $B-L$ quantum number of 2 to the field h^+. Conservation of $U(1)_Q$ dictates that h^+ must acquire a vanishing VEV. Thus, there are no Majorana masses at tree level.

In order to generate nonzero neutrino masses, we have to introduce a second scalar doublet ϕ' which is a copy of the SM scalar doublet ϕ. Therefore, the trilinear coupling $\mu\phi^T \mathrm{i}\sigma_2\phi' h^+ + \text{h.c.}$ violates $B-L$ by two units. For the case of just one scalar doublet, this term would vanish due to the antisymmetric combination of fields. In the process of symmetry breaking, a linear combination of ϕ^+ and ϕ'^+ will be eaten by the W^+ gauge boson. The remaining two physical scalars S and S' are linear combinations of ϕ^+, ϕ'^+, and h^+. Consequently, these scalars break $B-L$ and thus generate Majorana neutrino masses at the one–loop level as shown in Fig. 2.2.

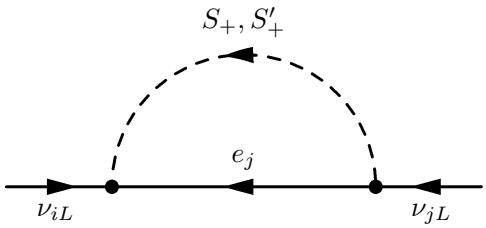

Figure 2.2: Neutrino mass generation at the one–loop level in Zee's model.

One might worry that the process shown in Fig. 2.2 could lead to an infinite contribution to neutrino masses. The reason is that there are no tree–level mass terms and one could not define counterterms which are absorbed into tree–level mass terms in order to cancel possibly infinite contributions. However, finite masses are guaranteed by the renormalizability of this model.

In order to read off the resulting neutrino mass matrices, let us redraw Fig. 2.2 in more detail, as shown in Fig. 2.3. We can simplify the situation by assuming that the Yukawa couplings of ϕ are much larger than those of ϕ', while their VEVs v and v' are of the same order, *i.e.*, $v \sim v'$. The consequence is that the charged lepton masses get a dominant contribution from ϕ. Fig. 2.3 gives a total contribution $Y_{hij}m^2_{e_i}$ to the neutrino masses. However, we also have to take into account the analogous diagram involving h^+ and ϕ^+, which gives rise to a term $Y_{hji}m^2_{e_j}$. Due to the antisymmetry of Y_{hij}, the total mass matrix becomes:

$$M_{ij} = AY_{hij}(m^2_{e_i} - m^2_{e_j}), \tag{2.44}$$

where A is a constant. The anti–symmetry of Y_{hij} furthermore implies that M_{ij} in Eq. (2.44) is indeed symmetric, as we would expect it for a representation in the Majorana basis.

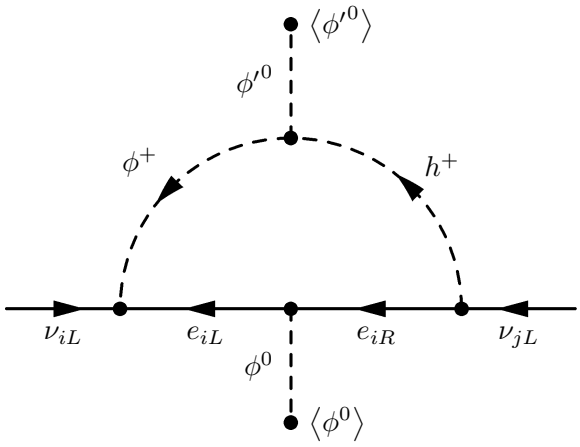

Figure 2.3: Detailed graph for the neutrino mass generation at the one–loop level in Zee's model.

Now, let us discuss the case of an additional doubly charged singlet k^{++} [48], which leads to a Lagrangian of the form

$$-\mathcal{L} = Y_{kij}\overline{e}^c_{iL}e_{jR}k^{++} + \text{h.c.} \tag{2.45}$$

Again, k^{++} carries two units of $B-L$. In order to generate Majorana masses, we need a $B-L$ violating term. However, due to the absence of trilinear couplings, the neutrinos must remain massless to all orders in perturbation theory. The situation changes when we also add a singly charged scalar h^+ as before. This scalar leads to the desired trilinear couplings $\mu h^- h^- k^{++}$, which break $B-L$ and can thus generate neutrino masses at the two-loop level as shown in Fig. 2.4. This two-loop diagram

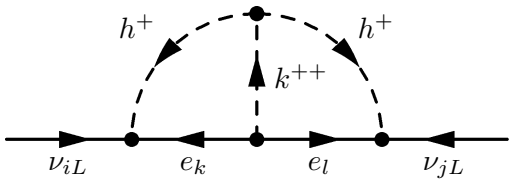

Figure 2.4: Neutrino mass generation at the two loop level in Babu's model.

gives rise to the following mass matrix

$$M_{ij} = 8\mu \sum_{e_k,e_l} m_{e_k} m_{e_l} Y_{hik} Y_{klk} Y^\dagger_{hlj} I_{kl}, \tag{2.46}$$

where

$$\begin{aligned} I_{kl} &= \int \frac{d^4k}{(2\pi)^4} \int \frac{d^4q}{(2\pi)^4} \frac{1}{k^2 - m_{e_k}^2} \frac{1}{q^2 - m_{e_l}^2} \\ &\times \frac{1}{k^2 - m_h^2} \frac{1}{q^2 - m_h^2} \frac{1}{(k-q)^2 - m_k^2}. \end{aligned} \tag{2.47}$$

Obviously, the neutrino mass eigenvalues have to be small due to the suppression factors from the two-loop integration.

In Secs. 2.2.3 and 2.2.4, we have discussed basic models for generating small neutrino masses in four dimensions. There are, however, also interesting proposals for small neutrino masses from extra dimensions [49, 50], which we will use in Chapter 7 to obtain realistic neutrino masses in the model defined on three throats.

Chapter 3

Leptogenesis

In this Chapter, we discuss the basic conditions and features of leptogenesis for Majorana as well as for Dirac neutrinos. Furthermore, we give some examples for alternative scenarios.

3.1 Sakharov's Conditions

Even in a homogeneous and baryon–symmetric Universe, a tiny number of baryons and antibaryons [51]

$$\frac{n_B}{s} = \frac{n_{\overline{B}}}{s} = 10^{-20} \tag{3.1}$$

(s is the entropy) would be left over after freeze–out. However, this tiny abundance is by far to small to explain BBN and CMB data. Thus, an effective mechanism must have taken place in the history of the Universe, which led to the observed asymmetry $\eta_B \sim 10^{-10}$. There are three indispensable ingredients needed in order to generate a baryon asymmetry starting initially with $B = 0$. These three conditions, generally referred to as Sakharov's [3] conditions are

- B–violation,
- C– and CP–violation, and
- decays out of thermal equilibrium.

The necessity of the first condition is obvious: When $B = 0$ is given initially, B has to be violated somehow in order to generate a baryon asymmetry, *i.e.*, we must have $B \neq 0$. In the context of leptogenesis, the B–violation is caused by sphaleronic processes as it will be outlined in more detail in Sec. 3.3.

The second condition requires processes which violate C and CP. In order to illustrate this requirement, consider a process of the form

$$X \to Y + Z, \tag{3.2}$$

where Y represents a symmetric initial state, with $B = 0$ and $L = 0$, and there are no intrinsic asymmetries: $B_L = B_R = L_L = L_R = 0$ in Eq. (3.2). Y and Z are final states, one of which carries a non-vanishing extrinsic or intrinsic B or L. Thus, if this process is invariant under C–transformation, acting on a complex scalar ϕ and a fermion ψ as

$$C: \quad \phi \;\to\; \phi^*, \tag{3.3a}$$
$$C: \quad \psi \;\to\; \mathrm{i}\gamma^2\psi, \quad \psi_L \to \mathrm{i}\sigma_2\psi_R^*, \quad \psi_R \to -\mathrm{i}\sigma_2\psi_L^*, \tag{3.3b}$$

it holds that

$$\Gamma(X \to Y + Z) = \Gamma(\overline{X} \to \overline{Y} + \overline{Z}), \tag{3.4}$$

where $\Gamma(\dots)$ is the decay width (see Chapter 5). As a consequence, no asymmetry A can be produced, since the net rate of asymmetry production is proportional to the difference between the decay rates:

$$\frac{\mathrm{d}A}{\mathrm{d}t} \sim \Gamma(X \to Y + Z) - \Gamma(\overline{X} \to \overline{Y} + \overline{Z}) \overset{C}{=} 0. \tag{3.5}$$

Furthermore CP, acting on ϕ and ψ as

$$CP: \quad \phi(t,\mathbf{x}) \;\to\; \pm\phi^*(t,-\mathbf{x}), \tag{3.6a}$$
$$\begin{aligned} CP: \quad \psi(t,\mathbf{x}) &\to \mathrm{i}\gamma^2\psi(t,-\mathbf{x}), \\ \psi_L(t,\mathbf{x}) &\to \mathrm{i}\sigma_2\psi_R^*(t,-\mathbf{x}), \\ \psi_R(t,\mathbf{x}) &\to -\mathrm{i}\sigma_2\psi_L^*(t,-\mathbf{x}), \end{aligned} \tag{3.6b}$$

must be violated. Consider decays of the form

$$X \to Y_L + \overline{Z}_R \quad \text{and} \quad X \to Y_R + \overline{Z}_L. \tag{3.7}$$

where $\overline{Y}_R$ denotes the antiparticle of Y_R. Thus, $\overline{Y}_R$ is actually a LH particle, since the indices L and R keep, in this notation, track of whether a particle is an $SU(2)_L$ doublet (L) or singlet (R). CP–conservation ($Y_L \to \overline{Y}_R$ and $Y_R \to \overline{Y}_L$) would imply

$$\Gamma(X \to Y_L + \overline{Z}_R) + \Gamma(X \to Y_R + \overline{Z}_L) = \Gamma(\overline{X} \to \overline{Y}_R + Z_L) + \Gamma(\overline{X} \to \overline{Y}_L + Z_R), \tag{3.8}$$

i.e., again no asymmetry could be generated. However, although it holds that

$$\Gamma(X \to Y_L\overline{Z}_R) \neq \Gamma(\overline{X} \to \overline{Y}_L Z_R), \tag{3.9}$$

due to C– and CP–violation, this can only lead to a temporary excess if $n_X = n_{\overline{X}}$ initially, and in the end everything would be equilibrated again. This contradiction is resolved by the CPT theorem, which requires at least one additional decay channel. CPT guarantees that the total process rates for particles and antiparticles are equal.

Combining this with the requirement that B has to be violated, we see that there have to take place at least two processes

$$B_i \to B_{f1} + B_i \to B_{f2} \overset{CPT}{=} \overline{B}_i \to \overline{B}_{f1} + \overline{B}_i \to \overline{B}_{f2}, \tag{3.10}$$

which generate different baryon numbers $B_{f1} \neq B_{f2}$ in the final states.

The third Sakharov condition requires out of thermal equilibrium decays. To see this, we have to consider the fact that B is odd under both C– and CP–transformations. A system in thermal equilibrium is described by the density operator $\rho = e^{-H/T}$. Requiring furthermore that the Hamiltonian H is invariant under CPT, we find the following relation for the average B in equilibrium at a time $T = 1/\beta$:

$$\begin{aligned} \langle B \rangle_T &= \mathrm{tr}\,[e^{-\beta H} B] = \mathrm{tr}\,[(CPT)(CPT)^{-1} e^{-\beta H} B] \\ &= \mathrm{tr}\,[e^{-\beta H} (CPT)^{-1} B (CPT)] = -\mathrm{tr}[e^{-\beta H} B] = 0. \end{aligned} \tag{3.11}$$

For the process $X \to Y + Z$, thermal equilibrium would mean

$$\Gamma(X \to Y + Z) = \Gamma(X \to Y + Z), \tag{3.12}$$

i.e., every net asymmetry has to average out to zero. Out–of–equilibrium means that the temperature at the time $\tau = 1/\Gamma(X \to Y + Z)$, when the decay takes place, has to be smaller than the mass of the decaying particle, *i.e.*, $T < M_X$. The inverse decay processes are then for kinematical reasons Boltzmann-suppressed

$$\Gamma(Y + Z \to X) \sim e^{-M_X/T}, \tag{3.13}$$

and can thus not equilibrate the generated asymmetry.

3.2 Baryogenesis

There are several scenarios for baryogenesis. These can be classified according to the mechanism by which they induce the departure from thermal equilibrium. GUT baryogenesis scenarios [52–56] consider the out-of-equilibrium decay of heavy particles. In fact, GUT models seem to be predestinated to fullfill Sakharov's conditions. B–violation is an inherent feature of GUT models, due to the fact that quarks and leptons are unified in the same representations [*cf.*for example [57] for $SU(5)$]. Furthermore, there can occur additional complex phases compared to the SM, and last but not least, the decay rates of the heavy gauge bosons and scalars are necessarily out–of–equilibrium because of their high mass scale. However, $B + L$ violating sphaleron processes will wash out every asymmetry except for $B - L$. Since $B - L$ is conserved in $SU(5)$, there is no way to generate it dynamically. But, in $SO(10)$, $B - L$ is a gauged subgroup and must thus be broken spontaneously. Therefore, only the decay of heavy particles X with $M_X < M_{B-L}$ can generate a baryon asymmetry. An alternative to GUT baryogenesis is EW baryogenesis [58, 59], which has the advantage to be

testable in future collider experiments. Here, the departure from thermal equilibrium is caused by a strong first order phase transition. In the Affleck-Dine scenario [60], η_B is generated by the evolution of a cosmological scalar fields which carries a baryon number.

3.3 Sphalerons

Some properties of gauge groups cannot be treated in terms of conventional perturbation theory. This is due to the fact that gauge field configurations show a non–trivial vacuum structure. According to 't Hooft [8], B can be violated, even in the SM, by non–perturbative effects due to triangle anomalies. Since the Adler–Bell–Jackiw triangular anomalies [61, 62] do not vanish, B and L are anomalous at the quantum level [52,63]. This anomalous non–conservation of B can also be encountered by transitions between the different vacua, separated by potential barriers. Thus, each tunnel-

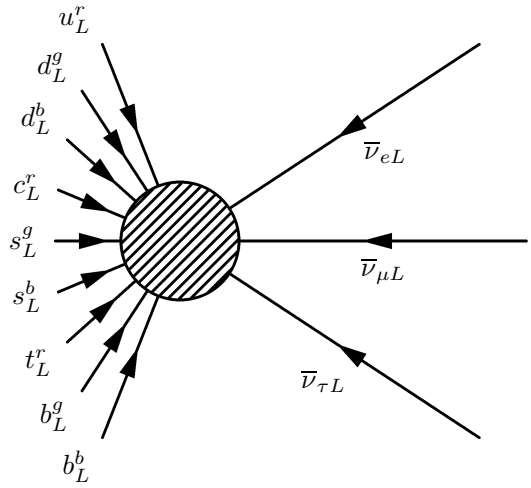

Figure 3.1: A Feynman–like diagram of a $SU(2)_L$ sphaleron process. The indices r, g, and b, are color indices.

ing process between the vacua would violate B and L by three units. These anomalies lead to a violation of B and L by three units each, *i.e.*, $\Delta B = \Delta L = \pm 3$. Since quarks carry $B = 1/3$, we see that in every sphaleron process 3 leptons and 9 quarks are involved. However, the probability of an instanton transition is $P \sim e^{-8\pi^2/g^2} \sim 10^{-173}$. Compared with the lifetime of the Universe, a process like this is most unlikely to have ever happend. A typical sphaleron process is shown in Fig. 3.1.

On the other hand, it was recognized by Kuzmin, Rubakov, and Shaposhnikov [64] that for $T \gtrsim 100\,\mathrm{GeV}$ there is enough thermal energy for the way over the barrier between the vacua. Below the EW phase transition, *i.e.*, for $T < T_c \sim 100\,\mathrm{GeV}$, the sphaleronic transition rate is Boltzmann–suppressed [65]. But extrapolating the

transition rate to a high–temperature symmetric phase [66–69], *i.e.*, $T > T_c$, it turns out that at high energies, sphaleronic baryon number violation plays an important role.

In Ref. [70], it has been shown that sphaleron–like processes can also occur in finite–temperature QCD. The reason is that above the EW symmetry breaking scale, QCD and the EW theory can be understood quite analogous. In the case of QCD, sphaleronic transitions lead to a strong non–conservation of chirality because of chiral anomalies. Thus, the chiral charge is the only charge that can be generated by transitions from one vacuum to another. Strong $SU(3)$ sphalerons thus lead to a change of chirality by 12 units, *i.e.*, by two for each flavor.

3.4 Thermal Leptogenesis

A very popular approach to explain the baryon asymmetry η_B has been formulated by of Fukugita and Yanagida [4] (see also Refs. [5–7]); the standard leptogenesis scenario *i.e.*, the generation of a baryon number asymmetry via the generation of a lepton number asymmetry. The striking idea is the postulation of a connection between this asymmetry and the smallness of the neutrino masses, a problematic phenomenon that cannot be explained within the SM. Assuming that neutrinos are Majorana particles, the masses of the RH singlets $N = \nu_R + \nu_R^c$ are not restricted by arguments of naturalness (see Sec. 2.2.3). Thus, we can, on the one hand, explain the smallness of the neutrino masses due to the type–I seesaw mechanism, and, on the other hand, the RH neutrinos N serve as the heavy particles needed for the generation of a particle–antiparticle asymmetry.

3.4.1 Standard Leptogenesis

In the standard leptogenesis scenario, heavy RH Majorana neutrinos N decay as

$$N \to \psi_L H \quad \text{and} \quad N \to \overline{\psi}_L \overline{H}, \tag{3.14}$$

where H is the SM $SU(2)$ Higgs doublet and ψ_L the LH $SU(2)$ lepton doublet. These decays can generate an lepton number asymmetry, which will later on be converted into a B asymmetry by sphaleron processes.
The total decay width Γ_{Di} of the ith ($i, j = 1, 2, 3$ are flavor indices) RH neutrino N_i at tree–level is given by

$$\begin{aligned} \Gamma_{Di} &= \sum_j \Big[\Gamma(N_i \to H + \psi_{Lj}) + \Gamma(N_i \to \overline{H} + \overline{\psi}_{Lj}) \Big] \\ &= \frac{1}{8\pi} (Y_\nu Y_\nu^\dagger)_{ii} M_i, \end{aligned} \tag{3.15}$$

where M_i denotes the mass of the ith RH neutrino N_i. Here, we will assume, for simplicity, that only the decay of the lightest RH neutrino is responsible for the

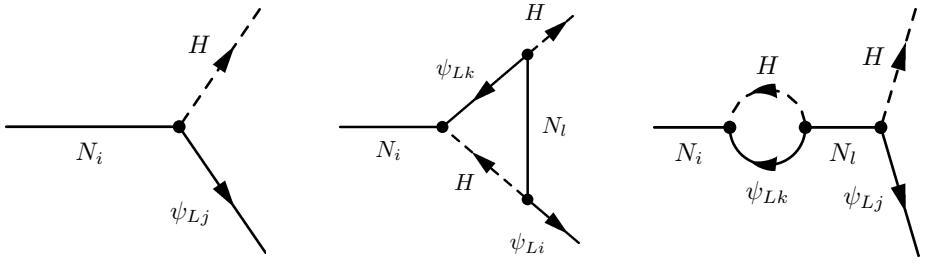

(a) (b) (c)

Figure 3.2: Decay diagrams of the RH Majorana neutrinos in the standard leptogenesis, where i, j are flavor indices. The lepton asymmetry is generated by the interference of tree–level decays (a) with the one–loop vertex (b) and wave–function correction.

generation of the asymmetry[1]. The condition for an out–of–equilibrium decay, as required by Sakharov, reads

$$r = \frac{\Gamma_{D1}}{H(M_1)} = \frac{M_{\rm Pl}}{1.7 \cdot 32\pi\sqrt{g_*}} \frac{(Y_\nu Y_\nu^\dagger)_{11}}{M_1} < 1, \tag{3.16}$$

where $g_* \sim 100$ is the number of relativistic degrees of freedom and $H(M_i)$ denotes the Hubble parameter at the temperature $T = M_i$. In other words, Eq. (3.16) tells us that the expansion of the Universe has to be larger than the total decay width such that the particles are not any more able to follow the rapid change of the equilibrium particle distribution. One can, furthermore, derive a constraint on the effective light neutrino mass

$$\widetilde{m}_1 = (Y_\nu Y_\nu^\dagger)_{11} \frac{v^2}{M_1} \simeq 4\sqrt{g_*} \frac{v^2}{M_{\rm Pl}} \frac{\Gamma_{D1}}{H(M_1)} < 10^{-3}\text{eV}, \tag{3.17}$$

where Y_ν is the 3×3 Yukawa coupling matrix and $v \sim 10^2\,\text{GeV}$. The CP asymmetry ε_1, generated by the interference between tree–level decays of N_1 and their one-loop corrections, take the form

$$\begin{aligned} \varepsilon_1 &= \frac{\sum_j \Big[\Gamma(N_i \to H + \psi_j) - \Gamma(N_i \to \overline{H} + \overline{\psi}_j)\Big]}{\sum_\alpha \Big[\Gamma(N_i \to H + \psi_j) + \Gamma(N_i \to \overline{H} + \overline{\psi}_j)\Big]} \\ &\simeq \frac{1}{8\pi} \frac{1}{(YY^\dagger)_{11}} \sum_{i=2,3} \text{Im}(YY^\dagger)_{1i}^2 \Big[f\Big(\frac{M_i^2}{M_1^2}\Big) + g\Big(\frac{M_i^2}{M_1^2}\Big)\Big], \end{aligned} \tag{3.18}$$

[1]For a discussion of the contributions from N_2 and N_3 see Ref. [71, 72]

where the functions $f(x)$ and $g(x)$, which describe the one–loop vertex correction [Fig. 3.2(b)] and the wave–function correction [Fig. 3.2(c)], respectively, are given by

$$f(x) = \sqrt{x}\Big[1-(1+x)\ln\Big(\frac{1+x}{x}\Big)\Big] \tag{3.19a}$$

$$g(x) = \frac{\sqrt{x}}{1-x} \tag{3.19b}$$

Notice that Eq. (3.19b) is only valid for $|M_i - M_1| \gg |\Gamma_i - \Gamma_1|$. Below this limit perturbation theory breaks down. In the case of a hierarchical mass structure for the RH neutrinos, *i.e.*, for $M_1 \ll M_2$, M_3, Eq. (3.18) reduces to

$$\varepsilon_1 \approx -\frac{3}{8\pi}\frac{1}{(Y_\nu Y_\nu^\dagger)_{11}}\sum_{i=2}^{3}\mathrm{Im}((Y_\nu Y_\nu^\dagger)^2_{1i})\frac{M_1}{M_i}. \tag{3.20}$$

However, the any produced L asymmetry can be washed out again by inverse decays and scattering processes (see Figs. 3.3 and 3.4). This wash–out effect is parametrized by κ:

$$\eta_L = \frac{n_L - n_{\overline{L}}}{s} = \kappa\frac{\varepsilon_1}{g_*}. \tag{3.21}$$

For the degree of wash–out, we can distinguish two cases depending on the size of r:

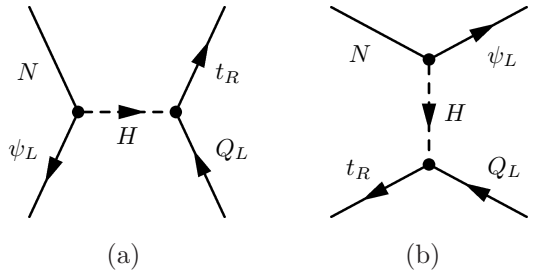

Figure 3.3: 2–2 scattering processes with $\Delta L = 1$.

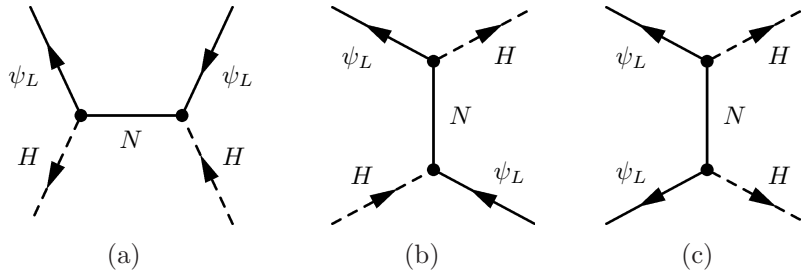

Figure 3.4: 2–2 scattering processes with $\Delta L = 2$.

- Case I: $r \ll 1$, *i.e.*, the weak wash–out regime: Here, the inverse decay width Γ_{ID} and 2–2 scattering processes described by Γ_S, are impotent, *i.e.*,

$$\frac{\Gamma_{ID}}{H} \sim \frac{M_X}{T}^{3/2} e^{-M_X/T} \cdot r \tag{3.22}$$

and

$$\frac{\Gamma_S}{H} \sim \alpha \frac{M_X}{T}^{5} \cdot r, \tag{3.23}$$

where r has been defined in Eq. (3.16) and M_X is the mass of the heavy decaying particle X. Since the number density n_X of X has a thermal distribution, *i.e.*, $n_X \simeq n_{\overline{X}} \simeq n_\gamma$ at $T \simeq T_D$, *i.e.*, at the temperature where the decays drop out of thermal equilibrium, we find for the produced lepton asymmetry

$$n_L = \varepsilon_1 \cdot n_X \simeq \varepsilon_1 \cdot n_\gamma. \tag{3.24}$$

- Case II: $r \gg 1$, *i.e.*, the strong wash–out regime: No asymmetry will be generated here, due to rapidly occurring inverse decays and scattering processes which keep the system in thermal equilibrium.

For values of r between these extrema, we have to solve the Boltzmann equations in order to see how strong the wash–out actually is, and how much asymmetry is produced. The resulting lepton asymmetry η_L is then transferred to a baryon asymmetry η_B via sphaleron processes:

$$\eta_B = c \cdot \eta_{B-L} = \frac{c}{c-1}\eta_L \approx -\frac{1}{3}\eta_L, \tag{3.25}$$

where c is a conversion factor describing the relation between B, L and $B - L$ by $B = c(B - L)$ and $L = (c - 1)(B - L)$.

However, it has been pointed out that such a flavor–independent discussion is a too strong simplification for hierarchical RH neutrino masses. The point is that all three flavors (e, μ, and τ) reach thermal equilibrium at different temperatures. In the case that leptogenesis takes place at $T \sim M_1 > 10^{12}\,\mathrm{GeV}$, *i.e.*, the temperature where the τ–flavor Yukawa interactions reach thermal equilibrium, all three flavors are out–of–equilibrium and thus we have a universal washout factor due to the fact that they are indistinguishable. The situation changes if leptogenesis takes place at temperatures below $10^{12}\,\mathrm{GeV}$, since then different flavors are distinguishable and we have to analyze the effect of every single flavor on its own. A detailed analysis shows an enhancement of the asymmetry by a factor of 2–3 [73–75].

3.4.2 Dirac Leptogenesis

Standard leptogenesis relies on the assumption that neutrinos are Majorana particles. However, even for Dirac neutrinos, a leptogenesis–like scenario exists [27]. The following three characteristics of the sphalerons are crucial for Dirac leptogenesis: (i) In

sphaleron processes only LH particles are involved. (ii) Sphalerons violate $B+L$ but conserve $B-L$. (iii) Sphalerons are in thermal equilibrium for $T \gtrsim T_c$ and Boltzmann–suppressed at $T < T_c$. The basic idea in Dirac leptogenesis is that an asymmetry is generated between the LH and RH neutrino sector due to out–of–equilibrium decays. Suppose a negative lepton number is produced for the LH neutrinos, *i.e.*, $\Delta L_L < 0$, and a positive lepton number for the RH neutrinos, *i.e.*, $\Delta L_R < 0$. At this point, the total lepton asymmetry remains constant, *i.e.*, $L = L_{\rm init}$. Now, sphaleron processes lead to a transfer of the asymmetry from the LH lepton sector to the baryon sector. Thus, a part of the negative ΔL_L gives rise to a positive LH baryon number which leads to a total positive baryon asymmetry in both LH and RH sectors due to LR equilibration. As long as the asymmetry stored in the RH neutrino sector is, due to the small Dirac neutrino Yukawa couplings, conserved above T_c, a total baryon asymmetry can evolve. When the temperature drops below T_c, the remaining negative ΔL_L equilibrates with the positive ΔL_R and a total positive lepton asymmetry is generated. In order to avoid a LR equilibration of the neutrinos above T_c, we have

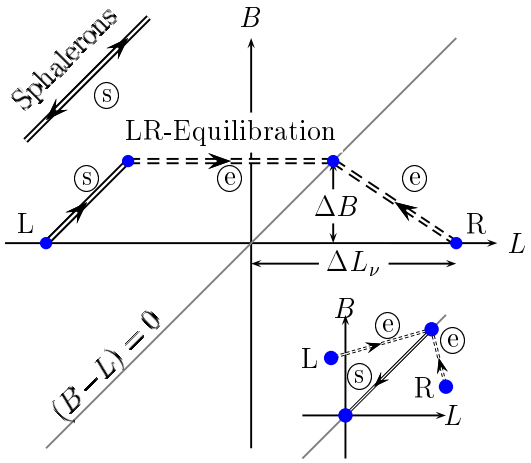

Figure 3.5: Comparison of the evolution of B and L due to $SU(2)_L$ sphaleronic ⓢ and LR–equilibration ⓔ processes in the case of neutrinos and SM particles (insertion). For SM particles, both processes occur approximately simultaneously and thus no baryon number can be generated for $B-L=0$. (taken from Ref. [27]).

to require that

$$\Gamma_{LR} \sim \lambda^2 g^2 T \lesssim H \sim \frac{T^2}{M_{\rm Pl}}, \tag{3.26}$$

where λ symbolizes the Dirac neutrino Yukawa couplings to the SM Higgs boson. For $g \sim 1$, $T = T_c \sim 100\,\text{GeV}$ and $M_{\rm Pl} \sim 10^{18}\,\text{GeV}$, we get

$$\lambda \lesssim \sqrt{\frac{T_c}{M_{\rm Pl}}} \sim 10^{-8}. \tag{3.27}$$

Thus, Dirac leptogenesis works for Dirac neutrino masses $m_{\rm D}$ up to

$$m_{\rm D} \sim \lambda T_c \lesssim 1\text{keV}. \tag{3.28}$$

This limit can be refined up to $m_{\rm D} \lesssim 10\,{\rm keV}$, in detailed numerical computations of the Boltzmann equations. A realistic supersymmetric Dirac leptogenesis scenario has been proposed in Ref. [76].

3.4.3 Gravitino Problem

In scenarios like the standard leptogenesis scenario where the RH neutrinos are produced thermally, we have to require that the reheating temperature $T_{\rm rh}$ is greater than the mass of the lightest RH neutrino, *i.e.*, $T_{\rm rh} > M_R$. A high $T_{\rm rh}$ can cause problems, since it can also lead to an overproduction of light particles, such as gravitinos [77–82]. If the gravitino is unstable, it must have a long lifetime, long enough to trouble BBN [83], leading to a decrease of η_B. The number density of gravitinos at the thermalization stage after inflation is

$$\frac{n_{3/2}}{s} \simeq 10^{-2} \frac{T_{\rm rh}}{M_{\rm Pl}}. \tag{3.29}$$

From the observed abundance of D $+^3$ He, we can derive a constraint on the gravitino number density and thus on the reheating temperature:

$$\frac{n_{3/2}}{s} \lesssim 10^{-12} \Rightarrow T_{\rm rh} < 10^{8-9}\,{\rm GeV}. \tag{3.30}$$

If the neutrino mass spectrum of the RH neutrinos is strongly hierarchical, *i.e.*, $M_1 \ll M_2 \ll M_3$, an upper bound for the asymmetry generated by the decay of the lightest RH neutrino, the so–called Davidson-Ibarra bound [84], can be found:

$$|\varepsilon_1| \leq \frac{3}{16\pi} \frac{M_1 (m_3 - m_2)}{v^2}, \tag{3.31}$$

where $v \sim 100\,{\rm eV}$. We know from experiments that $|m_3 - m_2| = \sqrt{\Delta m^2_{32}} \sim 0.05\,{\rm eV}$, leading to a lower bound $M_1 \geq 2 \cdot 10^9\,{\rm GeV}$. Due to the fact that the lightest RH neutrino has to be generated during the epoch of reheating at the end of inflation, the Davidson-Ibarra bound also implies a lower bound for $T_{\rm rh}$. However, this bound conflicts with the upper bound for $T_{\rm rh}$ derived from the requirement to avoid an overproduction of gravitinos in supersymmetric models.

3.5 Alternative Leptogenesis Scenarios

In order to overcome the conflicts arising from the gravitino problem (see Sec. 3.4.3), several alternative leptogenesis scenarios have been proposed. These scenarios include so–called resonant leptogenesis [85], using a resonant enhancement of the wave–function contribution to η_B due to degenerate RH neutrino masses. The one–loop wave–function correction dominates the asymmetry in the resonant limit $M_i^2 - M_2^2 \sim \Gamma_{N2}^2$. Thus, the mass scale of the RH neutrinos can be lowered even down to the

TeV scale. Besides the standard scenario of generating CP–violation via heavy particle decays, there is the alternative of soft leptogenesis [86–91], in which the relation between η_B and the RH neutrino masses is relaxed. Here, particle mixing can lead to a CP–violation, due to a mismatch between CP–eigenstates and mass eigenstates, analogously to the Kaon system $K^0 - \overline{K}^0$ (see, for example, [92]). Another possibility is non–thermal leptogenesis [93], where the relation between $T_{\rm rh}$ and the RH neutrino masses is relaxed. In this scenario, the RH neutrinos are generated non–thermally via the decay of the inflaton, the scalar responsible for inflation. The inflaton can be assumed to decay dominantly into the lightest RH neutrino, which then generates η_B in the usual way. There is also another class of models, which establish a connection between low energy CP–violation (occurring in neutrino oscillations and neutrinoless double beta decay) and high energy CP–violation as necessary for leptogenesis. However, such scenarios face the problem of additional phases and mixing angles which are introduced by the heavy neutrinos. There are two basic ideas to deal with this problem: One possibility is to reduce the number of additional parameters, for example, by restricting the number of heavy neutrinos to two instead of three [94]. An alternative approach is to postulate a common origin for both low–energy and high–energy CP–violation [95].

Chapter 4

Left–Right Symmetry and Extra Dimensions

Existing models of Dirac leptogenesis suffer from the lack of an attractive scenario which offers in an elegant way heavy states for the out–of–equilibrium decays as well as a connection to low–energy observables. In order to overcome these white spots on the map, we will, in this Chapter, discuss two model building ingredients that might be usefull for a realistic implementation of Dirac leptogenesis: LR symmetry and extra dimensions.

4.1 Left–Right Symmetry

As mentioned in the introduction, LR–symmetric theories could provide a natural framework for Dirac neutrino masses. They are based on the LR–symmetric gauge group G_{LR} given in Eq. (1.5). These models postulate that the parity violating processes we are observing are only the low–energy limit and that on a fundamental level, all forces are parity–conserving. For these models, we consequently have to add RH neutrinos. On the other hand, we know that neutrinos are massive and thus such an extension of the SM is attractive. Moreover, in the SM, the hypercharge $U(1)$ generators are arbitrary in the sense that they are just adjusted to give the desired electric charge. But on its own, it has no direct physical meaning. However, in the LR–symmetric models all the $U(1)$ generators can be identified with the $B-L$ quantum number and, thus, do have a physical meaning. In LR symmetry, the electric charge formula is then given by

$$Q = I_{3L} + I_{3R} + \frac{B-L}{2}. \tag{4.1}$$

There are a few more arguments favoring LR symmetry: In fundamental theories like string theory [96, 97] it is easier to derive a LR–symmetric structure of the gauge sector than the SM gauge structure [98]. Furthermore, for every model postulating a

unified substructure of quarks and leptons like preons [99, 100], we would expect G_{LR} to be a more natural symmetry than $G_{\rm SM}$.

4.1.1 Original Model with Dirac Neutrino Masses

The original version of the LR–symmetric model [22–24] would predict Dirac neutrinos. The quarks and leptons transform under G_{LR} as follows

$$\begin{aligned} Q_L = \begin{pmatrix} u \\ d \end{pmatrix}_L : \quad \left(\tfrac{1}{2}, 0, \tfrac{1}{3}\right), \quad Q_R = \begin{pmatrix} u \\ d \end{pmatrix}_R : \quad \left(0, \tfrac{1}{2}, \tfrac{1}{3}\right), \\ \psi_L = \begin{pmatrix} \nu \\ e \end{pmatrix}_L : \quad \left(\tfrac{1}{2}, 0, -1\right), \quad \psi_R = \begin{pmatrix} \nu \\ e \end{pmatrix}_R : \quad \left(0, \tfrac{1}{2}, -1\right). \end{aligned} \tag{4.2}$$

Due to a discrete parity symmetry, there are only two weak gauge couplings above SSB: The couplings associated with $SU(2)_L$ and $SU(2)_R$, g_{2L} and g_{2R}, are equal and can be identified with g_2 in the Glashow–Weinberg–Salam theory, *i.e.*, $g_2 = g_{2L} = g_{2R}$. Furthermore, we can identify the coupling g_1' of $U(1)_{B-L}$ by $g_1 = g_1' g_2 / ({g_1'}^2 + g_2^2)^{1/2}$ and thus find $\tan\theta_W = \tan\theta = g_1/g_2 = g_1/({g_1'}^2 + g_2^2)^{1/2}$, where θ_W is the usual Weinberg angle. In analogy to $SU(2)_L$ in the SM, also the breaking of $SU(2)_R$ leads to two charged gauge bosons $W_R^\pm$ and one neutral Z_R with masses M_{W_R} and M_{Z_R}, respectively. The gauge symmetry breaking has the pattern

$$\begin{array}{c} SU(2)_L \times SU(2)_R \times U(1)_{B-L} \\ \big\downarrow M_{W_R}, M_{Z_R} \\ SU(2)_L \times U(1)_Y \\ \big\downarrow M_{W_L} \\ U(1)_Q. \end{array} \tag{4.3}$$

In this scenario M_{W_R} breaks the discrete parity and $SU(2)_R \times U(1)_{B-L}$ at the same stage. Otherwise, the gauge couplings would be different at $\mu \geq M_{W_R}$, *i.e.*, $g_{2L} \neq g_{2R}$. Such a decoupling of the two processes of symmetry breaking would require a parity–odd, neutral scalar field σ, which acquires a non–zero VEV.

The Lagrangian of the LR–symmetric model contains the three parts

$$\mathcal{L} \supset \mathcal{L}^f_{\rm kin} + \mathcal{L}_Y - V, \tag{4.4}$$

where $\mathcal{L}^f_{\rm kin}$ is the fermionic kinetic term, $\mathcal{L}_Y$ are the Yukawa interactions, and V is the scalar potential. The fermionic kinetic energy is given by

$$\mathcal{L}^f_{\rm kin} = -\overline{Q} \not{D}^q Q - \psi \not{D}^\ell \psi, \tag{4.5}$$

where the covariant derivatives $D_\mu^{q,\ell}$ for quarks q and leptons ℓ are

$$D_\mu^{q,\ell} = \partial_\mu - \frac{\mathrm{i}g}{2} \sigma_a W^a_{L\mu} - \frac{\mathrm{i}g}{2} \sigma_a W^a_{R\mu} - \frac{\mathrm{i}g'}{6,2} B_\mu. \tag{4.6}$$

The Higgs sector consits of two Higgs doublets

$$\chi_{L,R} = \begin{pmatrix} \chi^+ \\ \chi^0 \end{pmatrix}_{L,R} \tag{4.7}$$

and a bi–doublet

$$\phi_1 = \begin{pmatrix} \phi_1^0 & \phi_1^\dagger \\ \phi_2^- & \phi_2^0 \end{pmatrix}, \qquad \phi_2 = \sigma_2 \phi_1^* \sigma_2 = \begin{pmatrix} \phi_2^{0*} & -\phi_2^\dagger \\ -\phi_1^- & \phi_1^{0*} \end{pmatrix}. \tag{4.8}$$

These scalars carry the G_{LR} quantum numbers

$$\chi_L : \left(\frac{1}{2}, 0, 1\right) \qquad \chi_L : \left(0, \frac{1}{2}, 1\right) \qquad \phi : \left(\frac{1}{2}, \frac{1}{2}, 0\right), \tag{4.9}$$

where LR symmetry implies $\chi_L \leftrightarrow \chi_R$ and $\phi \leftrightarrow \phi^\dagger$. The most general renormalizable parity– and gauge–invariant potential for $\chi_{L,R}$ and ϕ is then given by

$$\begin{aligned} V(\chi_L, \chi_R, \phi) &= -\mu^2(\chi_L^\dagger \chi_L + \chi_R^\dagger \chi_R) - \sum_{i,j} \mu_{ij}^2 \mathrm{tr}(\phi_i^\dagger \phi_j) + c_1[(\chi_L^\dagger \chi_L)^2 + (\chi_R^\dagger \chi_R)^2] \\ &+ c_2(\chi_L^\dagger \chi_L)(\chi_R^\dagger \chi_R) + \sum_{i,j,k,l} \lambda_{ijkl} \mathrm{tr}(\phi_i^\dagger \phi_j) \mathrm{tr}(\phi_k^\dagger \phi_l) \\ &+ \sum_{i,j,k,l} \widetilde{\lambda}_{ijkl} \mathrm{tr}(\phi_i^\dagger \phi_j \phi_k^\dagger \phi_l) + \sum_{i,j} \alpha_{i,j}(\chi_L^\dagger \chi_L + \chi_R^\dagger \chi_R) \mathrm{tr}(\phi_i^\dagger \phi_j) \\ &+ \sum_{i,j} \beta_{i,j}(\chi_L^\dagger \phi_i \phi_j^\dagger \chi_L + \chi_R^\dagger \phi_i^\dagger \phi_j \chi_R) + \mathrm{h.c.} \end{aligned} \tag{4.10}$$

A suitable choice of parameters gives the following VEV structure:

$$\langle \chi_L \rangle = 0, \quad \langle \Delta_{L,R} \rangle = \begin{pmatrix} 0 \\ v_R \end{pmatrix} \quad \text{and} \quad \langle \phi \rangle = \begin{pmatrix} \kappa & 0 \\ 0 & \kappa' \end{pmatrix}. \tag{4.11}$$

After SSB, there are 4 charged and 6 real neutral Higgs fields.

The fermion mass matrices are symmetric, due to the transformation $\phi \leftrightarrow \phi^\dagger$. The most general Yukawa couplings are

$$\mathcal{L}_Y = \overline{f}_{iL}(a_{ij}\phi + b_{ij}\widetilde{\phi}) f_{jR} + \overline{f}_{jR}(a_{ij}^* \phi^\dagger + b_{ij}^* \widetilde{\phi}^\dagger) f_{iL}, \tag{4.12}$$

where $f = (Q, \psi)$. Since $a_{ij} = a_{ij}^*$ and $b_{ij} = b_{ij}^*$ holds because of LR symmetry, we find the fermion mass matrices

$$M_{1ij} = a_{ij}k + b_{ij}k'^* \quad \text{and} \quad M_{1ij} = a_{ij}k' + b_{ij}k^*, \tag{4.13}$$

where the index $i, j = 1, 2$ denotes fermions with $T_3 = 1/2$ and $T_3 = -1/2$, respectively. In this model, the charged physical $W_{1,2}$ bosons are linear combinations of $W_{L,R}$:

$$\begin{aligned} W_1 &= W_L \cos\zeta + W_R \sin\zeta, & M_{W_1}^2 &\simeq \tfrac{1}{4} g^2(\kappa^2 + \kappa'^2) \\ W_2 &= -W_L \sin\zeta + W_R \cos\zeta, & M_{W_2}^2 &\simeq \tfrac{1}{4} g^2(\kappa^2 + \kappa'^2 + 2v^2) \end{aligned}$$

where $\tan 2\zeta = 2\kappa\kappa'/v^2$. The neutral gauge bosons are

$$\begin{aligned} A &= (W_{3L} + W_{3R})\sin\theta + B_\mu\sqrt{\cos 2\theta}, \\ Z_L &\simeq \cos\theta W_{3L} - \sin\theta\tan\theta W_{3R} - \tan\theta\sqrt{\cos 2\theta}B, \\ Z_R &\simeq \frac{\sqrt{\cos 2\theta}}{\cos\theta}W_{3R} - \tan\theta B. \end{aligned} \tag{4.14}$$

with

$$M_A = 0, \quad M_{Z_L} = \frac{M_{W_L}}{\cos\theta}, \quad \text{and} \quad M_{Z_R} = \frac{M_{W_R}\cos\theta}{\sqrt{\cos 2\theta}}. \tag{4.15}$$

Here, we are facing the basic problems of flavor changing neutral currents (FCNCs) in LR–symmetric models: The experimental limits on $W_1 - W_2$ mixing are consistent even for $\kappa = \kappa'$, *i.e.*, maximal mixing (see Ref. [101]). Thus, one is seduced to conclude that the low–energy limits on the relative magnitudes of κ and κ' are negligible. However, in Ref. [102] it was pointed out that it is not possible to avoid FCNCs in LR–symmetric models with three generations of fermions. When both κ and κ' are non–zero, the Higgs bosons have to be very massive in order to avoid FCNC interactions, which might lead to problems with respect to unitarity in the W sector.

4.1.2 Model with Higgs Triplets

The original LR–symmetric model described in Sec. 4.1.1 was, later on, modified by introducing the Higgs triplets $\Delta_{L,R}$ [42]:

$$\Delta_{L,R} = \frac{1}{\sqrt{2}}\sigma\delta_{L,R} = \begin{pmatrix} \delta^+/\sqrt{2} & \delta^{++} \\ \delta^0 & -\delta^+/\sqrt{2} \end{pmatrix}_{L,R}, \tag{4.16}$$

which transform under G_{LR} according to

$$\Delta_L : \Big(1, 0, 2\Big) \quad \text{and} \quad \Delta_R : \Big(0, 1, 2\Big), \tag{4.17}$$

where LR symmetry implies $\Delta_L \leftrightarrow \Delta_R$. The most general renormalizable parity– and gauge–invariant potential of $\Delta_{L,R}$ and ϕ is then given by

$$\begin{aligned} V(\Delta_L, \Delta_R, \phi) &= V(\Delta_L, \Delta_R) - \sum_{i,j}\mu_{i,j}^2 \mathrm{tr}(\phi_i^\dagger\phi_j) + \sum_{i,j,k,l}\lambda_{ijkl}\mathrm{tr}(\phi_i^\dagger\phi_j)\mathrm{tr}(\phi_k^\dagger\phi_l) \\ &+ \sum_{i,j,k,l}\widetilde{\lambda}_{ijkl}\mathrm{tr}(\phi_i^\dagger\phi_j\phi_k^\dagger\phi_l) + \sum_{i,j}\alpha_{i,j}\mathrm{tr}(\phi_i^\dagger\phi_j)\mathrm{tr}(\Delta_L^\dagger\Delta_L + \Delta_R^\dagger\Delta_R) \\ &+ \sum_{i,j}\beta_{i,j}\mathrm{tr}(\phi_i^\dagger\phi_j\Delta_L^\dagger\Delta_L + \phi_i^\dagger\phi_j\Delta_R^\dagger\Delta_R) \\ &+ \sum_{i,j}(\gamma_{ij}\mathrm{tr}(\Delta_L^\dagger\phi_i\Delta_R\phi_j^\dagger) + \mathrm{h.c.}), \end{aligned} \tag{4.18}$$

where

$$\begin{aligned} V(\Delta_L,\Delta_R) &= -\mu^2\mathrm{tr}(\Delta_L^\dagger\Delta_L+\Delta_R^\dagger\Delta_R)+\rho_1[(\mathrm{tr}(\Delta_L^\dagger\Delta_L))^2+(\mathrm{tr}(\Delta_R^\dagger\Delta_R))^2] \\ &+ \rho_2[\mathrm{tr}(\Delta_L^\dagger\Delta_L)^2+\mathrm{tr}(\Delta_R^\dagger\Delta_R)^2]+\rho_3[\mathrm{tr}(\Delta_L^\dagger\Delta_L)\mathrm{tr}(\Delta_R^\dagger\Delta_R)] \\ &+ \rho_4[\mathrm{tr}(\Delta_L^\dagger\Delta_L^\dagger)\mathrm{tr}(\Delta_L\Delta_L)+\mathrm{tr}(\Delta_R^\dagger\Delta_R^\dagger)\mathrm{tr}(\Delta_R\Delta_R)]. \end{aligned} \tag{4.19}$$

This potential has a minimum for the VEVs

$$\langle\Delta_{L,R}\rangle=\begin{pmatrix}0&0\\ v_{L,R}&0\end{pmatrix}\quad\text{and}\quad\langle\phi\rangle=\begin{pmatrix}\kappa&0\\0&\kappa'\end{pmatrix}e^{\mathrm{i}\alpha}. \tag{4.20}$$

These VEVs break G_{LR} down to G_{SM}. The physical $W_{1,2}$ are the same as in Eq. (4.14), but with the masses

$$M_{W_1}^2\simeq\frac{1}{2}g^2(\kappa^2+\kappa'^2)\quad\text{and}\quad M_{W_2}^2\simeq\frac{1}{2}g^2(\kappa^2+\kappa'^2+2v_R^2). \tag{4.21}$$

Also the neutral gauge bosons take the same form as in Eq. (4.14). The massless photon eigenstate is given by A, while the other two massive eigenstates are

$$Z_1=Z_L\cos\xi+Z_R\sin\xi\quad\text{and}\quad Z_2=-Z_L\sin\xi+Z_R\cos\xi, \tag{4.22}$$

where $\tan 2\xi\simeq 2\sqrt{\cos 2\theta_W}(M_{Z_L}^2/M_{Z_R}^2)$ and

$$\begin{aligned} M_{Z_L}^2 &\simeq \frac{g^2}{2\cos^2\theta_W}(\kappa^2+\kappa'^2+4v_L^2), \\ M_{Z_R}^2 &\simeq \frac{g^2}{2\cos^2\theta_W\cos 2\theta_W}(4v_R^2\cos^4\theta_W+(\kappa^2+\kappa'^2)\cos^2\theta_W+4v_L^2\sin^4\theta_W). \end{aligned} \tag{4.23}$$

The most general gauge–invariant Yukawa couplings in the LR–symmetric model reads

$$\begin{aligned} \mathcal{L}_Y &= \sum_{i,j}\big(Y_{qij}\overline{Q}_{Li}\phi Q_{Rj}+\widetilde{Y}_{qij}\overline{Q}_{Li}\widetilde{\phi}Q_{Rj}+Y_{\ell ij}\overline{\psi}_{Li}\phi\psi_{Rj}+\widetilde{Y}_{\ell ij}\overline{\psi}_{Li}\widetilde{\phi}\psi_{Rj} \\ &+ F_{ij}(\psi_{Li}^TC^{-1}\sigma_2\Delta_L\psi_{Lj}+\psi_{Ri}^TC^{-1}\sigma_2\Delta_R\psi_{Rj})+\mathrm{h.c.}\big), \end{aligned} \tag{4.24}$$

leading after SSB to the fermionic mass matrices

$$M_{ij}^u=M_{ij}^{d\,*}=Y_{qij}\kappa e^{\mathrm{i}\alpha}+\widetilde{Y}_{qij}\kappa' e^{-\mathrm{i}\alpha},\quad\text{and}\quad M_{ij}^e=Y_{\ell ij}\kappa e^{-\mathrm{i}\alpha}+\widetilde{Y}_{\ell ij}\kappa' e^{\mathrm{i}\alpha}. \tag{4.25}$$

In the low–energy limit, where $SU(2)_L$ is a good approximation, we see from Eq. (4.1) that

$$\Delta I_{3R}=-\frac{1}{2}\Delta(B-L). \tag{4.26}$$

For pure leptonic processes, we find $\Delta L=2\Delta I_{3R}$. Since $|\Delta I_{3R}|=1$ for neutrino interactions, we see that they are Majorana particles. The gauge–symmetry breaking

leads to the following neutrino mass matrix M_ν:

$$\begin{array}{c} SU(2)_L \times SU(2)_R \times U(1)_{B-L} \\ \downarrow \\ \langle \Delta_L^0 \rangle \simeq 0, \quad \langle \Delta_R^0 \rangle = v_R \neq 0, \quad M_\nu = \begin{pmatrix} 0 & 0 \\ 0 & v_R \end{pmatrix} \\ \downarrow \\ SU(2)_L \times U(1)_Y \\ \downarrow \\ \langle \phi \rangle = \begin{pmatrix} \kappa & 0 \\ 0 & \kappa' \end{pmatrix}, \quad M_\nu = \begin{pmatrix} 0 & \frac{1}{2} Y_\ell \kappa \\ \frac{1}{2} Y_\ell \kappa & F v_R \end{pmatrix} \\ \downarrow \\ U(1)_{\rm em}. \end{array} \tag{4.27}$$

The corresponding neutrino mass eigenstates and masses are

$$\begin{array}{ll} \nu = \nu_L \cos\xi + \nu_R \sin\xi, & m_\nu \simeq Y_\ell^2 \kappa^2 / 2 F v_R \\ N = -\nu_L \sin\xi + \nu_R \cos\xi, & m_N \simeq 2 F v_R, \end{array}$$

where $\tan\xi = (m_\nu / m_N)^{1/2}$. It can easily be seen that for $v_R \to \infty$, we get vanishing neutrino masses: $m_\nu \to 0$. We can parametrize the neutrino masses in terms of m_e and m_{W_R} as $m_\nu \simeq (r^2/\beta)(m_e^2/m_{W_R})$ and $m_N \simeq \beta m_{W_R}$, where r and β are free dimensionless parameters.

4.2 Extra Dimensions

The other idea that, as argued in the introduction, might be useful for a realistic implementation of Dirac leptogenesis are extra dimensions. We will therefore briefly review here the basic ideas and notions of extra dimensions, following closely the review article in Ref. [103] (for other reviews on extra dimensions see, *e.g.*, Refs. [104, 105]).

The first context in which the idea of extra dimensions occurred was the attempt to unify gravity and gauge interactions. Kaluza [106] and Klein [107] noticed that a unified theory of gravity and electromagnetism could be beautifully formulated by embedding our four–dimensional (4D) world into an extra dimensional space that has been compactified. However, the Kaluza–Klein (KK) scenario was based on a classical understanding of gravity. It was recognized half a century later that extra dimensions also offer an approach to a quantization of gravitational interactions. String theory, which is regarded as the most promising scenario for a theory of quantum gravity, can only be formulated consistently with six or seven extra spatial dimensions. Motivated by string theory, there are also a number of more phenomenological applications of

extra dimensions. The most important examples include the large extra dimensions scenario of Arkani-Hamed, Dimopoulos, and Dvali (ADD) [108–110], which describes the case of flat extra dimensions, and the Randall-Sundrum model [111, 112], formulated in warped extra dimensions. The benefit of these scenarios, in the first place, is an alleviation of the hierarchy problem. Other models with extra dimensions can offer a new approach to GUT model building [113–115], provide candidates for dark matter [116–118], or new mechanisms of EWSB [119–124].

4.2.1 Kaluza-Klein States

In the KK approach, extra dimensions are compactified to a small size R, which accounts the fact that we have not observed extra dimensions in Nature yet. The compactification of extra dimensions has interesting physical implications, which become observable at energy scales comparable to $1/R$.

The compactification of an extra space dimension can be simply illustrated, by considering a five–dimensional (5D) hypercylindrical spacetime as shown in Fig. 4.1, where the fifth dimension is compactified on a circle S^1. The extra dimension is parametrized as $x_5 = \varphi R$, where R is the radius of the circle and φ denotes the angular coordinate that runs over the range $-\pi \leq \varphi \leq \pi$.

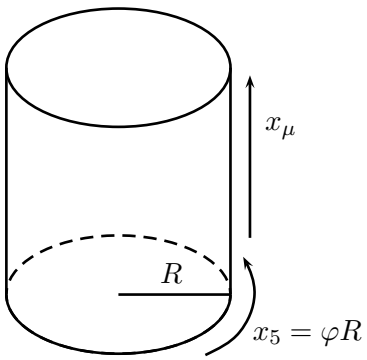

Figure 4.1: 5D hypercylindrical spacetime compactified on a circle S^1.

In the $(4 + 1)$–dimensional spacetime, we use for the metric tensor the convention $g = \mathrm{diag}(-1, +1, +1, +1, +1, +1)$. For a real scalar field $\Phi(x_\mu, y)$, where $\mu = 0, 1, 2, 3$, denote the usual four spacetime dimensions and $y = x_5 = \varphi R$ describes the extra dimension, the Lagrangian density takes the form

$$\mathcal{L} = -\frac{1}{2}\partial_M \Phi \partial^M \Phi, \tag{4.28}$$

where $M = 0, 1, 2, 3, 5$. Due to the circle structure of the compactified extra dimension, the scalar field should be periodic with respect to $y \to y + 2\pi R$, *i.e.*,

$$\Phi(x, y) \;=\; \Phi(x, y + 2\pi R). \tag{4.29}$$

We can expand this field on the circle as

$$\Phi(x, y) \;=\; \sum_{n=-\infty}^{+\infty} \phi_n(x)\, e^{\mathrm{i}ny/R}, \tag{4.30}$$

where $\phi_n^*(x) = \phi_{-n}(x)$. Using this expansion, we can rewrite the Lagrangian density in Eq. (4.28) as

$$\mathcal{L} = -\frac{1}{2} \sum_{n,m=-\infty}^{+\infty} \Big(\partial_\mu \phi_n \partial^\mu \phi_m - \frac{nm}{R^2} \phi_n \phi_m \Big) e^{i(n+m)y/R}, \tag{4.31}$$

Integrating with respect to y, the action becomes

$$\mathcal{S} = \int d^4x \int_0^{2\pi R} dy \mathcal{L} = -\frac{2\pi R}{2} \int d^4x \sum_{n=-\infty}^{+\infty} \Big(\partial_\mu \phi_n \partial^\mu \phi_n^* + \frac{n^2}{R^2} \phi_n \phi_n^* \Big). \tag{4.32}$$

This equation contains an infinite number of 4D fields $\phi_n(x)$. We can introduce the shorthand notation

$$\varphi_n = \sqrt{2\pi R} \phi_n. \tag{4.33}$$

and rewrite the action in the form

$$\mathcal{S} = \int d^4x \Big(-\frac{1}{2} \partial_\mu \varphi_0 \partial^\mu \varphi_0 \Big) - \int d^4x \sum_{k=1}^{+\infty} \Big(\partial_\mu \phi_k \partial^\mu \phi_k^* + \frac{k^2}{R^2} \phi_k \phi_k^* \Big). \tag{4.34}$$

As we can see in Fig. 4.2, the compactification of the extra dimension has led to an infinite spectrum of massive states, the so–called KK modes. In this case, the KK modes consist of a single real massless scalar field, *i.e.*, the zero-mode φ_0, and an infinite number of massive complex scalar fields with mass–squares $m_k^2 = k^2/R^2$ (see Fig. 4.2). In the low–energy limit, *i.e.*, for $E \ll 1/R$, only the zero mode is significant, while for higher energies $E \gtrsim 1/R$, all the KK modes become important.

Considering Abelian gauge fields $A_M(x_\mu, y)$ in a 5D spacetime, we also have to take the local gauge invariance into account. The Lagrangian density is in this case

$$\mathcal{L} = -\frac{1}{4g_5^2} F_{MN} F^{MN}, \tag{4.35}$$

where the Abelian gauge fields A_M have mass dimension $+1$, while the coupling constant g_5 has mass dimension -1. For the same type of compactification as before,

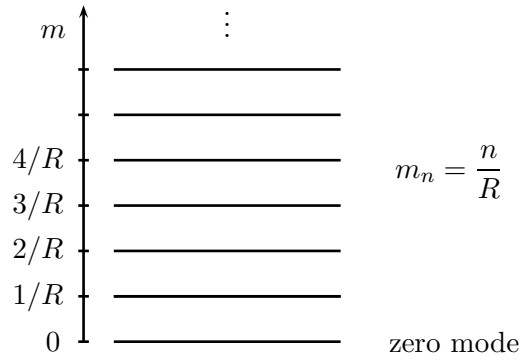

Figure 4.2: 4D KK spectrum of a 5D scalar.

we can decompose the field strength tensors as $F_{MN}^2 = F_{\mu\nu}^2 + 2(\partial_\mu A_5 - \partial_5 A_\mu)^2$, and expand the fields A_μ and A_5 on the circle as

$$A_\mu(x,y) = \sum_{n=-\infty}^{+\infty} A_\mu^{(n)}(x)\, e^{iny/R} \quad \text{and} \quad A_5(x,y) = \sum_{n=-\infty}^{+\infty} A_5^{(n)}(x)\, e^{iny/R}. \tag{4.36}$$

As in the scalar example, the effective 4D action can be calculated by integration with respect to y:

$$\mathcal{S} = \int d^4x \int_0^{2\pi R} dy\, \mathcal{L}, \tag{4.37}$$

where we can write the effective 4D Lagrangian by using a gauge transformation as

$$\int_0^{2\pi R} dy\mathcal{L} = -\frac{1}{4g_4^2}\Big[F_{\mu\nu}^{(0)}F^{(0)\mu\nu} + 2\sum_{k=1}^{+\infty}\Big(F_{\mu\nu}^{(k)}F^{*(k)\mu\nu} + \frac{2k^2}{R^2}A_\mu^{(k)}A^{*(k)\mu}\Big) + 2(\partial_\mu A_5^{(0)})^2\Big]. \tag{4.38}$$

Therefore, we can see that the effective 4D spectrum for Abelian gauge fields consists of a massless zero-mode gauge field $A_\mu^{(0)}$ with the gauge coupling $g_4^2 = g_5^2/(2\pi R)$, an infinite number of massive KK gauge bosons with masses $m_k^2 = k^2/R^2$, and a massless scalar field $A_5^{(0)}$.

Let us have a closer look at the 5D local gauge transformations $A_M(x_\mu, y) \to A_M(x_\mu, y) + \partial_m \alpha(x_\mu, y)$. The compactification of the fifth dimension leads to an infinite number of 4D gauge transformations, *i.e.*, one for each KK mode: $A_\mu^{(n)}(x_\mu) \to A_\mu^{(n)}(x_\mu) + \partial_\mu \alpha^{(n)}(x)$ $(n = 0, 1, 2, \ldots, \infty)$. However, only the zero-mode is a massless gauge field, while all the higher KK modes are massive. We can interpret this in terms of the Higgs mechanism which takes place at each massive KK level: For every KK mode, a massless gauge field "eats" one massless scalar $A_5^{(n)}$ $(n > 0)$ and consequently becomes a massive gauge field with 3 physical degrees of freedom. At the level of zero modes, we find a 4D massless gauge field with 2 physical degrees of freedom plus one real massless scalar $A_5^{(0)}$ which could perhaps serve as the SM Higgs.

4.2.2 Effect of the Bulk Volume

Let us now consider two important implications of integrating out extra dimensions: the possibility of lowering the fundamental Planck scale and the suppression of Yukawa couplings by the bulk volume. For this purpose, let us, in generalization of Sec. 4.2.1, assume a number of δ flat extra spatial dimensions with common compactification radius R. We denote the δ coordinates of the extra dimensions by $y_i \in [0, \pi R]$, where $i = 1, \ldots, \delta$ labels the ith extra dimension. Generalizing the Gauss law for gravity to δ extra dimensions, one arrives at the famous relation

$$M_{\rm Pl}^2 = M_*^{2+\delta} R^\delta = M_*^2 (M_* R)^\delta = M_*^2 N, \tag{4.39}$$

between the usual 4D Planck scale $M_{\rm Pl} \simeq 10^{18}\,\text{GeV}$ and the δ–dimensional fundamental Planck scale M_*. In Eq. (4.39), N is the total number of KK modes in all δ extra dimensions. Solving for M_*, we thus find that the fundamental scale is lowered by the bulk volume to the value

$$M_* = \left(\frac{M_{\rm Pl}^2}{R^\delta} \right)^{1/(2+\delta)} \leq M_{\rm Pl}. \tag{4.40}$$

For large (sub–mm) extra dimensions, M_* could be as small as several TeV [108–110]. Note that for fixed M_*, the number of KK modes N is independent of δ, but the mass of the first excitation becomes

$$N = (M_* R)^\delta \Rightarrow R^{-1} = M_* N^{-1/\delta}. \tag{4.41}$$

Tab. 4.1 shows the masses of the first KK modes as a function of δ for $N \simeq 10^{14}$ KK modes.

number of extra dimensions	mass of the first KK mode
$\delta = 1$	1 MeV
$\delta = 2$	10^4 GeV
$\delta = 3$	10^6 GeV
$\delta = 4$	10^7 GeV
$\delta = 5$	10^8 GeV
$\delta = 6$	10^8 GeV

Table 4.1: Masses of the first KK modes increasing with the number δ of flat extra dimensions for a fixed number of $N \simeq 10^{14}$ KK modes. Note the large jump by 7 orders of magnitude when going from $\delta = 1$ to $\delta = 2$.

Next, we will assume LH and RH fermions ψ_L and ψ_R that are localized as 4D fields at the origin $y_1 = y_2 = \cdots = y_\delta = 0$. The fermions couple to a scalar X which

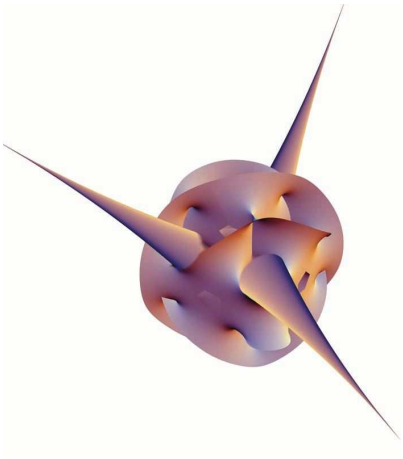

Figure 4.3: Generic Calabi-Yau manifold with three throats (taken from Ref. [125]).

propagates in the bulk of the δ extra dimensions. Now, we want to estimate the volume suppression of the Yukawa couplings to the scalar. On dimensional grounds, we can see that the Yukawa interactions are of the type

$$\overset{4+\delta}{\mathcal{L}_Y} \supset (\sqrt{\overset{-\frac{\delta}{2}}{M_*}})^{-\delta} \prod_{i=1}^{\delta} \overset{1}{\delta}(y_i) Y \overset{\frac{3}{2}}{\overline{\psi}_L} \overset{\frac{2+\delta}{2}}{X} \overset{\frac{3}{2}}{\psi_R}, \tag{4.42}$$

where Y are the Yukawa couplings and the numbers above the different terms indicate the mass dimensions. The spin–$\frac{1}{2}$ fields have mass dimension $(\delta-1)/2$, while spin–1 fields have mass dimension $(\delta-2)/2$. It is obvious that in the case of δ extra dimensions a factor of $(\sqrt{M_*})^{-\delta}$ has to be multiplied in order to keep the correct overall dimension: $\delta+4+\delta/2-\delta/2 = 4+\delta$. This factor represents a volume suppression of the Yukawa couplings. Taking the wave–function normalization factor $(\sqrt{R})^{-\delta}$ of X into account, we get the following overall suppression of the Yukawa couplings:

$$\frac{Y}{(\sqrt{M_* R})^{\delta}} = \frac{Y}{\sqrt{N}}. \tag{4.43}$$

For $N \simeq 10^{14}$ the Yukawa couplings are suppressed by a factor of 10^{-7}. Again, for large extra dimensions, Y could be suppressed by a factor as small as $\sim 10^{-12}$ [49].

4.2.3 Calabi-Yau Manifolds and Throats

The most conventional superstring models consider ten dimensions out of which six have been compactified. If the six–dimensional manifold is an Calabi-Yau manifold, $N = 1$ supersymmetry in four dimensions remains unbroken after compactification [126]. A generic type of geometry arising from so–called flux compactifications[1] is a

[1] A flux can in this context be understood as a generalization of an electromagnetic field strength.

Calabi-Yau manifold with multiple throats hanging out from it [28–30] (*cf.* Fig. 4.3). The throats are strongly warped regions in spacetime that arise from stacks of so–called branes (solitonic solutions of supergravity) transverse to the compactification manifold. This can be seen as follows: The tension (energy density) of a brane curves the space around it, and the back reaction is proportional to the total number of branes in a certain region of space. A large stack of branes can therefore alter the metric on a compactified manifold and create throats with a warped geometry. In such a configuration, the degrees of freedom localized at the end of a throat can be seen to be dual to the infrared (IR) excitations of the low–energy field theory, while the excitations near the mouth of the throat are dual to the ultraviolet (UV) degrees of freedom (*cf.* AdS/CFT correspondence).

Geometries with multiple throats could offer a number of advantages for model building, such as a relatively simple implementation of multiple scales, a straightforward way to separate fields, and the generation of small numbers, even in the flat limit [125, 127, 128]. In Chapter 7, we will make use of these possibilities and consider a model for Dirac leptogenesis with three 5D throats in the flat limit.

Chapter 5

Heavy Scalar Decay

In this Chapter, we analyze the generation of a lepton asymmetry by the CP–violating decays of heavy $SU(2)_L$ scalars into LH lepton doublets and RH neutrinos.

5.1 CP–Violation

CP–violation can occur when there are complex couplings in a theory. Let us therefore consider the following Yukawa couplings for leptons

$$\begin{aligned}\mathcal{L}_{Y_\nu}^{(n)} &= Y_{\nu_1}\overline{\psi}_L\phi^{(n)}\nu_R + Y_{\nu_2}\overline{\psi}_L\xi^{(n)}\nu_R \\ &+ Y_{e_1}\overline{\psi}_L\phi^{c(n)}e_R + Y_{e_2}\overline{\psi}_L\xi^{c(n)}e_R + \text{h.c.},\end{aligned} \tag{5.1}$$

where $X^{c(n)} = \mathrm{i}\sigma_2 X^{*(n)}$ for $X^{(n)} = \phi^{(n)}, \xi^{(n)}$. These doublets $X^{(n)} = (X_1^{0(n)}, X_2^{-(n)})^T$ have the masses $M_n(X)$. The superscript (n) will become important later on in Chapters 6, 7, and 8, when we identify them with KK in a higher–dimensional scenario. In Sakharov's three conditions for the generation of baryon asymmetry, the presence of a CP–violating process is the second indispensable ingredient (see Chapter 3). For this purpose, we will turn our discussion to the decay of heavy scalars and assume that the baryon asymmetry is generated via Dirac leptogenesis [27,76,129,130] by the decay of the scalar doublets $\phi^{(n)}$ and $\xi^{c(n)}$ (*cf.* Fig. 5.1). Consequently, the leptonic CP–violating decay channels are of the form

$$\overline{X}^{(n)} \to \overline{\psi}_L + \nu_R \quad \text{and} \quad X^{(n)} \to \overline{\psi}_L + e_R. \tag{5.2}$$

In more detail, the decay of the heavy scalars into LH leptons ψ_L and RH neutrinos ν_R, as shown in Fig. 5.2, consists of the decay channels

$$\begin{aligned}\overline{\phi}^{(n)} \to \overline{\psi}_L + \nu_R \;&:\quad \phi_1^{0*(n)} \to \overline{\nu}_L + \nu_R, \quad \phi_2^{+(n)} \to \overline{e}_L + \nu_R, \\ \overline{\chi}^{(n)} \to \overline{\psi}_L + \nu_R \;&:\quad \chi_1^{0*(n)} \to \overline{\nu}_L + \nu_R, \quad \chi_2^{+(n)} \to \overline{e}_L + \nu_R,\end{aligned} \tag{5.3}$$

The decays into LH leptons ψ_L and RH charged leptons e_R read

$$\begin{aligned}\phi^{(n)} \to \overline{\psi}_L + e_R \;&:\quad \phi_1^{0(n)} \to \overline{e}_L + e_R, \quad \phi_2^{-(n)} \to \overline{\nu}_L + e_R, \\ \chi^{(n)} \to \overline{\psi}_L + e_R \;&:\quad \chi_1^{0(n)} \to \overline{e}_L + e_R, \quad \chi_2^{-(n)} \to \overline{\nu}_L + e_R.\end{aligned} \tag{5.4}$$

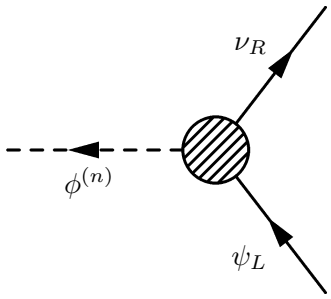

Figure 5.1: Decay of a heavy bulk scalar $\phi^{(n)}$ into leptons with possible one–loop–corrections indicated by the blob.

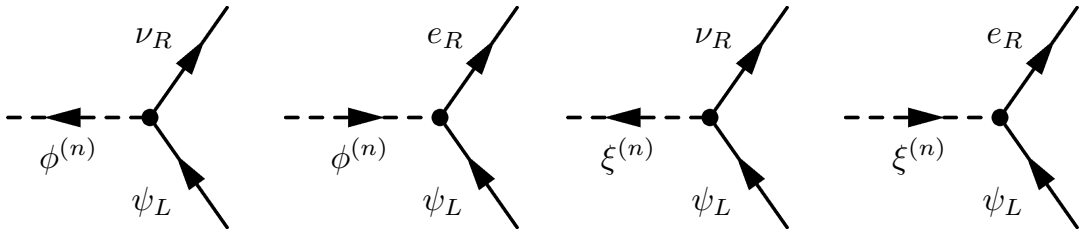

Figure 5.2: Tree–level decays of the heavy scalars $\phi^{(n)}$ and $\xi^{(n)}$.

Similar equations hold for the scalar decays into quarks. Notice that all these decays can be CP–violating due to loop effects as we will show later in this Chapter. However, they do not change the baryon number B or lepton number L, since the overall difference between of the number of particles and antiparticles in the lepton as well as in the quark sector remains unchanged. In this case, CP–violation can only lead to a number–difference of particles and antiparticles between the LH and the RH sector. When we are talking about an asymmetry in the following, we mean this matter–antimatter asymmetry between LH and RH particles.

We are interested in the physical decay asymmetries $\varepsilon_X^{(n)}$ arising from the decays of the scalars $\phi^{(n)}$ and $\xi^{(n)}$. Let us define the quantity ε_X as the net ratio of particles which is generated when a certain number density n_X of particles X and a corresponding number density $n_{\overline{X}}$ of antiparticles $\overline{X}$ decay. As long as X and $\overline{X}$ are in thermal equilibrium, decays and inverse decays will cancel out each other. However, when a critical temperature $T = M(X)$ is reached, where the particles drop out of thermal equilibrium, a net number density n_Y of the decay products Y can survive, *i.e.*,

$$n_Y = \varepsilon_X n_X \quad \text{for} \quad n_X = n_{\overline{X}}. \tag{5.5}$$

The interesting number in the context of this thesis is the net number of weakly coupled RH particles, since every asymmetry produced by strongly coupled particles

would most likely be washed out by inverse decays. Thus, we write ε_X as the sum of the differences of decay widths for decays in which RH particles are produced, divided by the sum over decay widths of all possible weakly coupled decays which change the net number density of X and $\overline{X}$:

$$\varepsilon_X = \frac{\sum_{b_R}[\Gamma(X \to \overline{a}_L b_R) - \Gamma(\overline{X} \to a_L \overline{b}_R)]}{\sum_c \sum_d [\Gamma(X \to \overline{c} d) + \Gamma(\overline{X} \to c\overline{d})]}, \tag{5.6}$$

where Γ denotes the decay width, and a_L are all the possible LH particle states which can be produced together with the RH states b_R by the decay of X and $\overline{X}$. On the other hand, c and d denote every possible state including a_L and b_R. The form of the denominator is due to the fact that all the different decay channels are competing with each other. The decay width for the decay of one initial particle into f final states is defined by

$$\Gamma = \frac{1}{2M_i}\Big(\int \prod_f \frac{d^3 p_f}{(2\pi)^3} \frac{1}{2E_f} \Big) |\mathcal{M}(M_i \to p_f)|^2 (2\pi)^4 \delta^{(4)}(p_i - \sum_f p_f), \tag{5.7}$$

where M_i and p_i are the mass and momentum of the initial particle, while E_f and p_f are the energy and momentum of the final particle f. We are only considering weakly coupled decay processes, since strongly coupled processes are longer in equilibrium and thus do not change the net number density of X and $\overline{X}$ at that time. The CP–violating contribution for a certain RH species, for example ν_R, is given by

$$\varepsilon^{(n)}_{X_1,\nu_R} = \frac{\Gamma(X_1^{(n)} \to \overline{\psi}_L \nu_R) - \Gamma(\overline{X}_1^{(n)} \to \psi_L \overline{\nu}_R)}{\Gamma^{(n)}_{X_1} + \Gamma^{(n)}_{\overline{X}_1}}. \tag{5.8}$$

Here, $\Gamma^{(n)}_{X_1}$ denotes the total decay width of the particle $X_1^{(n)}$, *i.e.*, the sum of all possible decay channels

$$\Gamma^{(n)}_{X_1} = \Gamma^{(n)}(X_1^{(n)} \to \overline{\psi}_L \nu_R) + \Gamma^{(n)}(X_1^{(n)} \to \overline{\psi}_L e_R) \tag{5.9}$$

and $\Gamma^{(n)}_{\overline{X}_1}$ is defined in an analogous way. The decay width (*cf.* Appendix A)

$$\Gamma^{(n)} = \Gamma^{(n)}(X_1^{(n)} \to \overline{\psi}_L \nu_R) = \frac{1}{16\pi M_n(X_1)} |\mathcal{M}_{X_1^{(n)} \to \overline{\psi}_L \nu_R}|^2, \tag{5.10}$$

includes the sum over all internal degrees of freedom, *i.e.*, spins and isospins. Thus, in a bath which contains an equal number of particles X_1 and antiparticles $\overline{X}_1$ the net amount of RH neutrinos produced by CP–violating decays will be

$$n_{\nu_R} = \sum_{n=0}^{n_{\max}} \varepsilon^{(n)}_{X_1,\nu_R} n^{(n)}_{X_1}. \tag{5.11}$$

Let us in the following discussion concentrate on the asymmetry of the RH neutrinos. The asymmetries for all the other RH particles can be calculated and analyzed in exactly the same way. All we have to do is to replace correspondingly the Yukawa couplings and multiply by a factor of three for quarks.

5.2 Generation of CP–Asymmetry

After having defined the notation, let us now have a closer look at how a CP–asymmetry can be generated by the scalar decays. First, notice that in a tree–level approximation, no CP–violation can be generated. The decay amplitudes for particles and antiparticles in the tree–level approximation are

$$\begin{aligned} \mathrm{i}\mathcal{M}_{\overline{X}_1^{(n)}\to\overline{\psi}_{iL}\nu_{jR}} &= \mathrm{i}(Y_{\nu_1})^*_{ij}\bar{u}(p)P_R v(q), \qquad (5.12)\\ \mathrm{i}\mathcal{M}_{X_1^{(n)}\to\psi_{iL}\overline{\nu}_{jR}} &= \mathrm{i}(Y_{\nu_1})_{ij}\bar{u}(q)P_L v(p)\\ &= \mathrm{i}(Y_{\nu_1})_{ij}v^T(q)\gamma^0 C^{-1}\gamma^0 P_L C^{-1}C\gamma^0 C^{-1}u^*(p)\\ &= \mathrm{i}(Y_{\nu_1})_{ij}(\bar{u}(p)P_L v(q))^T = \mathrm{i}(Y_{\nu_1})_{ij}\bar{u}(p)P_L v(q), \qquad (5.13)\end{aligned}$$

where i and j are flavor indices, *i.e.*, $e_{1R}=e_R$, $e_{2R}=\mu_R$, $e_{3R}=\tau_R$, *etc.* Here, we have made use of the identities

$$u(p) = C\bar{v}^T, \quad C^{-1}\gamma^\mu C = -(\gamma^\mu)^T. \qquad (5.14)$$

At this accuracy, the absolute value squares of the spin-summed amplitudes are identical:

$$\begin{aligned}\Sigma_{Tij} &= \sum_{\text{spins}}|\mathcal{M}_{\overline{X}_1^{(n)}\to\overline{\psi}_{iL}\nu_{jR}}|^2 = \sum_{\text{spins}}|\mathcal{M}_{X_1^{(n)}\to\psi_{iL}\overline{\nu_1}_{jR}}|^2 = \sum_{\text{spins}}|\bar{u}(p)\mathrm{i}(Y_{\nu_1})^*_{ij}P_R v(q)|^2\\ &= (Y_{\nu_1})^*_{ij}(Y_{\nu_1})_{ij}Tr\Big[\frac{1}{2}(1+\gamma^5)\not{q}\not{p}\Big] = |(Y_{\nu_1})_{ij}|^2 M_n^2(X_1), \qquad (5.15)\end{aligned}$$

i.e., complex phases are irrelevant at tree–level. Summing over all flavors, we get

$$\Sigma_T = \sum_{ij}\Sigma_{Tij} = \mathrm{tr}(Y^\dagger_{\nu_1}Y_{\nu_1})M_n^2(X_1), \qquad (5.16)$$

since $\sum_{ij}^n A^*_{ji}B_{ji} = \sum_{ij}^n A^\dagger_{ij}B_{ji} = \sum_i^n (A^\dagger B)_{ii} = \mathrm{tr}(A^\dagger B)$, where A and B are general complex $n\times n$ matrices. For two diagonal matrices A^{diag} and B^{diag} this formula simplifies to $\sum_{ij}^n A^{\mathrm{diag}*}_{ji}B^{\mathrm{diag}}_{ji} = \mathrm{tr}(A^{\mathrm{diag}*}B^{\mathrm{diag}})$. In the case of just one Yukawa coupling matrix, this might allways be possible. However, since we are considering more than one general Yukawa coupling matrix, and as we will see later on, even products of these matrices, we can in general not assume that A and B are diagonal. The amplitudes for the decay channels of $\phi^{(n)}$ and $\overline{\phi}^{(n)}$ are given by

$$\begin{aligned}\sum_{ij}\sum_{\text{spins}}|\mathcal{M}_{\overline{\phi}^{(n)}\to\overline{\psi}_{iL}\nu_{jR}}|^2 &= \mathrm{tr}(Y^\dagger_{\nu_1}Y_{\nu_1})M_n^2(\phi), \qquad (5.17a)\\ \sum_{ij}\sum_{\text{spins}}|\mathcal{M}_{\overline{\phi}^{(n)}\to\overline{\psi}_{iL}e_{jR}}|^2 &= \mathrm{tr}(Y^\dagger_{e_1}Y_{e_1})M_n^2(\phi). \qquad (5.17b)\end{aligned}$$

The remaining decays of ξ and $\overline{\xi}$ can be treated similarly, all we have to do is to correspondingly replace the Yukawa coupling matrices and the squared masses of the decaying scalars. The sum of the decay widths in tree approximation is

$$\Gamma_T^{(n)}(\overline{X}_1^{(n)} \to \overline{\psi}_L \nu_R) + \Gamma_T^{(n)}(X_1^{(n)} \to \psi_L \overline{\nu}_R) = \frac{\mathrm{tr}(Y_{\nu_1}^\dagger Y_{\nu_1})}{4\pi} M_n(X_1). \tag{5.18}$$

We have thus to go to the next order and calculate the interference between the tree–level amplitude and the one–loop corrections for the numerator in Eq. (5.8). At one–loop level, we have to consider vertex–corrections as well as wave–function corrections.

At this accuracy, an imaginary part can arise as a consequence of unitarity of the S-matrix, *i.e.*, $S^\dagger S = \mathbb{1}$. With $S = \mathbb{1} + \mathrm{i}T$, we get $-\mathrm{i}(T - T^\dagger) = T^\dagger T$. In terms of the amplitudes, this expression becomes

$$-\mathrm{i}(\mathcal{M}_{p_i \to p_f} - \mathcal{M}^*_{p_f \to p_i}) = \sum_a d\Pi_a \mathcal{M}_{p_i \to p_a} \mathcal{M}^*_{p_f \to p_a}, \tag{5.19}$$

where the sum over a indicates the summation over all possible on–shell intermediate states and $d\Pi_a$ is the Lorentz–invariant phase–space measure. For $\mathcal{M}^*_{p_f \to p_i} = \mathcal{M}^*_{p_i \to p_f}$, we can rewrite Eq. (5.19) in terms of the optical theorem as

$$\mathcal{M}_{p_i \to p_f} - \mathcal{M}^*_{p_f \to p_i} = 2\mathrm{i}\mathrm{Im}\,(\mathcal{M}_{p_i \to p_f}), \tag{5.20}$$

i.e., the imaginary part of the forward scattering amplitude is proportional to the total cross section. Therefore, the right–hand–side in Eq. (5.20) implies that an imaginary part develops if intermediate states can go on–shell. This is always true as long as the decaying particle is heavier than the intermediate states or the decays take place at sufficiently high energies.

5.3 One–loop Corrections

Let us analyze the one–loop level diagrams, which are generating the CP–asymmetry. There are two types of diagrams. A CP–asymmetry ε^v can arise from vertex–corrections [56] and another CP–asymmetry ε^w is generated by wave–function corrections [131]. The total asymmetry ε is hence given by the sum $\varepsilon = \varepsilon^v + \varepsilon^w$ of vertex– and wave–function corrections.

The interference amplitude of the tree–level with the vertex–correction as, shown in Fig. 5.3, can be written as

$$\mathrm{i}\mathcal{M}_{ij}^{\varepsilon^v} = \mathrm{i}\Big[(Y_{\nu_1})^*_{ij} \mathcal{T}_{ij} + (Y_{\nu_2}^\dagger Y_{e_1} Y_{e_2}^\dagger)_{ji} \mathcal{V}_{ij}\Big], \tag{5.21}$$

where the function $\mathcal{T}$ denotes the tree–level amplitude

$$\mathcal{T} = \bar{u}(p) P_R v(q) \tag{5.22}$$

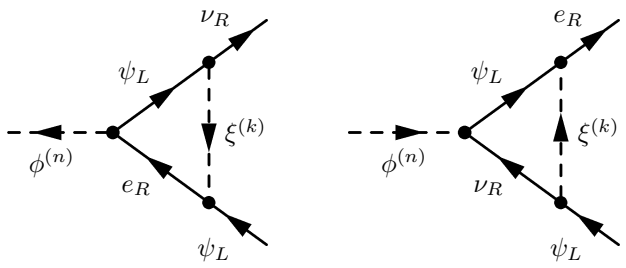

Figure 5.3: Vertex-corrections for the decays of $\phi^{(n)}$. The diagrams for $\xi^{(n)}$ can be obtained by exchanging the scalar fields.

and $\mathcal{V}$ is the amplitude of the vertex–correction:

$$\begin{aligned}\mathcal{V} &= \mathrm{i}\bar{u}(p)\int\frac{d^4k'}{(2\pi)^4}P_R\frac{\not{p}'}{p'^2+\mathrm{i}\varepsilon}P_L\frac{\not{q}'}{q'^2+\mathrm{i}\varepsilon}P_R\frac{1}{k'^2-M_n(X_2)+\mathrm{i}\varepsilon}v(q)\\ &= \mathrm{Re}(\mathcal{V})+\mathrm{i}\,\mathrm{Im}(\mathcal{V}).\end{aligned} \tag{5.23}$$

Furthermore, in writing the product of the Yukawa coupling matrices, we have used the identity

$$(A^\dagger BC^\dagger)_{ij}=\sum_{l=1}^{n}(A^\dagger B)_{il}C^*_{jl}=\sum_{k=1}^{n}\sum_{l=1}^{n}A^*_{ki}B_{kl}C^*_{jl}, \tag{5.24}$$

where A, B, and C, are general complex $n\times n$ matrices. In the limit of massless leptonic states, *i.e.*, for $M_n(X_1)\gg m_{\psi_L},m_{\nu_R}$, the amplitudes $\mathcal{T}$ and $\mathcal{V}$ are flavor–independent.
The creation of a rate asymmetry can be calculated in the following way:

$$\mathcal{M}^{\varepsilon^v}_{\overline{X}_1^{(n)}\to\overline{\psi}_{iL}\nu_{jR}} = ((Y_{\nu_1})^*_{ij}\mathcal{T}+\hat{Y}^*_{ji}\mathcal{V}), \tag{5.25}$$

$$\mathcal{M}^{\varepsilon^v}_{X_1^{(n)}\to\psi_{iL}\overline{\nu}_{jR}} = ((Y_{\nu_1})_{ij}\mathcal{T}+\hat{Y}_{ji}\mathcal{V}), \tag{5.26}$$

where $\hat{Y}=(Y^T_{\nu_2}Y_{e_1}{}^*Y^T_{e_2})_{ji}$. The difference between the decay probabilities of particles $\overline{X}_1^{(n)}$ and antiparticles $X_1^{(n)}$ is then

$$\begin{aligned}&|\mathcal{M}^{\varepsilon^v}_{\overline{X}_1^{(n)}\to\overline{\psi}_{iL}\nu_{jR}}|^2-|\mathcal{M}^{\varepsilon^v}_{X_1^{(n)}\to\psi_{iL}\overline{\nu}_{jR}}|^2\\ =\;&((Y_{\nu_1})_{ij}\mathcal{T}^*+\hat{Y}_{ji}\mathcal{V}^*)((Y_{\nu_1})^*_{ij}\mathcal{T}+\hat{Y}^*_{ji}\mathcal{V})-((Y_{\nu_1})^*_{ij}\mathcal{T}^*+\hat{Y}^*_{ji}\mathcal{V}^*)((Y_{\nu_1})_{ij}\mathcal{T}+\hat{Y}_{ji}\mathcal{V})\\ =\;&((Y_{\nu_1})_{ij}\hat{Y}^*_{ji}\mathcal{T}^*\mathcal{V}+\hat{Y}_{ji}(Y_{\nu_1})^*_{ij}\mathcal{T}\mathcal{V}^*-(Y_{\nu_1})^*_{ij}\hat{Y}_{ji}\mathcal{T}^*\mathcal{V}-\hat{Y}^*_{ji}(Y_{\nu_1})_{ij}\mathcal{T}\mathcal{V}^*)\\ =\;&[((Y_{\nu_1})_{ij}\hat{Y}^*_{ji}-(Y_{\nu_1})^*_{ij}\hat{Y}_{ji})\mathcal{T}^*\mathcal{V}-(\hat{Y}^*_{ji}(Y_{\nu_1})_{ij}-\hat{Y}_{ji}(Y_{\nu_1})^*_{ij})\mathcal{T}\mathcal{V}^*]\\ =\;&2\mathrm{i}((Y_{\nu_1})_{ij}\hat{Y}^*_{ji}-(Y_{\nu_1})^*_{ij}\hat{Y}_{ji})\mathrm{Im}(\mathcal{T}^*\mathcal{V})=-4\,\mathrm{Im}\,((Y_{\nu_1})_{ij}\hat{Y}^*_{ji})\mathrm{Im}(\mathcal{T}^*\mathcal{V})\\ =\;&-4\,\mathrm{Im}\left[(Y_{\nu_1})_{ij}(Y^\dagger_{\nu_2}Y_{e_1}Y_{e_2}{}^\dagger)_{ji}\right]\mathrm{Im}(\mathcal{T}^*\mathcal{V}).\end{aligned} \tag{5.27}$$

Taking all flavors into account, we get

$$|\mathcal{M}^{\varepsilon^v}_{\overline{X}_1^{(n)}\to\overline{\psi}_L\nu_R}|^2 - |\mathcal{M}^{\varepsilon^v}_{X_1^{(n)}\to\psi_L\overline{\nu}_R}|^2 = \sum_{ij}^{3} |\mathcal{M}^{\varepsilon^v}_{\overline{X}_1^{(n)}\to\overline{\psi}_{iL}\nu_{jR}}|^2 - |\mathcal{M}^{\varepsilon^v}_{X_1^{(n)}\to\psi_{iL}\overline{\nu}_{jR}}|^2$$
$$= -4\,\mathrm{Im}\,\mathrm{tr}(Y_{\nu_1}Y^\dagger_{\nu_2}Y_{e_1}Y^\dagger_{e_2})\mathrm{Im}(\mathcal{T}^*\mathcal{V}). \qquad (5.28)$$

As we can now easily see, if $\mathrm{tr}(Y_{\nu_1}Y^\dagger_{\nu_2}Y_{e_1}Y^\dagger_{e_2})$ contains a phase, this phase will result in an asymmetry. The sum of decay probabilities is, on the other hand, given by

$$|\mathcal{M}^{\varepsilon^v}_{X_1^{(n)}\to\overline{\psi}_L\nu_R}|^2 + |\mathcal{M}^{\varepsilon^v}_{\overline{X}_1^{(n)}\to\psi_L\overline{\nu}_R}|^2 = 2\,\mathrm{tr}(Y^\dagger_{\nu_1}Y_{\nu_1})|\mathcal{T}|^2 + 2\,\mathrm{tr}(\hat{Y}^\dagger\hat{Y})|\mathcal{V}|^2$$
$$+ \; 4\mathrm{Re}\,\mathrm{tr}(Y_{\nu_1}Y^\dagger_{\nu_2}Y_{e_1}Y^\dagger_{e_2})\mathrm{Re}(\mathcal{T}^*\mathcal{V}). \qquad (5.29)$$

Since the Yukawa couplings are all very small, *i.e.*, $Y_{\nu_i}, Y_{e_i} \ll 1$, we can safely neglect in Eq. (5.29) factors proportional to $Y^6_{\nu_i}$ and $Y^6_{e_i}$. Furthermore, compared to the tree–level term $\mathrm{tr}(Y^\dagger_{\nu_1}Y_{\nu_1})|\mathcal{T}|^2$, we can also neglect in Eq. (5.29) the last term. Especially, if the asymmetry is maximal, we write

$$\mathrm{tr}(Y_{\nu_1}Y^\dagger_{\nu_2}Y_{e_1}Y^\dagger_{e_2}) \in \mathbb{C} \quad \Rightarrow \quad \mathrm{Re}\,\mathrm{tr}(Y_{\nu_1}Y^\dagger_{\nu_2}Y_{e_1}Y^\dagger_{e_2})\,\mathrm{Re}(\mathcal{T}^*\mathcal{V}) = 0. \qquad (5.30)$$

In total, Eq. (5.29) simplifies to

$$|\mathcal{M}^{\varepsilon^v}_{X_1^{(n)}\to\overline{\psi}_L\nu_R}|^2 + |\mathcal{M}^{\varepsilon^v}_{\overline{X}_1^{(n)}\to\psi_L\overline{\nu}_R}|^2 = 2\,\mathrm{tr}(Y^\dagger_{\nu_1}Y_{\nu_1})|\mathcal{T}|^2. \qquad (5.31)$$

The CP–violating one–loop wave–function correction diagrams for the decays of $\phi^{(n)}$ and $\xi^{(n)}$ are shown in Fig. 5.4. The interference amplitude with the wave–function

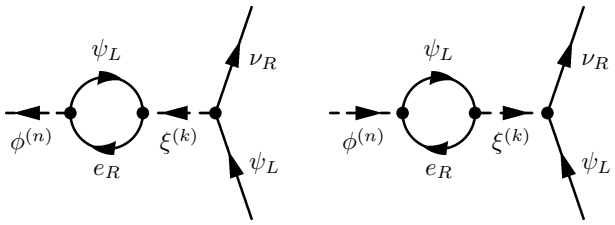

Figure 5.4: Wave–function corrections for the decays of $\phi^{(n)}$. The diagrams for $\xi^{(n)}$ can be obtained by exchanging the scalar fields.

correction is, given by

$$\mathrm{i}\mathcal{M}^{\varepsilon^w}_{ij} = \mathrm{i}\Big[(Y_{\nu_1})^*_{ij} + Y^*_{\nu_2 ij}\,\mathrm{tr}(Y^\dagger_{e_2}Y_{e_1})\mathcal{W}\Big], \qquad (5.32)$$

where, in this case, the one–loop-amplitude Π is

$$\mathcal{W} = \mathrm{i}^5\bar{u}(p)\Big[\frac{P_R}{k'^2 - M_n(X_2) + \mathrm{i}\varepsilon}\int\frac{d^4q'}{(2\pi)^4}\frac{-\mathrm{tr}(P_R\not{p}'P_L\not{q}')}{(p'^2+\mathrm{i}\varepsilon)(q'^2+\mathrm{i}\varepsilon)}\Big]v(q)$$
$$= \mathrm{Re}(\mathcal{W}) + \mathrm{i}\;\mathrm{Im}(\mathcal{W}). \qquad (5.33)$$

For the wave–function correction, the difference between the decay probabilities is

$$|\mathcal{M}^{\varepsilon^w}_{\overline{X}_1^{(n)}\to\overline{\psi}_{iL}\nu_{iR}}|^2 - |\mathcal{M}^{\varepsilon^w}_{X_1^{(n)}\to\psi_{iL}\overline{\nu}_{iR}}|^2 = -4\,\mathrm{Im}\,[(Y_{\nu_1})_{ij}Y^*_{\nu_2 ij}\,\mathrm{tr}(Y_{e_1}Y^\dagger_{e_2})]\mathrm{Im}(\mathcal{T}^*\mathcal{W}). \quad (5.34)$$

The flavor-summed difference is then

$$\begin{aligned}|\mathcal{M}^{\varepsilon^w}_{\overline{X}_1^{(n)}\to\overline{\psi}_L\nu_R}|^2 - |\mathcal{M}^{\varepsilon^w}_{X_1^{(n)}\to\psi_L\overline{\nu}_R}|^2 &= \sum_{ij}^{3} |\mathcal{M}^{\varepsilon^w}_{\overline{X}_1^{(n)}\to\overline{\psi}_{iL}\nu_{iR}}|^2 - |\mathcal{M}^{\varepsilon}_{X_1^{(n)}\to\psi_{iL}\overline{\nu}_{iR}}|^2 \\ &= -4\,\mathrm{Im}\,[\mathrm{tr}(Y_{\nu_1}Y^\dagger_{\nu_2})\,\mathrm{tr}(Y^\dagger_{e_2}Y_{e_1})]\mathrm{Im}(\mathcal{T}^*\mathcal{W}),\end{aligned} \quad (5.35)$$

while the sum can be approximated as

$$|\mathcal{M}^{\varepsilon^w}_{X_1^{(n)}\to\overline{\psi}_L\nu_R}|^2 + |\mathcal{M}^{\varepsilon^w}_{\overline{X}_1^{(n)}\to\psi_L\overline{\nu}_R}|^2 = 2\,\mathrm{tr}(Y^\dagger_{\nu_1}Y_{\nu_1})|\mathcal{T}|^2. \quad (5.36)$$

In Eq. (5.1), it can be see that $\mathrm{tr}(Y_{\nu_1}Y^\dagger_{\nu_2})\,\mathrm{tr}(Y^\dagger_{e_2}Y_{e_1}) = [\mathrm{tr}(AB^\dagger)]^2$ and $\mathrm{tr}(Y_{\nu_1}Y^\dagger_{\nu_2}Y_{e_1}Y^\dagger_{e_2}) = \mathrm{tr}[(AB^\dagger)^2]$, where A and B are general real $n\times n$ matrices. The crucial point in the trace product is that $\mathrm{tr}[(AB^\dagger)^2] \neq [\mathrm{tr}(AB^\dagger)]^2$. We can substitute $C = AB^\dagger$. Even if we rotate to the basis where all the matrices are diagonal, we find $\mathrm{tr}[(AB^*)^2] \neq [\mathrm{tr}(AB^*)]^2$, since $\mathrm{tr}[C^2] = \sum_{i=1}^3 C_{ii}^2$ while $[\mathrm{tr}\,C]^2 = \left(\sum_{i=1}^3 C_{ii}\right)^2$. The relation $\mathrm{tr}[C^2] = [\mathrm{tr}\,C]^2$ would only hold if we additionally assumed that one Yukawa coupling in the diagonal matrix dominates and the others are neglected. But this would be a quite strong restriction, so we will not assume anything like that in the following discussion.

5.3.1 Vertex Correction

We shall assume the limit where the leptons are massless compared to the mass of the decaying scalars. Focussing on the calculation of $\mathcal{V}$, we have

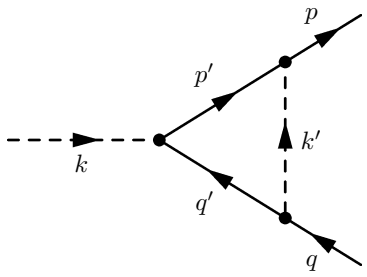

Figure 5.5: Vertex-correction for the decay of a heavy scalar with the associated momenta.

$$\mathcal{V} = \mathrm{i}\bar{u}(p)\Big[P_R\int\frac{d^4k'}{(2\pi)^4}\frac{\not{p}'}{p'^2+\mathrm{i}\varepsilon}\frac{\not{q}'}{q'^2+\mathrm{i}\varepsilon}\frac{1}{k'^2-M_k(X_2)^2+\mathrm{i}\varepsilon}\Big]v(q), \quad (5.37)$$

where conservation of momentum dictates the relations

$$p' = p + k' \quad \text{and} \quad q' = -q + k'. \tag{5.38}$$

To combine the propagator denominators, we can use an integral over Feynman parameters

$$\frac{1}{\prod_{i=1}^{n} A_i} = \int_0^1 \prod_{i=1}^{n} dx_i \delta\Big(\sum_{i=1}^{n} x_i - 1\Big) \frac{(n-1)!}{(\sum_{i=1}^{n} x_i A_i)^n}, \tag{5.39}$$

where A_i are the denominators of the contributing propagators, obtaining

$$\frac{1}{(p'^2 + \mathrm{i}\varepsilon)(q'^2 + \mathrm{i}\varepsilon)(k'^2 - M_k(X_2)^2 + \mathrm{i}\varepsilon)} = \int_0^1 dx\, dy\, dz \delta(x + y + z - 1) \frac{2}{D^3}, \tag{5.40}$$

where D is given by

$$\begin{aligned} D &= x((p+k')^2 + \mathrm{i}\varepsilon) + y((-q+k')^2 + \mathrm{i}\varepsilon) + z(k'^2 - M_k(X_2)^2 + \mathrm{i}\varepsilon) \\ &= 2xpk' - 2yqk' - zM_k(X_2)^2 + k'^2 + \mathrm{i}\varepsilon \\ &= (k' + xp - yq)^2 + xyM_n(X_1)^2 - zM_k(X_2)^2 + \mathrm{i}\varepsilon \\ &= \ell^2 - \Delta. \end{aligned} \tag{5.41}$$

Here, we have treated the final states to be on–shell and massless, *i.e.*, $p^2 = q^2 = 0$ and $(p+q)^2 = 2pq = M_n(X_1)^2$. Furthermore, we have introduced $\ell = k' + xp - yq$ and $\Delta = -xyM_n(X_1)^2 + zM_k(X_2)^2 - \mathrm{i}\varepsilon$. In order to express in Eq. (5.37) also the numerator in terms of ℓ, we can use the following identities:

$$\int \frac{d^4\ell}{(2\pi)^4} \frac{\ell^\mu}{D^3} = 0 \quad \text{and} \quad \int \frac{d^4\ell}{(2\pi)^4} \frac{\ell^\mu \ell^\nu}{D^3} = \int \frac{d^4\ell}{(2\pi)^4} \frac{\frac{1}{4} g^{\mu\nu} \ell^2}{D^3}. \tag{5.42}$$

The numerator therefore takes the form

$$\begin{aligned} \not{p}'\not{q}' &= (\not{p} + \not{\ell} - x\not{p} + y\not{q})(-\not{q} + \not{\ell} - x\not{p} + y\not{q}) \\ &= \ell^2 - \not{p}\not{q}(1 - x + y + xy) - xy\not{q}\not{p}\not{p}, \end{aligned} \tag{5.43}$$

where we have used $\not{\ell}\not{\ell} = \frac{1}{4} g^{\mu\nu} \ell^2 \gamma_\mu \gamma_\nu = \frac{1}{4} \ell^2 \gamma_\mu \gamma^\mu = \ell^2$. As a consequence, the integral becomes

$$\int_0^1 dx\, dy\, dz \delta(x + y + z - 1) \int \frac{d^4\ell}{(2\pi)^4} \frac{2(\ell^2 - \not{p}\not{q}(1 - x + y + xy) - xy\not{q}\not{p}\not{p})}{D^3}. \tag{5.44}$$

Note that the numerator is sandwiched between $\bar{u}(p) P_R$ and $v(q)$. Using the identity $\sum_{\text{all spins}} [\bar{u}(p)\Gamma_1 u(q)][\bar{u}(p)\Gamma_2 u(q)]^* = \mathrm{tr}[\Gamma_1(\not{q} + m_q)\bar{\Gamma}_2(\not{p} + m_p)]$, where Γ_1 and Γ_2 are two 4×4 matrices and $\bar{\Gamma}_2 = \gamma^0 \Gamma_2^\dagger \gamma^0$, we see that we get terms of the form

$$[\bar{u}(p) P_R v(q)]^* [\bar{u}(p) P_R v(q)] = \mathrm{tr}[\gamma^0 P_R^\dagger \gamma^0 \not{q} P_R \not{p}] = \mathrm{tr}[P_L \not{q} P_R \not{p}]. \tag{5.45}$$

This leads to the identities

$$\begin{aligned}
[\bar{u}(p)P_R v(q)]^* [\bar{u}(p)P_R v(q)] &= \mathrm{tr}[\frac{1}{2}(1+\gamma^5)\not{q}\not{p}] = 2pq, \\
\left[\bar{u}(p)P_R \not{p}\not{q} v(q)\right]^* \left[\bar{u}(p)P_R \not{p}\not{q} v(q)\right] &= 0, \\
\left[\bar{u}(p)P_R \not{q}\not{p} v(q)\right]^* \left[\bar{u}(p)P_R \not{q}\not{p} v(q)\right] &= \mathrm{tr}[\frac{1}{2}(1+\gamma^5)\not{q}\not{p}\not{q}\not{p}] \\
&= 4(pq)^2. \qquad (5.46)
\end{aligned}$$

We can then replace the numerator by $2(\ell^2 - xyM_n(X_1)^2)$. In order to solve the integral, it can be splitted up

$$I_1 = \int dx\, dy\, dz \delta(x+y+z-1) \int_\ell \frac{2\ell^2}{D^3}, \qquad (5.47)$$

$$I_2 = \int dx\, dy\, dz \delta(x+y+z-1) \int_\ell \frac{-2xyM_n(X_1)^2}{D^3}. \qquad (5.48)$$

Using the following d–dimensional integrals in Minkowski space

$$\int \frac{d^d\ell}{(2\pi)^d} \frac{1}{(\ell^2-\Delta)^n} = \frac{(-1)^n \mathrm{i}}{(4\pi)^{d/2}} \frac{\Gamma(n-d/2)}{\Gamma(n)} \Big(\frac{1}{\Delta}\Big)^{n-d/2}, \qquad (5.49)$$

$$\int \frac{d^d\ell}{(2\pi)^d} \frac{\ell^2}{(\ell^2-\Delta)^n} = \frac{(-1)^{n-1} \mathrm{i}}{(4\pi)^{d/2}} \frac{d}{2} \frac{\Gamma(n-d/2-1)}{\Gamma(n)} \Big(\frac{1}{\Delta}\Big)^{n-d/2-1}, \qquad (5.50)$$

The first integral I_1 reads

$$\begin{aligned}
I_1 &= \frac{2\mathrm{i}}{(4\pi)^{d/2}} \frac{d}{2} \frac{\Gamma(2-d/2)}{\Gamma(3)} \\
&\times \int_0^1 dx \int_0^{1-x} dy \Big(\frac{\mu^2}{(1-x-y)M_n(X_1)^2 - xyM_k(X_2)^2}\Big)^{2-d/2}, \qquad (5.51)
\end{aligned}$$

where $z \geq 0$, *i.e.*, $y \leq 1-x$. We have introduced here the arbitrary mass scale μ^2 to make the integral dimensionally correct. This integral diverges at $d=4$. To analyze its behavior, one expands the integrand as well as the gamma function around the critical point:

$$\begin{aligned}
\Big(\frac{1}{\Delta}\Big)^{2-d/2}\Big|_{d=4} &= 1 - (2-\frac{d}{2}) \ln\Delta + \ldots, \\
\Gamma(x)\Big|_{x=0} &= \frac{1}{x} - \gamma + \mathcal{O}(x), \qquad (5.52)
\end{aligned}$$

where γ is the Euler-Mascheroni constant, $\gamma \approx 0.5772$. Using the modified minimal substraction scheme ($\overline{\mathrm{MS}}$) [132], *i.e.*, the the renormalization scale $\mu\, e^{\frac{\gamma}{2}}/(4\pi)^{\frac{1}{2}}$, we can replace

$$\begin{aligned}
\frac{\Gamma(2-d/2)}{(4\pi)^{d/2}} \Big(\frac{\mu^2}{\Delta}\Big)^{2-d/2} &\approx \frac{1}{(4\pi)^2} \Big(\frac{2}{\epsilon} - \gamma + \ln(4\pi) - \ln\Big(\frac{\Delta}{\mu^2}\Big)\Big) \\
&\to \frac{1}{(4\pi)^2} \Big(\ln\Big(\frac{\mu^2}{\Delta}\Big)\Big). \qquad (5.53)
\end{aligned}$$

Here, the parameter $\epsilon = 4-d$ contains the divergent part of the integral. The integral thus yields

$$\begin{aligned} I_1 &= \frac{2\mathrm{i}}{(4\pi)^2}\int_0^1 dx\int_0^{1-x} dy\,\ln\Big(\frac{\mu^2}{(1-x-y)M_k(X_2)^2 - xyM_n(X_1)^2}\Big) \\ &= \frac{2\mathrm{i}}{(4\pi)^2}\int_0^1 dx\Big\{(1-x) \\ &\quad + \frac{1-x}{M_k(X_2)^2 + xM_n(X_1)^2}\Big[M_k(X_2)^2\ln\Big(\frac{\mu^2}{(1-x)M_k(X_2)^2}\Big) \\ &\quad + xM_n(X_1)^2\ln\Big(-\frac{\mu^2}{x(1-x)M_n(X_1)^2}\Big)\Big]\Big\}. \end{aligned} \tag{5.54}$$

We are interested in the imaginary part of the amplitude, since only this part can generate a nonzero asymmetry. Remember that in the expression for the amplitude Eq. (5.37), there still is a second imaginary unit. Therefore, the only imaginary part that remains in the end must result from the last term of the integral over x, since $\ln(-x) = \ln|x| + \mathrm{i}\pi\theta(x)$ ($\theta(x)$ denotes here and for the rest of the chapter the Heaviside step function with $\theta(0) = 0$):

$$\begin{aligned} \mathrm{Im}\, I_1 &= -\frac{2\pi M_n(X_1)^2}{(4\pi)^2}\int_0^1 dx\frac{x(1-x)}{M_k(X_2)^2 + xM_n(X_1)^2} \\ &= -\frac{2\pi}{(4\pi)^2}\Big(\frac{1}{2} + \frac{M_k(X_2)^2}{M_n(X_1)^2} \\ &\quad - \frac{M_k(X_2)^2(M_n(X_1)^2 + M_k(X_2)^2)}{M_n(X_1)^4}\ln\Big(\frac{M_n(X_1)^2 + M_k(X_2)^2}{M_k(X_2)^2}\Big)\Big). \end{aligned} \tag{5.55}$$

Note that this imaginary part is independent of μ. In a similar way, one can discuss the second integral

$$\begin{aligned} I_2 &= \frac{\mathrm{i}}{(4\pi)^2}\int dx\,dy\,dz\delta(x+y+z-1)\frac{xyM_n(X_1)^2}{\Delta} \\ &= \frac{\mathrm{i}}{(4\pi)^2}\int_0^1 dx\int_0^{1-x} dy\frac{xyM_n(X_1)^2}{(1-x-y)M_k(X_2)^2 - xyM_n(X_1)^2} \\ &= \frac{\mathrm{i}M_n(X_1)^2}{(4\pi)^2}\int_0^1 dx\Big[\frac{x(1-x)M_k(X_2)^2}{(M_k(X_2)^2 + xM_n(X_1)^2)^2} \\ &\quad \ln\Big(-\frac{xM_n(X_1)^2}{M_k(X_2)^2}\Big) + \frac{x(1-x)}{M_k(X_2)^2 + xM_n(X_1)^2}\Big]. \end{aligned} \tag{5.56}$$

The imaginary part we are looking for thus turns out to be

$$\begin{aligned}\mathrm{Im}\, I_2 &= -\frac{\pi M_n(X_1)^2}{(4\pi)^2}\int_0^1 dx \frac{x(1-x)M_k(X_2)^2}{(M_k(X_2)^2 + xM_n(X_1)^2)^2} \\ &= -\frac{\pi}{(4\pi)^2}\frac{M_k(X_2)^2}{M_n(X_1)^2}\Big[\frac{M_n(X_1)^2 + 2M_k(X_2)^2}{M_n(X_1)^2} \\ &\quad \ln\Big(\frac{M_n(X_1)^2 + M_k(X_2)^2}{M_k(X_2)^2}\Big) - 2\Big]. \end{aligned} \tag{5.57}$$

This leads to

$$\mathrm{Im}(I_1 + I_2) = -\frac{1}{16\pi}\Big[1 - \frac{M_k(X_2)^2}{M_n(X_1)^2}\ln\Big(1 + \frac{M_n(X_1)^2}{M_k(X_2)^2}\Big)\Big], \tag{5.58}$$

and for $\mathrm{Im}(\mathcal{T}^*\mathcal{V})$ we obtain the result:

$$\mathrm{Im}(\mathcal{T}^*\mathcal{V}) = -\frac{M_n(X_1)^2}{16\pi}\Big[1 - \frac{M_k(X_2)^2}{M_n(X_1)^2}\ln\Big(1 + \frac{M_n(X_1)^2}{M_k(X_2)^2}\Big)\Big]. \tag{5.59}$$

Besides this vertex contribution to the CP–violation, we have to take wave–function corrections into account.

5.3.2 Wave–Function Correction

In order to calculate the wave–function corrections at high energies, we treat the leptons as massless particles. We start with the wave–function factor

$$\mathcal{W} = \mathrm{i}\bar{u}(p)\Big[\frac{P_R}{k'^2 - M_k(X_2)^2 + \mathrm{i}\varepsilon}\underbrace{\int\frac{d^4q'}{(2\pi)^4}\frac{\mathrm{tr}[P_R \not{p}' P_L \not{q}']}{(p'^2 + \mathrm{i}\varepsilon)(q'^2 + \mathrm{i}\varepsilon)}}_{=I}\Big]v(q). \tag{5.60}$$

The integral over the Feynman parameters is

$$\frac{1}{(p'^2 + \mathrm{i}\varepsilon)(q'^2 + \mathrm{i}\varepsilon)} = \int_0^1 dx\, dy \delta(x + y - 1)\frac{1}{D^2}, \tag{5.61}$$

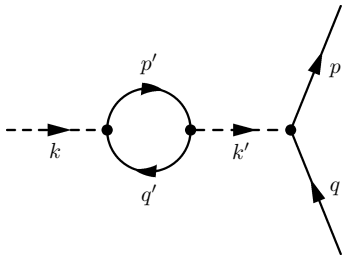

Figure 5.6: Wave–function correction for the decay of a heavy scalar with the associated momenta.

where D is given by

$$\begin{aligned} D &= (1-x)((q')^2+\mathrm{i}\varepsilon)+x((q'+k')^2+\mathrm{i}\varepsilon) = q'^2+2xq'k'+xk'^2+\mathrm{i}\varepsilon \\ &= (q'+xk')^2+x(1-x)M_k(X_2)^2+\mathrm{i}\varepsilon = \ell^2-\Delta. \end{aligned} \tag{5.62}$$

The numerator in Eq. (5.60) can be written as

$$\mathrm{tr}[P_R \not{p}' P_L \not{q}'] = -2p'q' = -2(\ell^2+x(x-1)k^2), \tag{5.63}$$

and the integral I yields

$$\begin{aligned} I &= 2\int_0^1 dx\,\mu^{4-d}\int_\ell \frac{d^d\ell}{(2\pi)^d}\frac{\ell^2+\Delta}{(\ell^2-\Delta)^2} \\ &= 2\int_0^1 dx \frac{-\mathrm{i}\,\mu^{4-d}}{(4\pi)^{d/2}}\left(\frac{\frac{d}{2}\Gamma(1-\frac{d}{2})}{\Delta^{1-d/2}}-\frac{\Delta\Gamma(2-\frac{d}{2})}{\Delta^{2-d/2}}\right) \\ &= -\frac{2\mathrm{i}\,(d-1)\,\mu^{4-d}}{(4\pi)^{d/2}}\int_0^1 dx\frac{\Gamma(1-\frac{d}{2})}{\Delta^{1-d/2}}. \end{aligned} \tag{5.64}$$

where we have used the relation $\Gamma(1+x) = x\Gamma(x)$. Expanding $\Gamma(x)$ near $x = -n$ ($n \in \mathbb{N}$) as

$$\Gamma(x) = \frac{(-1)^n}{n!}\left(\frac{1}{x+n}-\gamma+1\cdots+\frac{1}{n}+\mathcal{O}(x+n)\right), \tag{5.65}$$

we get

$$\frac{\mu^{d-4}\,\Gamma(1-\frac{d}{2})}{(4\pi)^{(d/2)}}\left(\frac{1}{\Delta}\right)^{1-\frac{d}{2}} \approx \frac{-\Delta}{(4\pi)^2}\left(\frac{2}{\epsilon}-\ln\left(\frac{\Delta}{\mu^2}\right)-\gamma+\ln(4\pi)+1\right). \tag{5.66}$$

Therefore, using the $\overline{\mathrm{MS}}$ scheme I takes in the limit $d \to 4$, *i.e.*, $(d-1) \to 3-\epsilon$, the form

$$\begin{aligned} I &= \frac{6\mathrm{i}}{(4\pi)^2}\int_0^1 dx(-x(1-x)k^2)\Big(-\ln\Big(-\frac{x(1-x)k^2}{\mu^2}\Big)+1\Big) \\ &- \frac{4\mathrm{i}}{(4\pi)^2}\int_0^1 dx(-x(1-x)k^2). \end{aligned} \tag{5.67}$$

Since the above integral I gives $I = \mathrm{i}(1/4\pi)^2k^2\Big[\Big(3\ln\big(\frac{|k^2|}{\mu^2}\big)+3\mathrm{i}\pi\theta(k^2)-8\Big)/3+4/6\Big]$, just the real part of I contributes to $\mathrm{Im}\,\mathcal{W}$. For $k^2 = M_n^2(X_1)$ this contribution yields a factor

$$\mathrm{Re}\,I = \frac{M_n^2(X_1)}{16\pi}. \tag{5.68}$$

Putting everything together, we end up with

$$\mathrm{Im}(\mathcal{T}^*\mathcal{W}) = \frac{M_n(X_1)^2}{16\pi}\Big[\frac{M_n(X_1)^2}{M_n(X_1)^2-M_k(X_2)^2}\Big]. \tag{5.69}$$

The total CP–violation is then generated by the sum $\mathrm{Im}\,(\mathcal{T}^*\mathcal{V}+\mathcal{T}^*\mathcal{W})$ given in Eqs. (5.59) and (5.69).

5.4 CP–Asymmetry

The loop calculations above lead to the following differences in the decay widths:

$$\begin{aligned}\Delta_V^{(n)} &= \Gamma^{(n)}(X_1^{(n)} \to \overline{\psi}\nu) - \Gamma^{(n)}(\overline{X}_1^{(n)} \to \psi\overline{\nu}) \qquad (5.70a)\\ &= \frac{M_n(X_1)}{32\pi^2}\mathrm{Im}\ \mathrm{tr}(Y_{\nu_1}Y_{\nu_2}^\dagger Y_{e_1}Y_{e_2}^\dagger)\Big[1 - \frac{M_k(X_2)^2}{M_n(X_1)^2}\ln\Big(1+\frac{M_n(X_1)^2}{M_k(X_2)^2}\Big)\Big],\\ \Delta_W^{(n)} &= -\frac{M_n(X_1)}{32\pi^2}\mathrm{Im}\ [\mathrm{tr}(Y_{\nu_1}Y_{\nu_2}^\dagger)\ \mathrm{tr}(Y_{e_1}Y_{e_2}^\dagger)]\frac{M_n(X_1)^2}{M_n(X_1)^2 - M_k(X_2)^2}. \qquad (5.70b)\end{aligned}$$

The result for $\Delta_W^{(n)}$ holds in the limit $(M_n(X_1) - M_k(X_2))^2 \gg (\Gamma_{X_1}^{(n)} - \Gamma_{X_2}^{(k)})^2$. For example in Chapters 7 and 8, we are interested in resonant mass splittings of the order $(M_n^2(X_1) - M_n^2(X_2))/M_n^2(X_1) \sim 10^{-14}$. For $\mathrm{tr}(Y_{\nu_1}^\dagger Y_{\nu_1}) \simeq \mathrm{tr}(Y_{\nu_2}^\dagger Y_{\nu_2})$, we see that

$$(\Gamma_{X_1}^{(n)} - \Gamma_{X_2}^{(k)})^2 \simeq \frac{\mathrm{tr}(Y_{\nu_1}^\dagger Y_{\nu_1})^2}{(8\pi)^2}(M_n(X_1) - M_k(X_2))^2. \qquad (5.71)$$

Consequently, our calculation in Sec. 5.3.2 should be valid as long as $\mathrm{tr}(Y_{\nu_1}^\dagger Y_{\nu_1}) \simeq \mathrm{tr}(Y_{\nu_2}^\dagger Y_{\nu_2}) \ll 1$ even in the resonant limit, *i.e.*, $k = n$. But to be on the safe side, we will have a closer look at the resonant limit in the next Section.

The total lepton asymmetry generated by the heavy scalar decay including both vertex– and wave–function corrections, reads

$$\begin{aligned}\epsilon_{X_1}^{(n)} &= \frac{\Delta_W^{(n)} + \Delta_V^{(n)}}{\Sigma_T^{(n)}} = \frac{1}{8\pi\ [\mathrm{tr}(Y_{\nu_1}Y_{\nu_1}^\dagger) + \mathrm{tr}(Y_{e_1}Y_{e_1}^\dagger)]}\\ &\times \Bigg[\mathrm{Im}\ \mathrm{tr}(Y_{\nu_1}Y_{\nu_2}^\dagger Y_{e_1}Y_{e_2}^\dagger)\Big(1 - \frac{M_k(X_2)^2}{M_n(X_1)^2}\ln\Big(1+\frac{M_n(X_1)^2}{M_k(X_2)^2}\Big)\Big)\\ &- \mathrm{Im}\ [\mathrm{tr}(Y_{\nu_1}Y_{\nu_2}^\dagger)\ \mathrm{tr}(Y_{e_1}Y_{e_2}^\dagger)]\Big(\frac{M_n(X_1)^2}{M_n(X_1)^2 - M_k(X_2)^2}\Big)\Bigg],\end{aligned} \qquad (5.72)$$

where we have used in the denominator the tree–level approximation. Note that our result in Eq. (5.72) disagrees with the corresponding expression given in Ref. [27]. The most important difference between Eq. (5.72) and Ref. [27] is the way how the complex conjugation has been applied to the Yukawa coupling matrices.

5.5 Resonant Limit

Our approximations for the wave–function correction in Sec. 5.3.2 break down in a "resonant" limit $(M_n(X_1) - M_n(X_2))^2 \approx (\Gamma_{X_1}^{(n)} - \Gamma_{X_2}^{(n)})^2$. But we are interested in an "enhanced scenario" for lepton–asymmetry. To ensure that we are on the safe side with our calculations, we will now repeat the calculations in an approach which

accounts for the resonant case. The method we use is Pilaftsis' resummation approach for scalars [85, 133, 134] (for another treatment see, *e.g.*, Ref. [135]). For two complex scalars X_1 and X_2, the effective resummation approach for unstable particle mixing can be discussed as follows. The unrenormalized fields X_i^0 $(i = 1, 2)$ with masses M_i^0 are expressed in terms of renormalized quantities as

$$X_i^0 = \sum_{j=1}^{2} Z_{ij}^{1/2} X_j = \sum_{j=1}^{2} (\delta_{ij} + \frac{1}{2}\delta Z_{ij}) X_j \tag{5.73}$$

and

$$(M_i^0)^2 = M_i^2 + \delta M_i^2. \tag{5.74}$$

We can determine the wave–function and mass renormalization constants $Z_{ij}^{1/2}$ and δM_i from renormalization conditions which are imposed on the two-point correlation functions $\Pi_{ij}(p^2)$ in some physical scheme for the transition $X_j \to X_i$. First, we have to calculate all the $X_i X_j$ Greens functions. Then, summing up a geometric series of self–energies $\Pi_{ij}(p^2)$, the full propagators are given by the inverse propagator matrix

$$\Delta_{ij}^{-1}(p^2) = \begin{pmatrix} p^2 - (M_1^0)^2 + \Pi_{11}(p^2) & \Pi_{12}(p^2) \\ \Pi_{21}(p^2) & p^2 - (M_2^0)^2 + \Pi_{22}(p^2) \end{pmatrix}. \tag{5.75}$$

After inverting this matrix, the propagators take the forms

$$\Delta_{11}(p^2) = \Big[p^2 - (M_1^0)^2 + \Pi_{11}(p^2) - \frac{\Pi_{12}(p^2)\Pi_{21}(p^2)}{p^2 - (M_2^0)^2 + \Pi_{22}(p^2)}\Big]^{-1}, \tag{5.76a}$$

$$\Delta_{22}(p^2) = \Big[p^2 - (M_2^0)^2 + \Pi_{22}(p^2) - \frac{\Pi_{12}(p^2)\Pi_{21}(p^2)}{p^2 - (M_1^0)^2 + \Pi_{11}(p^2)}\Big]^{-1}, \tag{5.76b}$$

$$\Delta_{12}(p^2) = -\Delta_{11}(p^2)\Pi_{12}(p^2)\Big[p^2 - (M_2^0)^2 + \Pi_{22}(p^2)\Big]^{-1}, \tag{5.76c}$$

$$\Delta_{21}(p^2) = -\Delta_{22}(p^2)\Pi_{21}(p^2)\Big[p^2 - (M_1^0)^2 + \Pi_{11}(p^2)\Big]^{-1}. \tag{5.76d}$$

We therefore see that the off-diagonal resummed scalar propagators $\Delta_{12}(p^2)$ and $\Delta_{21}(p^2)$ can also be written as

$$\Delta_{12}(p^2) = -\Big[p^2 - (M_1^0)^2 + \Pi_{11}(p^2)\Big]^{-1}\Pi_{12}(p^2)\Delta_{22}(p^2), \tag{5.77}$$

$$\Delta_{21}(p^2) = -\Big[p^2 - (M_2^0)^2 + \Pi_{22}(p^2)\Big]^{-1}\Pi_{21}(p^2)\Delta_{11}(p^2). \tag{5.78}$$

This unrenormalized scalar propagator $\Delta_{ij}(p^2)$ is related to the renormalized propagator $\widehat{\Delta}_{ij}(p^2)$ by

$$\Delta_{ij}(p^2) = Z_{im}^{1/2}\widehat{\Delta}_{mn}(p^2)Z_{nj}^{1/2\dagger} \tag{5.79}$$

and can be obtained from Eqs. (5.76a) by replacing M_i^0 by M_i and $\Pi_{ij}(p^2)$ by $\widehat{\Pi}_{ij}(p^2)$. As a consequence, Eq. (5.78) also holds for $\widehat{\Delta}_{ij}(p^2)$.

The question is how to find the effective resummed decay amplitude $\widehat{\mathcal{M}}_{X_i}$ for the decay of X_i into n light stable scalars $X_{i_1}, \ldots, X_{i_n}$. We start in analogy with the LSZ formalism [136] with the Greens function and then amputate the legs by their inverse propagators. The procedure which can be extended to the external line describing the X_iX_j system, is summarized as

$$\begin{aligned}
\widehat{\mathcal{M}}_{i\ldots} &= \lim_{p^2\to M_i^2} \mathcal{M}^{\rm amp}_{k\ldots} Z^{1/2}_{km} \widehat{\Delta}_{mn}(p^2) Z^{1/2\dagger}_{nj} Z^{-1/2\dagger}_{ji} \widehat{\Delta}^{-1}_{ii}(p^2) \\
&= \lim_{p^2\to M_i^2} \left(\mathcal{M}^{\rm amp}_{k\ldots} Z^{1/2}_{ki} - \mathcal{M}^{\rm amp}_{k\ldots} Z^{1/2}_{km} \frac{\widehat{\Pi}_{mi}(p^2)(1-\delta_{mi})}{p^2 - M_m^2 + \widehat{\Pi}_{mm}(p^2)} \right) \\
&= \mathcal{M}_{i\ldots} - \mathcal{M}_{j\ldots} \frac{\widehat{\Pi}_{ji}(M_i^2)(1-\delta_{ij})}{M_i^2 - M_j^2 + \widehat{\Pi}_{jj}(M_i^2)},
\end{aligned} \tag{5.80}$$

where $\mathcal{M}_{i\ldots}$ and $\mathcal{M}_{j\ldots}$ are the renormalized transition elements evaluated in the stable particle approximation. It is important to notice that the on–shell renormalized self–energies $\widehat{M}_j^2$ contain nonvanishing absorptive parts, since renormalization can only modify dispersive parts. This is due to the fact that the counter term Lagrangian must be Hermitian in contrast to absorptive parts which are anti-Hermitian. As it can be easily seen, $X_{i\ldots}$ is analytic in the limit $M_i^2 \to M_j^2$ because of the remaining imaginary term $\mathrm{i}\,\mathrm{Im}\,\widehat{\Pi}_{jj}(M_i^2)$ in the denominator. It must be stressed that the decaying particle cannot serve as an initial state. Consequently, the resummed decay amplitude must be regarded as being effectively embedded into the resummed S-matrix element. The resulting S-matrix describes the dynamics of the following process: Some asymptotic states produce the considered unstable particle which resides only in the intermediate state. Then it decays subsequently either directly or indirectly through mixing into some observed final states which are stable.

Given the effective resummed decay amplitude in Eq. (5.80), we can obtain an equation for the transition $\mathcal{M}_1^{\varepsilon^w}$ amplitude responsible for the CP–violation induced by the wave–function correction:

$$\mathcal{M}_1^{\varepsilon^w} = Y^\dagger_{\nu_1} \overline{u}_\nu P_R v_\psi - i Y^\dagger_{\nu_2} \overline{u}_\nu P_R [p^2 - M_2^2 + i\Pi^{\rm abs}_{22}(p^2)]^{-1} \Pi^{\rm abs}_{21}(p^2) v_\psi, \tag{5.81}$$

where the superscript "abs" denotes the absorptive part The absorptive part of the one–loop transitions is

$$\Pi^{\rm abs}_{ij}(p^2) = \frac{\mathrm{tr}(Y_{e_i} Y^\dagger_{e_j})}{16\pi} M^2(X_i), \tag{5.82}$$

such that

$$\mathcal{M}_1^{\varepsilon^w} = \overline{u}_\nu P_R v_\psi \left[Y^\dagger_{\nu_1} - i \frac{Y^\dagger_{\nu_2} \mathrm{tr}(Y_{e_1} Y^\dagger_{e_2})}{16\pi} \frac{M_1^2 (M_1^2 - M_2^2 - \mathrm{i}\frac{\mathrm{tr}(Y_{e_2} Y^\dagger_{e_2})}{16\pi} M_1^2)}{(M_1^2 - M_2^2)^2 + \frac{\mathrm{tr}(Y_{e_2} Y^\dagger_{e_2})^2 M_1^4}{(16\pi)^2}} \right]. \tag{5.83}$$

The resummed amplitude for the CP-transformed decay $\overline{\mathcal{M}}_1^{\varepsilon^w}$ is

$$\begin{aligned}\overline{\mathcal{M}}_1^{\varepsilon^w} &= Y_{\nu_1}^\dagger \overline{u}_\psi P_L v_\nu + \mathrm{i} Y_{\nu_2}^\dagger \overline{u}_\psi \Pi_{12}^{\mathrm{abs}}(p^2)[p^2 - M_2^2 + \mathrm{i}\Pi_{22}^{\mathrm{abs}}(p^2)]^{-1} P_L v_\nu \\ &= Y_{\nu_1}^\dagger \overline{u}_\psi P_L v_\nu - \mathrm{i} Y_{\nu_2}^\dagger \overline{u}_\nu P_L [p^2 - M_2^2 + \mathrm{i}\Pi_{22}^{\mathrm{abs}}(p^2)]^{-1} \overline{\Pi}_{21}^{\mathrm{abs}}(p^2) v_\psi, \end{aligned} \tag{5.84}$$

where we have used that $\overline{\Pi}_{ij}^{\mathrm{abs}}(p^2) = \Pi_{ij}^{\mathrm{abs}\,*}(p^2)$. In the resummation approach, the difference in the decay widths of scalar and antiscalar due to the wave–function correction is

$$\begin{aligned}\Delta_W^{(n)} &= -\frac{M_n(X_1)}{32\pi^2} \mathrm{Im}\left[\mathrm{tr}(Y_{\nu_1} Y_{\nu_2}^\dagger)\, \mathrm{tr}(Y_{e_1} Y_{e_2}^\dagger)\right] \\ &\times \frac{M_n^2(X_1)}{M_n^2(X_1) - M_n^2(X_2) + \frac{\mathrm{tr}(Y_{e_2} Y_{e_2}^\dagger)^4}{(16\pi)^2} \frac{M_n^4(X_1)}{M_n^2(X_1) - M_k^2(X_2)}} \end{aligned} \tag{5.85}$$

It has to be emphasized here that due to the additional term in the denominator,

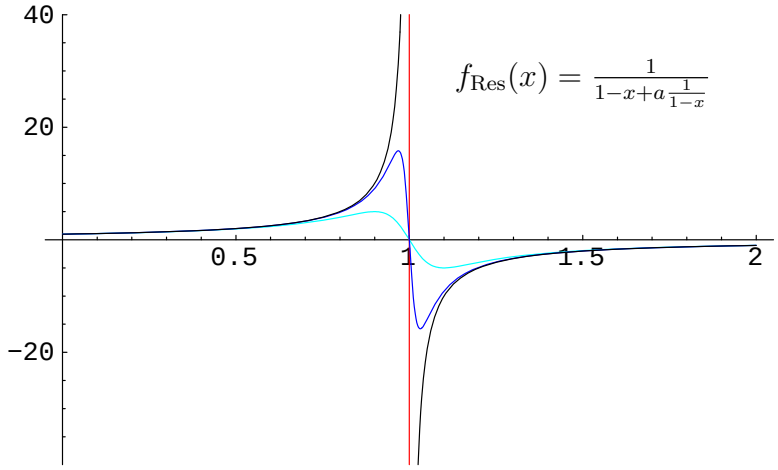

Figure 5.7: The function $f_{\mathrm{Res}}(x) = 1/[1 - x + a/(1-x)]$ in the range $[0, 2]$, where the turquoise, blue, and black refer to $a = 10^{-2}$, $a = 10^{-3}$, and $a = 0$, respectively.

$\Delta_W^{(n)}$ is well–behaved in the deeply resonant limit (*cf.* Fig. 5.7), *i.e.*,

$$\lim_{M_n(X_1) \to M_n(X_2)} \frac{M_n^2(X_1)}{M_n^2(X_1) - M_n^2(X_2) + \frac{\mathrm{tr}(Y_{e_2} Y_{e_2}^\dagger)^4}{(16\pi)^2} \frac{M_n^4(X_1)}{M_n^2(X_1) - M_n^2(X_2)}} = 0. \tag{5.86}$$

In particular, for a typical number $\mathrm{tr}(Y_{e_2} Y_{e_2}^\dagger) \sim 10^{-24}$ (see Chapters 7 and 8) and a relative mass splitting between X_1 and X_2 of the order of $\sim 10^{-14}$, we can estimate

$$\frac{\mathrm{tr}(Y_{e_2} Y_{e_2}^\dagger)^2}{(16\pi)^2} \frac{M_n^4(X_1)}{(M_n^2(X_1) - M_k^2(X_2))^2} < 10^{-28}. \tag{5.87}$$

For this reason, we can neglect in Eq. (5.85) the additional term in the denominator and thus reproduce our original result in Eq. (5.70b).

Chapter 6

Symmetry Breaking by a Bulk Scalar

In this Chapter, we will apply the two ideas of LR symmetry and extra dimensions, introduced in Chapter 4, to a scalar bi–doublet of the LR symmetric model that propagates on an interval in 5D flat space. In particular, we determine the minimum of the scalar potential after dimensional reduction in the 4D effective theory. The symmetry breaking $G_{LR} \to SU(2)_D \times U(1)_{B-L}$ induced by the bulk scalar VEV serves as an origin of EWSB. We also analyze the role of brane–localized operators.

6.1 The Potential

Consider a single 5D scalar bi–doublet X transforming under G_{LR} as $X \sim (\frac{1}{2}, \frac{1}{2}, 0)$ that propagates on an interval as shown in Fig. 6.1. The coordinate of the 5th dimension is $y \in [0, \pi R]$, where πR is the size of the extra dimension. We impose on X the following Neumann boundary conditions (BCs)

$$\text{at } y = 0 : \ \partial_y X|_{y=0} = 0 \quad \text{and} \quad \text{at } y = \pi R : \ \partial_y X|_{y=\pi R} = 0. \tag{6.1}$$

This ensures that there are scalar zero modes which can be identified with SM–like Higgs fields that acquire nonzero VEVs of the order of the EW scale $\sim 10^2$ GeV. The standard flat space KK expansion (see Sec.4.2.1) for the scalar X, consistent with the BCs in Eq. (6.1), is

$$X(x_\mu, y_1) = \frac{1}{\sqrt{\pi R}}\Big[X^{(0)}(x_\mu) + \sqrt{2}\sum_{n=1}^{+\infty} X^{(n)}(x_\mu)\cos\Big(\frac{n y_1}{R}\Big)\Big], \tag{6.2}$$

where $X^{(n)}(x_\mu)$ is the nth KK mode of X and $X^{(0)}(x_\mu)$ is the zero mode, both having mass dimension +1. The most general 5D potential for the bi–doublet X is

$$V(X) = -\sum_{i,j} \mu_{ij}^2 \,\mathrm{tr}\, X_i^\dagger X_j + \sum_{i,j,k,l} \lambda_{ijkl} \,\mathrm{tr}\, X_i^\dagger X_j \,\mathrm{tr}\, X_k^\dagger X_l + \sum_{i,j,k,l} \lambda'_{ijkl} \,\mathrm{tr}\, X_i^\dagger X_j X_k^\dagger X_l, \tag{6.3}$$

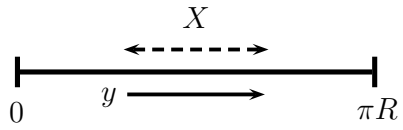

Figure 6.1: 5D scalar bi-doublet $X \sim (\frac{1}{2}, \frac{1}{2}, 0)$ propagating on an interval.

where $i, j, k, l = 1, 2$, and X_1 and X_2 are defined as $X_1 = X$ and $X_2 = \widetilde{X}$, respectively. (Thenotation for $X_{1,2}$ here should not be confused with that of Chapter 5). The potential V in Eq. (6.3) consists of $2^2 + 2 \cdot 2^4 = 36$ terms. In Eq. (6.3), it is obvious we must have

$$\lambda_{ijkl} = \lambda_{klij}. \tag{6.4}$$

Since the fields X_i transform under LR symmetry as $X_i \leftrightarrow X_i^\dagger$, we find

$$\begin{gathered} \mu_{ij} = \mu_{ji}, \\ \lambda_{1212} = \lambda_{2121}, \quad \lambda_{iijk} = \lambda_{iikj}, \quad \lambda_{ijkk} = \lambda_{jikk}, \\ \widetilde{\lambda}_{ijkl} = \widetilde{\lambda}_{lijk} = \widetilde{\lambda}_{klij} = \widetilde{\lambda}_{jkli}. \end{gathered} \tag{6.5}$$

These identities are a consequence of the reality of V. The parameters μ_{ij} have mass dimension $+1$, while λ_{ijkl} and $\widetilde{\lambda}_{ijkl}$ have mass dimension -1.

Now, we go from the 5D description of the scalars to the 4D effective theory. The 4D effective Lagrangian for the scalar $\mathcal{L}^{\rm eff}_{\rm scalar} = \int_0^{\pi R} dy[\mathcal{L}^{\rm kin}_{\rm scalar} - V(X)]$ is given by

$$\begin{aligned} \mathcal{L}^{\rm eff}_{\rm scalar} = -V_{\rm eff}(X) \;\; &+ \;\; \sum_{n=0}^{+\infty} \left\{ \left(K + \frac{K'_X}{\pi R}\right) \mathrm{tr} \left[\left(D_\mu X^{(n)}\right)^\dagger D^\mu X^{(n)} \right] \right. \\ &- \;\; \left. K \left(\frac{n}{\pi R}\right)^2 \mathrm{tr}\, X^{(n)\dagger} X^{(n)} \right\}, \end{aligned} \tag{6.6}$$

The scalar kinetic part of the Lagrangian is invariant under the Z_2 interchange symmetry $X \leftrightarrow \widetilde{X}$, *i.e.*,

$$\mathcal{L}^{\rm kin}_{\rm scalar} \supset \mathrm{tr}[(D_\mu X)^\dagger D^\mu X] = \mathrm{tr}[(D_\mu \widetilde{X})^\dagger D^\mu \widetilde{X}], \tag{6.7}$$

where the covariant derivative D_μ is defined by

$$D_\mu X = \partial_\mu X - \frac{\mathrm{i}g}{2}[\sigma_a A^a_L X - X \sigma_a A^a_R]. \tag{6.8}$$

In this equation, the index a runs over $1, 2, 3$. From the identities $\sigma_a^2 = \mathrm{diag}(1, 1)$ and $\sigma_2 \sigma_a \sigma_2 = -\sigma_a^*$ it follows that

$$\begin{aligned} D_\mu \widetilde{X} &= \partial_\mu(\sigma_2 X^* \sigma_2) - \frac{\mathrm{i}g}{2}[\sigma_a A^a_L \sigma_2 X^* \sigma_2 - \sigma_2 X^* \sigma_2 \sigma_a A^a_R] \\ &= \sigma_2[\partial_\mu X^* + \frac{\mathrm{i}g}{2}[\sigma_a^* A^a_L X^* - X^* \sigma_a^* A^a_R]\sigma_2 = \sigma_2 (D_\mu X)^* \sigma_2. \end{aligned} \tag{6.9}$$

The Lagrangian thus satisfies

$$\begin{aligned}\mathcal{L}_{\rm kin} &= \mathrm{tr}[(D_\mu \widetilde{X})^\dagger D^\mu \widetilde{X}] = \mathrm{tr}[(\sigma_2 (D_\mu X)^* \sigma_2)^\dagger \sigma_2 (D^\mu X)^* \sigma_2] \\ &= \mathrm{tr}[(D_\mu X)^\dagger (D^\mu X)]^* = \mathrm{tr}[(D_\mu X)^\dagger D^\mu X], \end{aligned} \tag{6.10}$$

where we have used in the last step that $\mathcal{L}_{\rm kin}$ is real. The 4D effective potential $V_{\rm eff}(X)$ for all the KK modes including the zero mode reads

$$\begin{aligned} V_{\rm eff}(X) &= -\sum_n \sum_{i,j} \mu_{ij}^2 \,\mathrm{tr}\, X_i^{(n)\dagger} X_j^{(n)} + \sum_{m,n,p,q} \sum_{i,j,k,l} \lambda_{ijkl}^{mnpq} \mathrm{tr}\, X_i^{(m)\dagger} X_j^{(n)} \,\mathrm{tr}\, X_k^{(p)\dagger} X_l^{(q)} \\ &+ \sum_{m,n,p,q} \sum_{i,j,k,l} \widetilde{\lambda}_{ijkl}^{mnpq} \mathrm{tr}\, X_i^{(m)\dagger} X_j^{(n)} X_k^{(p)\dagger} X_l^{(q)}, \end{aligned} \tag{6.11}$$

where, in the notation of Eq. (6.3), $X_i^{(n)}$ is the nth KK mode of X_i, and the summation indices run over $i,j,k,l = 1,2$, and $m,n,p,q = 0,1,\ldots,\infty$. In Eq. (6.11), the mass squares μ_{ij}^2 are the same as in Eq. (6.3), whereas λ_{ijkl}^{mnpq} and $\widetilde{\lambda}_{ijkl}^{mnpq}$ are dimensionless parameters, which are related to λ_{ijkl} and $\widetilde{\lambda}_{ijkl}$ in Eq. (6.3) by

$$\lambda_{ijkl}^{mnpq} = \lambda_{ijkl} \frac{1}{(\pi R)^2} a_m a_n a_p a_q \int_0^{\pi R} dy\, c_m(y) c_n(y) c_p(y) c_q(y), \tag{6.12a}$$

$$\widetilde{\lambda}_{ijkl}^{mnpq} = \widetilde{\lambda}_{ijkl} \frac{1}{(\pi R)^2} a_m a_n a_p a_q \int_0^{\pi R} dy\, c_m(y) c_n(y) c_p(y) c_q(y), \tag{6.12b}$$

where we have introduced $c_r(y) = \cos(ry/R)$, for $r = m,n,p,q$, as well as $a_s = 1$, for $s = 0$, and $a_s = \sqrt{2}$, for $s > 0$. If, in the 4D effective theory, λ_{ijkl}^{mnpq} and $\widetilde{\lambda}_{ijkl}^{mnpq}$ are of order one, while the 5D parameters λ_{ijkl} and $\widetilde{\lambda}_{ijkl}$ are of the order of the size of the extra dimension, *i.e.*, $\lambda_{ijkl}, \widetilde{\lambda}_{ijkl} \sim \pi R$. In the following, we will assume that K (which is dimensionless) and K'_X (which has mass dimension -1) are given by

$$K = \mathcal{O}(1) \quad \text{and} \quad K'_X \sim 1/M_*, \tag{6.13}$$

where for one flat extra dimension, *i.e.*, $\delta = 1$, $M_* = (M_{\rm Pl}^2/R)^{1/3}$ is the fundamental 5D Planck scale and $M_{\rm Pl} \simeq 10^{18}$ GeV is the usual 4D Planck scale. This is a general feature of theories with extra dimensions: The higher dimensional fundamental scale is lowered in the effective theory (*cf.* Sec. 4.2.2). Assuming, *e.g.*, $1/R \simeq 1$ TeV, we have $M_* \simeq 10^{11}$ GeV.

Now, we have to remember that there are also scalar mass terms arising from the bulk kinetic terms. We denote by $M_n^2(X)$ the mass-squared of the nth KK-mode $X^{(n)}$. In Eq. (6.6), we canonically normalize the kinetic terms of the fields X by applying the field-redefinition $X \to X' = [K + (K'_X/\pi R)]^{\frac{1}{2}} X$. Setting for simplicity $K = 1$ and

using a Taylor expansion, we find

$$\mathrm{tr}\, X^{(n)\dagger} X^{(n)} = \Big[1 - \tfrac{K'_X}{\pi R} + \ldots\Big] \mathrm{tr}\, X'^{(n)\dagger} X'^{(n)}, \tag{6.14a}$$

$$\mathrm{tr}\, X^{(m)\dagger} X^{(n)} \mathrm{tr}\, X^{(p)\dagger} X^{(q)} = \Big[1 - 2\tfrac{K'_X}{\pi R} + \ldots\Big] \mathrm{tr}\, X'^{(m)\dagger} X'^{(n)} \mathrm{tr}\, X'^{(p)\dagger} X'^{(q)}, \tag{6.14b}$$

$$\mathrm{tr}\, X^{(m)\dagger} X^{(n)} X^{(p)\dagger} X^{(q)} = \Big[1 - 2\tfrac{K'_X}{\pi R} + \ldots\Big] \mathrm{tr}\, X'^{(m)\dagger} X'^{(n)} X'^{(p)\dagger} X'^{(q)}, \tag{6.14c}$$

where the dots denote higher powers of $K'_X/\pi R$. For $1/R \simeq 1$ TeV and $M_* \simeq 10^{11}$ GeV, a mass splitting of the order $K'_X/\pi R \sim 10^{-9}$ is introduced. For our discussion of the potential in this Chapter we can neglect these small corrections safely, because of their smallness compared to the absolute mass of the scalars. However, later on they will become important and lead to resonant expressions in the equations for the generation of the lepton asymmetry. It is convenient at this point to redefine the effective potential in the form

$$V'_{\mathrm{eff}}(X) = V_{\mathrm{eff}}(X) + K\Big(\frac{n}{\pi R}\Big)^2 \mathrm{tr}\, X^{(n)\dagger} X^{(n)}. \tag{6.15}$$

Notice that calculating the following integrals $X^{(n)}$ in the bulk kinetic term has no subscript due to the fact that this term is invariant under $X_1^{(n)} \leftrightarrow X_2^{(n)}$. In order to write down an explicit expression of the 4D effective potential, we have to evaluate integrals over products of cosines up to the order of four. For these integrals, we can take advantage of the following identities in terms of delta functions:

$$\int_0^{\pi R} \cos\Big(\frac{ny}{R}\Big) dy = 0, \tag{6.16a}$$

$$\int_0^{\pi R} \cos\Big(\frac{ny}{R}\Big)\cos\Big(\frac{my}{R}\Big) dy = \frac{1}{2}\pi R \Delta(n,m), \tag{6.16b}$$

$$\int_0^{\pi R} \cos\Big(\frac{ny}{R}\Big)\cos\Big(\frac{my}{R}\Big)\cos\Big(\frac{ly}{R}\Big) dy = \frac{1}{4}\pi R \Delta(n,m,l), \tag{6.16c}$$

$$\int_0^{\pi R} \cos\Big(\frac{ny}{R}\Big)\cos\Big(\frac{my}{R}\Big)\cos\Big(\frac{ly}{R}\Big)\cos\Big(\frac{ky}{R}\Big) dy = \frac{1}{8}\pi R \Delta(n,m,l,k), \tag{6.16d}$$

where we have used that

$$\Delta(n,m) \equiv \delta(n-m), \tag{6.17a}$$

$$\Delta(n,m,l) \equiv \delta(n+m-l) + \delta(n-m+l) + \delta(n-m-l), \tag{6.17b}$$

$$\begin{aligned} \Delta(n,m,l,k) \equiv\ & \delta(n+m+l-k) + \delta(n+m-l+k) + \delta(n+m-l-k) \\ +\ & \delta(n-m+l+k) + \delta(n-m+l-k) + \delta(n-m-l+k) \\ +\ & \delta(n-m-l-k). \end{aligned} \tag{6.17c}$$

As a consequence, Eq. (6.11) becomes

$$
\begin{aligned}
V'_{\text{eff}}(X) &= \int_0^{\pi R} V(X)\, dy = \\
&- \sum_{i,j} \mu_{ij}^2 \Big\{ \operatorname{tr} X_i^{(0)\dagger} X_j^{(0)} + \sum_{n,m} \operatorname{tr} X_i^{(n)\dagger} X_j^{(m)} \Delta_{nm} \Big\} \\
&+ \sum_n K \Big(\frac{n}{\pi R}\Big)^2 \operatorname{tr} X_1^{(n)\dagger} X_1^{(n)} \\
&+ \sum_{i,j,k,l} \lambda_{ijkl} \Big\{ \frac{1}{(\pi R)} \operatorname{tr} X_i^{(0)\dagger} X_j^{(0)} \operatorname{tr} X_k^{(0)\dagger} X_l^{(0)} \\
&\quad + \frac{1}{\pi R} \sum_{n,m} \Big[\operatorname{tr} X_i^{(0)\dagger} X_j^{(0)} \operatorname{tr} X_k^{(n)\dagger} X_l^{(m)} \Delta_{nm} + \text{all permutations} \Big] \\
&\quad + \frac{1}{\sqrt{2}\pi R} \sum_{n,m,p} \Big[\operatorname{tr} X_i^{(0)\dagger} X_j^{(n)} \operatorname{tr} X_k^{(m)\dagger} X_l^{(p)} \Delta_{nmp} + \text{all permutations} \Big] \\
&\quad + \frac{1}{2\pi R} \sum_{n,m,p,q} \operatorname{tr} X_i^{(n)\dagger} X_j^{(m)} \operatorname{tr} X_k^{(p)\dagger} X_l^{(q)} \Delta_{nmpq} \Big\} \\
&+ \sum_{i,j,k,l} \widetilde{\lambda}_{ijkl} \Big\{ \frac{1}{(\pi R)} \operatorname{tr} X_i^{(0)\dagger} X_j^{(0)} X_k^{(0)\dagger} X_l^{(0)} \\
&\quad + \frac{1}{\pi R} \sum_{n,m} \Big[\operatorname{tr} X_i^{(0)\dagger} X_j^{(0)} X_k^{(n)\dagger} X_l^{(m)} \Delta_{nm} + \text{all permutations} \Big] \\
&\quad + \frac{1}{\sqrt{2}\pi R} \sum_{n,m,p} \Big[\operatorname{tr} X_i^{(0)\dagger} X_j^{(n)} X_k^{(m)\dagger} X_l^{(p)} \Delta_{nmp} + \text{all permutations} \Big] \\
&\quad + \frac{1}{2\pi R} \sum_{n,m,p,q} \operatorname{tr} X_i^{(n)\dagger} X_j^{(m)} X_k^{(p)\dagger} X_l^{(q)} \Delta_{nmpq} \Big\}. \qquad (6.18)
\end{aligned}
$$

Here, "all permutations" refers to all possible permutations between the zero mode and the higher KK modes. In this context, we are interested in VEVs of the form

$$
\langle X^{(0)} \rangle = \langle \widetilde{X}^{(0)*} \rangle = \kappa_X \cdot \operatorname{diag}(1,1), \quad \langle X^{(n)} \rangle = \langle \widetilde{X}^{(n)} \rangle = 0, \qquad (6.19)
$$

where the parameter κ_X is real and $n = 1, \ldots, \infty$. In Eq. (6.19), only the zero modes $X^{(0)}$ acquire nonzero VEVs. As we will demonstrate next, the VEVs of the zero modes $X^{(0)}$ in Eq. (6.19) lead in the bulk to the symmetry breaking $G_{LR} \to SU(2)_D \times U(1)_{B-L}$, where $SU(2)_D$ is the diagonal subgroup of $SU(2)_L \times SU(2)_R$.

6.2 Extremum of the Potential

In order to see that the VEVs in Eq. (6.19) indeed correspond to a local minimum, we have to analyze the effective 4D potential in more detail. What we want to show

is that the potential has a local minimum for the VEVs given in Eq. (6.19). Thus, by keeping in mind the simple structure of these VEVs, which are mostly zeros, one can reduce the complexity of this discussion significantly.

As a first step, we split the scalars into real and imaginary parts:

$$\begin{aligned} X_1 &= X = \begin{pmatrix} X_{11} & X_{12} \\ X_{21} & X_{22} \end{pmatrix} = \begin{pmatrix} R_{11} & R_{12} \\ R_{21} & R_{22} \end{pmatrix} + \mathrm{i} \begin{pmatrix} I_{11} & I_{12} \\ I_{21} & I_{22} \end{pmatrix} \\ X_2 &= \widetilde{X} = \sigma_2 X^* \sigma_2 \\ &= \begin{pmatrix} X_{22}^* & -X_{21}^* \\ -X_{12}^* & X_{11}^* \end{pmatrix} = \begin{pmatrix} R_{22} & -R_{21} \\ -R_{12} & R_{11} \end{pmatrix} + \mathrm{i} \begin{pmatrix} -I_{22} & I_{21} \\ I_{12} & -I_{11} \end{pmatrix}. \end{aligned} \tag{6.20}$$

Thus, we can describe each pair of scalars X and $\widetilde{X}$ in terms of eight independent parameters. Now, we can identify 16 structurally different extremizing conditions, which take the form

$$\left.\frac{\partial V'_{\text{eff}}(X)}{\partial R_{ab}^{(0)}}\right|_{\text{VEVs}} = \left.\frac{\partial V'_{\text{eff}}(X)}{\partial I_{ab}^{(0)}}\right|_{\text{VEVs}} = \left.\frac{\partial V'_{\text{eff}}(X)}{\partial R_{ab}^{(r)}}\right|_{\text{VEVs}} = \left.\frac{\partial V'_{\text{eff}}(X)}{\partial I_{ab}^{(r)}}\right|_{\text{VEVs}} = 0, \tag{6.21}$$

where the indices a, b, and r run over $a, b = 1, 2$ and $r = 1, 2, \ldots, \infty$. Note that only squared and quartic terms appear in the potential. It is important for our further analysis to notice that there are no cubic terms in $X_i^{(0)}$, since these are forbidden by the orthogonality of the y–integration. We can identify the basic building–blocks which build up the complete potential as

$$\begin{aligned} \operatorname{tr} A^\dagger B &= \operatorname{tr}\Big[\Big(A^R\Big)^T - \mathrm{i}\Big(A^I\Big)^T\Big]\Big[B^R + \mathrm{i}B^I\Big] \\ &= \operatorname{tr}\left\{\Big(A^R\Big)^T B^R + \Big(A^I\Big)^T B^I + \mathrm{i}\Big[\Big(A^R\Big)^T B^I - \Big(A^I\Big)^T B^R\Big]\right\} \\ &= \sum_{a,b}^{2}\left\{A_{ab}^R B_{ab}^R + A_{ab}^I B_{ab}^I + \mathrm{i}\Big[A_{ab}^R B_{ab}^I - A_{ab}^I B_{ab}^R\Big]\right\}, \end{aligned} \tag{6.22a}$$

$$\begin{aligned} \operatorname{tr} A^\dagger B \operatorname{tr} C^\dagger D &= \sum_{a,b}^{2}\left\{A_{ab}^R B_{ab}^R + A_{ab}^I B_{ab}^I + \mathrm{i}\Big[A_{ab}^R B_{ab}^I - A_{ab}^I B_{ab}^R\Big]\right\} \\ &\qquad \left\{C_{ab}^R D_{ab}^R + C_{ab}^I D_{ab}^I + \mathrm{i}\Big[C_{ab}^R D_{ab}^I - C_{ab}^I D_{ab}^R\Big]\right\}, \end{aligned} \tag{6.22b}$$

$$\begin{aligned} \operatorname{tr} A^\dagger B C^\dagger D &= \Big(A_{11}B_{11} + A_{21}B_{21}\Big)\Big(C_{11}D_{11} + C_{21}D_{21}\Big) \\ &+ \Big(A_{11}B_{12} + A_{21}B_{22}\Big)\Big(C_{12}D_{11} + C_{22}D_{21}\Big) \\ &+ \Big(A_{12}B_{11} + A_{22}B_{21}\Big)\Big(C_{11}D_{12} + C_{21}D_{22}\Big) \\ &+ \Big(A_{12}B_{12} + A_{22}B_{22}\Big)\Big(C_{12}D_{12} + C_{22}D_{22}\Big), \end{aligned} \tag{6.22c}$$

where A, B, C, and D, are arbitrary complex 2×2 matrices and the indices R and I denote the real and the imaginary parts, respectively. The product $A_{ab}B_{ab}$ is given by $A_{ab}B_{ab} = A^R_{ab}B^R_{ab} + A^I_{ab}B^I_{ab} + \mathrm{i}\big[A^R_{ab}B^I_{ab} - A^I_{ab}B^R_{ab}\big]$. Considering derivatives with respect to $R^{(0)}_{ab}$ or $I^{(0)}_{ab}$, we see that terms containing solely either $X^{(0)}_1$ or $X^{(0)}_2$ can be nonzero, *i.e.*, we are left with the 8 extremizing conditions

$$\left.\frac{\partial V'^0_{\text{eff}}(X)}{\partial R^{(0)}_{ab}}\right|_{\text{VEVs}} = \left.\frac{\partial V'^0_{\text{eff}}(X)}{\partial I^{(0)}_{ab}}\right|_{\text{VEVs}} = 0, \tag{6.23}$$

where

$$\begin{aligned} V'^0_{\text{eff}}(X) = \; & - \sum_{i,j} \mu^2_{ij} \mathrm{tr}\, X^{(0)\dagger}_i X^{(0)}_j + \frac{1}{(\pi R)} \sum_{i,j,k,l} \Big\{ \lambda_{ijkl} \mathrm{tr}\, X^{(0)\dagger}_i X^{(0)}_j \mathrm{tr}\, X^{(0)\dagger}_k X^{(0)}_l \\ & + \widetilde{\lambda}_{ijkl}\, \mathrm{tr}\, X^{(0)\dagger}_i X^{(0)}_j X^{(0)\dagger}_k X^{(0)}_l \Big\}. \end{aligned} \tag{6.24}$$

This result is a consequence of the fact that after differentiating with respect to $R^{(r)}_{ab}$ or $I^{(r)}_{ab}$, only terms which are linear in $X^{(0)}_1$ or $X^{(0)}_2$ can be nonzero. However, as mentioned above, there are no such terms, *i.e.*, the extremizing conditions

$$\left.\frac{\partial V'_{\text{eff}}(X)}{\partial R^{(r)}_{ab}}\right|_{\text{VEVs}} = \left.\frac{\partial V'_{\text{eff}}(X)}{\partial I^{(r)}_{ab}}\right|_{\text{VEVs}} = 0, \tag{6.25}$$

are always satisfied for the VEVs given here. Now, let us have a closer look at the non-vanishing derivatives in Eqs. (6.23). In Eqs. (6.22a) – (6.22c), only terms linear in the off–diagonal elements could be nonzero. Again, there are no such terms. The obvious consequence is that

$$\text{for } a \neq b: \qquad \left.\frac{\partial V'_{\text{eff}}(X)}{\partial R^{(0)}_{ab}}\right|_{\text{VEVs}} = \left.\frac{\partial V'_{\text{eff}}(X)}{\partial I^{(0)}_{ab}}\right|_{\text{VEVs}} = 0, \tag{6.26}$$

is always satisfied by construction. Furthermore, when taking the derivative with respect to the diagonal elements, we can ignore every term containing at least one off–diagonal element, since these will be zero anyway.

Thus, the rules for the remaining equations are: When differentiating with respect to the real parts, all terms containing one or more imaginary parts will vanish for our VEVs. In the case of derivatives for the imaginary parts, only terms linear in these can survive. The fact that there are no terms linear in the imaginary parts implies that

$$\left.\frac{\partial V'^0_{\text{eff}}(X)}{\partial I^{(0)}_{11}}\right|_{\text{VEVs}} = \left.\frac{\partial V'^0_{\text{eff}(X)}}{\partial I^{(0)}_{22}}\right|_{\text{VEVs}} = 0 \tag{6.27}$$

is always satisfied. Therefore, our only non–trivial extremum conditions are

$$\left.\frac{\partial V'^0_{\rm eff}(X)}{\partial R^{(0)}_{11}}\right|_{\rm VEVs} = \left.\frac{\partial V'^0_{\rm eff}(X)}{\partial R^{(0)}_{22}}\right|_{\rm VEVs} = -2\sum_{i,j}\mu^2_{ij}\kappa + \frac{4}{(\pi R)}\sum_{i,j,k,l}(2\lambda_{ijkl}+\widetilde{\lambda}_{ijkl})\kappa^3 = A\kappa + (B+C)\kappa^3 = 0, \tag{6.28}$$

where we have used the substitution $A = -2\sum_{i,j}\mu^2_{ij}$, $B = \frac{4}{(\pi R)}\sum_{i,j,k,l}2\lambda_{ijkl}$, and $C = \frac{4}{(\pi R)}\sum_{i,j,k,l}\widetilde{\lambda}_{ijkl}$. Apart from the trivial and undesirable solutions $\kappa = 0$ or $A = B + C = 0$, our extremizing conditions in Eq. (6.28) are solved by

$$\kappa = \pm\sqrt{\frac{-A}{B+C}}. \tag{6.29}$$

VEVs are in general complex, but we can always perform a global phase rotation and absorb one phase into the fermion fields. The parameter κ can consequently, without loss of generality, be assumed to be real, in other words

$$\frac{-A}{B+C} > 0 \quad \text{and} \quad B + C \neq 0. \tag{6.30}$$

In Sec. 6.3, we will find a whole range of parameters for $\lambda_{ijkl} \sim \widetilde{\lambda}_{ijkl}$, where $B+C \neq 0$, since $B + C$ is linear in λ_{ijkl} and $\widetilde{\lambda}_{ijkl}$.

6.3 Minimum of the Potential

For a local minimum of the potential $V'_{\rm eff}$, the symmetric Hessian matrix

$$H\big(V'_{\rm eff}\big) = \left(\frac{\partial^2 V'_{\rm eff}}{\partial A^{(n)}_a \partial A^{(m)}_c}\right) \tag{6.31}$$

must be positive semi–definite, *i.e.*, the eigenvalues ρ_i of $H\big(V'_{\rm eff}\big)$ have to satisfy $\rho_i \geq 0$. In Eq. (6.31), we have $A^{(n)}_1 = R^{(n)}_{11}$, $A^{(n)}_2 = R^{(n)}_{12}$, $A^{(n)}_3 = R^{(n)}_{21}$, $A^{(n)}_4 = R^{(n)}_{22}$, $A^{(n)}_5 = I^{(n)}_{11}$, $A^{(n)}_6 = I^{(n)}_{12}$, $A^{(n)}_7 = I^{(n)}_{21}$, $A^{(n)}_8 = I^{(n)}_{22}$, and the indices run over $n, m = 1, 2, \ldots, \infty$. The explicit results for the 2nd derivatives of $V'_{\rm eff}$ in Eq. (6.31) are given in the Appendix B.1. The Hessian matrix of these derivatives is of the block–diagonal form

$$H\big(V'_{\rm eff}\big) = \begin{pmatrix} H^{(0)} & & & \\ & H^{(1)} & & 0 \\ & & \ddots & \\ & 0 & & H^{(n)} \\ & & & & \ddots \end{pmatrix}. \tag{6.32}$$

Due to this block–structure, H can be diagonalized by $H_{\rm diag} = S^\dagger H S$, where S is also a block–diagonal matrix. Consequently, we can consider for every KK mode a diagonalization equation of the type

$$H^{(i)}_{\rm diag} = {S^{(i)}}^\dagger H^{(i)} S^{(i)}, \tag{6.33}$$

where the index i runs over $i = 0, 1, 2, \ldots, \infty$. The symmetric matrix $H^{(0)}$ is given by

$$H^{(0)} = \begin{pmatrix} a^{(0)} & 0 & 0 & b^{(0)} & 0 & 0 & 0 & 0 \\ & c^{(0)} & c^{(0)} & 0 & 0 & 0 & 0 & 0 \\ & & c^{(0)} & 0 & 0 & 0 & 0 & 0 \\ & & & a^{(0)} & 0 & 0 & 0 & 0 \\ & & & & d^{(0)} & 0 & 0 & d^{(0)} \\ & & & & & c^{(0)} & -c^{(0)} & 0 \\ & & & & & & c^{(0)} & 0 \\ & & & & & & & d^{(0)} \end{pmatrix}, \tag{6.34}$$

where $a^{(0)}$, $b^{(0)}$, $c^{(0)}$, and $d^{(0)}$ are defined in Appendix B.1 and the corresponding eigensystem is

$$\begin{array}{rcll} \rho_1^{(0)} &=& a^{(0)} + b^{(0)} & \leftrightarrow \quad v_1 = \frac{1}{\sqrt{2}}(1,0,0,1,0,0,0,0)^T, \\ \rho_2^{(0)} &=& 2c^{(0)} & \leftrightarrow \quad v_3 = \frac{1}{\sqrt{2}}(0,1,1,0,0,0,0,0)^T, \\ \rho_3^{(0)} &=& 0 & \leftrightarrow \quad v_4 = \frac{1}{\sqrt{2}}(0,-1,1,0,0,0,0,0)^T, \\ \rho_4^{(0)} &=& a^{(0)} - b^{(0)} & \leftrightarrow \quad v_2 = \frac{1}{\sqrt{2}}(-1,0,0,1,0,0,0,0)^T, \\ \rho_5^{(0)} &=& 2d^{(0)} & \leftrightarrow \quad v_5 = \frac{1}{\sqrt{2}}(0,0,0,0,1,0,0,1)^T, \\ \rho_6^{(0)} &=& 0 & \leftrightarrow \quad v_7 = \frac{1}{\sqrt{2}}(0,0,0,0,0,1,1,0)^T, \\ \rho_7^{(0)} &=& 2c^{(0)} & \leftrightarrow \quad v_8 = \frac{1}{\sqrt{2}}(0,0,0,0,0,-1,1,0)^T, \\ \rho_8^{(0)} &=& 0 & \leftrightarrow \quad v_6 = \frac{1}{\sqrt{2}}(0,0,0,0,-1,0,0,1)^T. \end{array} \tag{6.35}$$

The second derivatives of the higher KK modes can be arranged as

$$H^{(n)} = \begin{pmatrix} a^{(n)} & 0 & 0 & b^{(n)} & 0 & 0 & 0 & 0 \\ & c^{(n)} & e^{(n)} & 0 & 0 & 0 & 0 & 0 \\ & & c^{(n)} & 0 & 0 & 0 & 0 & 0 \\ & & & a^{(n)} & 0 & 0 & 0 & 0 \\ & & & & d^{(n)} & 0 & 0 & f^{(n)} \\ & & & & & c^{(n)} & -e^{(n)} & 0 \\ & & & & & & c^{(n)} & 0 \\ & & & & & & & d^{(n)} \end{pmatrix}, \tag{6.36}$$

where $n \geq 1$ and $a^{(n)}$, $b^{(n)}$, $c^{(n)}$, $d^{(n)}$, $e^{(n)}$, and $f^{(n)}$ are defined in Appendix B.1. This gives the following eigensystem with eight nonzero eigenvalues:

$$\begin{array}{rcll}
\rho_1^{(n)} &=& a^{(0)} + b^{(0)} + 2K\left(\frac{n}{\pi R}\right) & \leftrightarrow \quad v_1 = \frac{1}{\sqrt{2}}(1,0,0,1,0,0,0,0)^T, \\
\rho_2^{(n)} &=& 2c^{(0)} + 2K\left(\frac{n}{\pi R}\right) & \leftrightarrow \quad v_3 = \frac{1}{\sqrt{2}}(0,1,1,0,0,0,0,0)^T, \\
\rho_3^{(n)} &=& 2K\left(\frac{n}{\pi R}\right) & \leftrightarrow \quad v_4 = \frac{1}{\sqrt{2}}(0,-1,1,0,0,0,0,0)^T, \\
\rho_4^{(n)} &=& a^{(0)} - b^{(0)} + 2K\left(\frac{n}{\pi R}\right) & \leftrightarrow \quad v_2 = \frac{1}{\sqrt{2}}(-1,0,0,1,0,0,0,0)^T, \\
\rho_5^{(n)} &=& 2d^{(0)} + 2K\left(\frac{n}{\pi R}\right) & \leftrightarrow \quad v_5 = \frac{1}{\sqrt{2}}(0,0,0,0,1,0,0,1)^T, \\
\rho_6^{(n)} &=& 2K\left(\frac{n}{\pi R}\right) & \leftrightarrow \quad v_7 = \frac{1}{\sqrt{2}}(0,0,0,0,0,1,1,0)^T, \\
\rho_7^{(n)} &=& 2c^{(0)} + 2K\left(\frac{n}{\pi R}\right) & \leftrightarrow \quad v_8 = \frac{1}{\sqrt{2}}(0,0,0,0,0,-1,1,0)^T, \\
\rho_8^{(n)} &=& 2K\left(\frac{n}{\pi R}\right) & \leftrightarrow \quad v_6 = \frac{1}{\sqrt{2}}(0,0,0,0,-1,0,0,1)^T.
\end{array} \tag{6.37}$$

For the zero mode ($n = 0$), we get no further contributions from the kinetic terms. Hence, we find – in contrast to the higher modes – three Goldstone bosons for the zero mode. These are eaten to give mass to three spin–1 vector states of $SU(2)_L \times SU(2)_R/SU(2)_D$ in the course of the gauge symmetry breaking $SU(2)_L \times SU(2)_R \to SU(2)_D$. H is positive semi–definite when the potential satisfies the conditions

$$a^{(0)} > |b^{(0)}|, \quad c^{(0)} > 0, \quad d^{(0)} > 0. \tag{6.38}$$

Let us have a more detailed look at the definition of these eigenvalues in Eq. (B.7) – (B.10): The parameters μ_{ij} and the factor $1/R$ have mass dimension +1, while the parameters λ_{ijkl} and $\widetilde{\lambda}_{ijkl}$ have mass dimension −1. Furthermore, we see from Eq. (6.29) that the VEV has mass dimension +1 (as it must be), and the eigenvalues have mass dimension +2, since they are mass squares.

In order to discuss the parameter space in which the minimum conditions of Eq. (6.38) are satisfied, we can first consider the simple case of the SM Higgs potential (*cf.* Sec. (2.1.2). The SM Higgs VEV remains constant, when we change μ and λ to the same extent, *i.e.*, there are two extreme limits: (i) $\mu^2 \to 0$ and at the same time $\lambda \to 0$ and (ii) $\mu^2 \to \infty$ and simultaneously $\lambda \to \infty$. However, since the Higgs mass in the SM is given by $m_H = \sqrt{2\mu^2}$ and we have a lower limit of $m_H > 114\,\text{GeV}$ from LEP data, we know that (i) becomes unphysical when μ^2 becomes too small. For case (ii), which is known as the non–linear sigma model, we encounter the problem that the theory becomes non–perturbative for large values of λ.

In the following, we will show that it is always possible to find a reasonable parameter space, where Eqs. (6.28) and (6.38) are satisfied. As the radius of the extra dimension we will take $1/R \sim 100\,\text{TeV}$. Analogous to the SM case, we substitute $\lambda_{ijkl}/(\pi R) \simeq \widetilde{\lambda}_{ijkl}/(\pi R) = r_0^1$ and $\mu_{ij}^2 = (r_1^{100} \times 100\,\text{GeV})^2$, where r_0^1 and r_1^{100} denote random numbers in the range $[0,1]$ and $[1,100]$, respectively. In Eq. (B.11), one can convince oneself that the scaling of λ_{ijkl} and $\widetilde{\lambda}_{ijkl}$ does not much affect the minimum conditions for given μ_{ij}^2, but it has a significant effect on the VEV. Even if the absolute scaling is not crucial for the minimum conditions, the relative scaling is more

important, since it determines the sign of the eigenvalues of the Hessian matrix. We can analyze the parameter space for the minimum in more detail by using a large setup of random numbers for μ_{ij}, λ_{ijkl}, and $\widetilde{\lambda}_{ijkl}$. Fig. 6.2 shows the parameter range of the VEV κ, while Fig. 6.3 show the range of the eigenvalues $\rho_1^{(0)}$, $\rho_2^{(0)}$, $\rho_4^{(0)}$, and $\rho_5^{(0)}$, respectively. We have used here 10^4 random sets. The picture does not change much, if we enlarge the number of random sets up to 10^6. In this case, the range of the VEV is

$$\kappa \in [3.44 \times 10^{10}, 4.02 \times 10^{12}], \tag{6.39}$$

and the ranges of the eigenvalues are

$$\begin{aligned}
&\rho_1^{+(0)} \in [2.28 \times 10^{23}, 1.59 \times 10^{27}], && \rho_1^{-(0)} \in \varnothing, \\
&\rho_2^{+(0)} \in [4.96 \times 10^{20}, 6.24 \times 10^{26}], && \rho_2^{-(0)} \in [-5.14 \times 10^{26}, -6.55 \times 10^{19}], \\
&\rho_4^{+(0)} \in [8.25 \times 10^{19}, 5.63 \times 10^{26}], && \rho_4^{-(0)} \in [-5.27 \times 10^{26}, -9.50 \times 10^{19}], \\
&\rho_5^{+(0)} \in [3.64 \times 10^{19}, 6.19 \times 10^{26}], && \rho_5^{-(0)} \in [-6.71 \times 10^{26}, -3.56 \times 10^{20}],
\end{aligned} \tag{6.40}$$

where $\rho_i^{\pm(0)}$ denotes the positive (+) negative (-) values of the ith eigenvalues. Obviously, $\rho_1^{(0)}$ is positive for every setup. But for $\rho_2^{(0)}$, $\rho_4^{(0)}$, and $\rho_5^{(0)}$, the parameter space seems to be approximately symmetric with respect to zero. We thus have to count all the random number sets for which all eigenvalues are positive. For 10^4 and 10^6 random sets we find about 4×10^3 and 4×10^6 cases, where all eigenvalues are positive.

In order to see that the sign of the eigenvalues mainly depends on the relative ratio of the μ_{ij}, we can assume $\lambda_{ijkl} \simeq \widetilde{\lambda}_{ijkl} \simeq 1$ and view the eigenvalues $\rho_1^{(0)}$, $\rho_2^{(0)}$, $\rho_4^{(0)}$, and $\rho_5^{(0)}$, as functions of μ_{12} and $\mu_{11} = \mu_{22}$. This is shown in Fig. 6.4. Obviously, we can always find a parameter space where all eigenvalues are positive. But this positiveness is mainly determined by the μ_{ij}. In contrast to the zero mode, the mass matrix $H^{(n)}$ ($n \geq 1$) is positive definite if

$$a^{(0)} + 2K\Big(\frac{n}{\pi R}\Big) > |b^{(0)}|, \quad c^{(0)} + K\Big(\frac{n}{\pi R}\Big) > 0, \quad d^{(0)} + K\Big(\frac{n}{\pi R}\Big) > 0, \quad K > 0, \tag{6.41}$$

which is always satisfied as long as the compactification scale $1/R$ is large enough and $K > 0$. As a consequence, the mass squares are

$$M_n^2(X) = \Big[-\mu^2 + \Big(\frac{n}{\pi R}\Big)^2 \Big] \Big[1 - \frac{K'_X}{\pi R} + \ldots \Big], \tag{6.42}$$

where $n \geq 0$ and the mass–square μ^2 is determined by the coefficients in Eq. (6.18).

6.4 Brane–Localized Operator

The VEV in Eq. (6.19) is only determined up to a unitary transformation. This freedom can be fixed by introducing a suitable operator which can become important

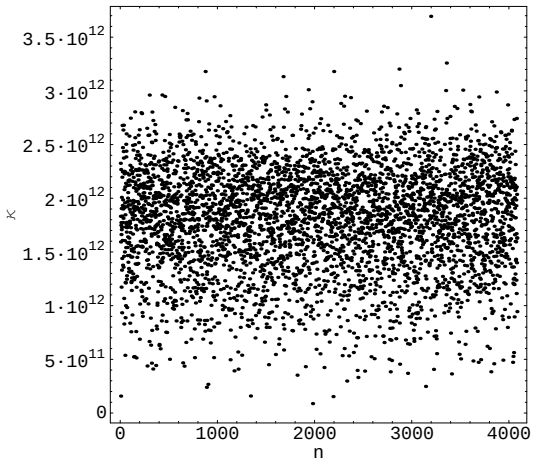

Figure 6.2: Different values of the VEV κ, using 10^4 random sets for the parameters μ_{ij}^2 and λ_{ijkl} and $\widetilde{\lambda}_{ijkl}$. The x–axis denotes the number n of the set. Only random number sets have been taken into account, for which all eigenvalues are non–negative.

for the vacuum alignment of several Higgs fields. We have the freedom to write down explicit terms on the branes, as long as they leave the local symmetries on the branes unbroken. At $y = \pi R$, let us therefore add the operator

$$V_B(X) = \delta(y - \pi R) \sum_{i,j} [-\mu_i^2 \, \mathrm{tr}(X_i) + \lambda_{ij} \, \mathrm{tr}(X_i)\mathrm{tr}(X_j) + \widetilde{\lambda}_{ij} \, \mathrm{tr}(X_i X_j)], \qquad (6.43)$$

which leaves $SU(2)_D$ invariant. In Eq. (6.43), μ_i, λ_{ij}, and $\widetilde{\lambda}_{ij}$ are real, such that these parameters satisfy

$$\mu_i = \mu_j, \quad \lambda_{ii} = \lambda_{jj}, \quad \lambda_{ij} = \lambda_{ji}, \quad \widetilde{\lambda}_{ii} = \widetilde{\lambda}_{jj}, \quad \text{and} \quad \widetilde{\lambda}_{ij} = \widetilde{\lambda}_{ji}. \qquad (6.44)$$

Now, we split the operator into $V_B(X) = A_B(X) + B_B(X)$, where $B_B(X)$ only consists of mixed terms in X and $\widetilde{X}$, while $A_B(X)$ contains all the remaining terms. After integrating over y, we get the 4D effective operator $V_{B\mathrm{eff}}(X) = A_{B\mathrm{eff}}(X) + B_{B\mathrm{eff}(X)}$. For the explicit expressions for $A_{B\mathrm{eff}}(X) = \int_0^{\pi R} dy A_B(X)$ and $B_{B\mathrm{eff}}(X) = \int_0^{\pi R} dy B_B(X)$ see Eqs. (B.21) and (B.22) in Appendix B.2. From the extremizing conditions of $V_B(X)$ in Appendix B.2, it can be seen that for real VEVs, $\langle X^{(n)} \rangle = \langle \widetilde{X}^{(n)} \rangle = 0$ $(n = 1, \ldots, \infty)$ and $\lambda_{11} \neq \lambda_{12}$ can only be satisfied, if the off–diagonal VEVs are

$$\langle R_{12}^{(0)} \rangle = \langle R_{21}^{(0)} \rangle = 0. \qquad (6.45)$$

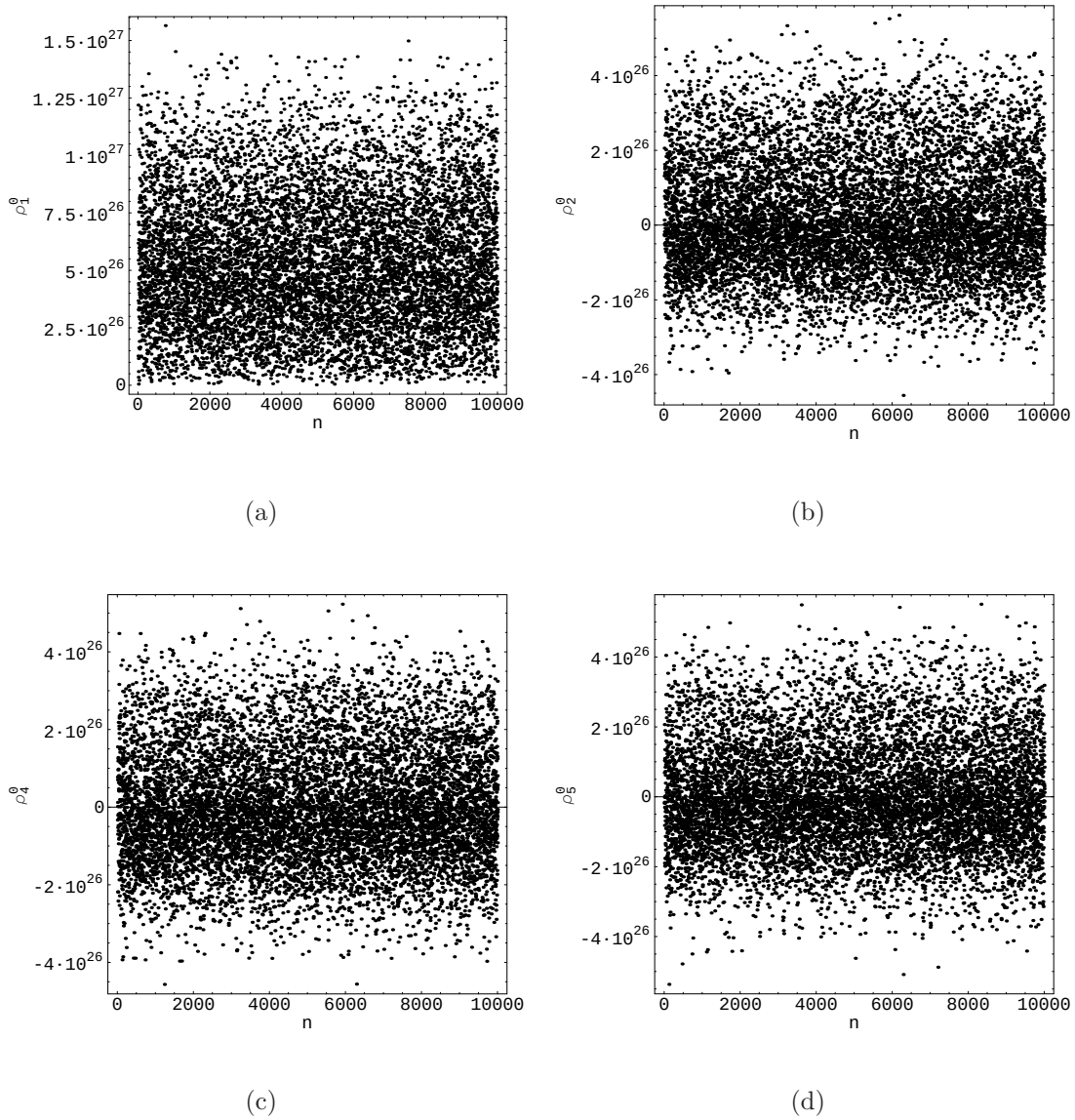

Figure 6.3: Different values of the zero–mode eigenvalues $\rho_1^{(0)}$ (a), $\rho_2^{(0)}$ (b), $\rho_4^{(0)}$ (c), and $\rho_5^{(0)}$ (d) , using 10^4 random sets for the parameters μ_{ij}^2 and λ_{ijkl} and $\widetilde{\lambda}_{ijkl}$. The x–axis shows the label n of the sets. For $\rho_1^{(0)}$, there are only positive values, while all the other eigenvalues are almost symmetrically arranged around zero. For 4×10^3 sets all eigenvalues are simultaneously non-negative. Thus, we see that there is always a reasonable parameter space for which the minimum conditions given in Eq. (6.38) are satisfied.

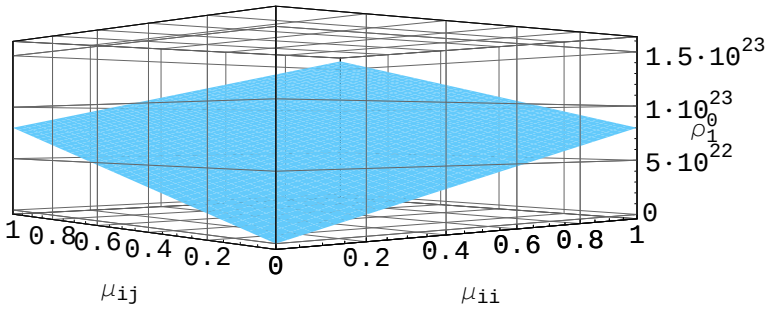

(a)

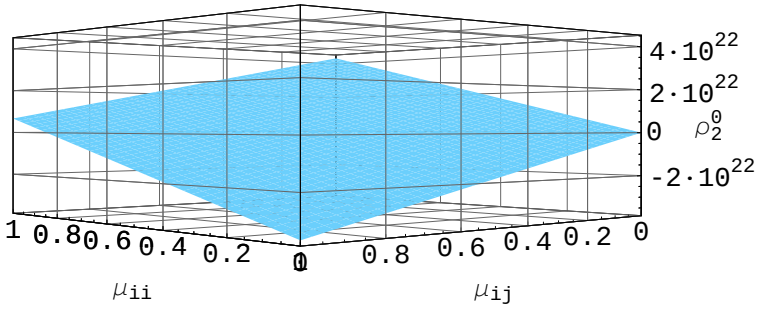

(b)

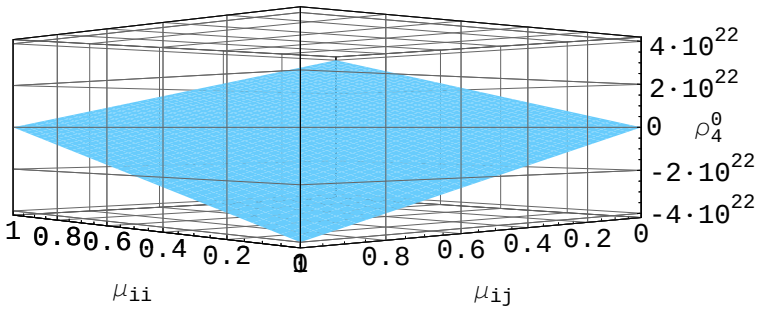

(c)

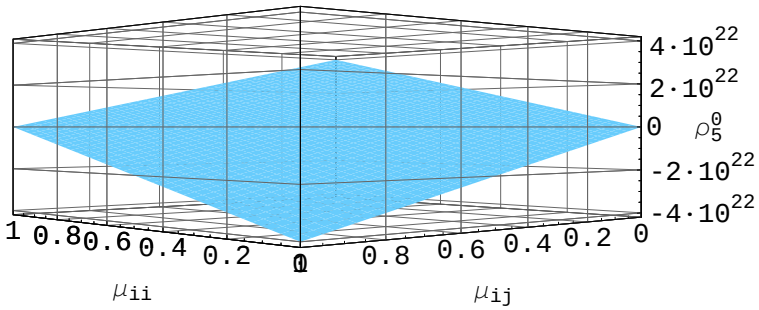

(d)

Figure 6.4: Different values of the zero–mode eigenvalues $\rho_1^{(0)}$ (a), $\rho_2^{(0)}$ (b), $\rho_4^{(0)}$ (c), and $\rho_5^{(0)}$ (d) as functions of μ_{12} and $\mu_{11} = \mu_{22}$, assuming $\lambda_{ijkl} \simeq \widetilde{\lambda}_{ijkl} \simeq 1$. As we can see $\rho_1^{(0)}$ is always positive, while the signs of all the other eigenvalues crucially depend on μ_{12} and $\mu_{11} = \mu_{22}$. Again, we can always find an reasonable space of parameters for which all eigenvalues are non-negative.

The diagonal VEVs have to satisfy

$$-\mu_1^2\frac{2}{\sqrt{\pi R}}+\frac{4}{\pi R}\left[(\lambda_{11}+\lambda_{12}+\widetilde{\lambda}_{11})\langle R_{11}^{(0)}\rangle+(\lambda_{11}+\lambda_{12}+\widetilde{\lambda}_{12})\langle R_{22}^{(0)}\rangle\right]=0, \quad (6.46)$$

$$-\mu_1^2\frac{2}{\sqrt{\pi R}}+\frac{4}{\pi R}\left[(\lambda_{11}+\lambda_{12}+\widetilde{\lambda}_{11})\langle R_{22}^{(0)}\rangle+(\lambda_{11}+\lambda_{12}+\widetilde{\lambda}_{12})\langle R_{11}^{(0)}\rangle\right]=0, \quad (6.47)$$

for $\mu_1 \neq 0$. Since $\langle R_{11}^{(0)}\rangle$ and $\langle R_{22}^{(0)}\rangle$ satisfy the same equations, they must be equal:

$$\langle R_{11}^{(0)}\rangle = \langle R_{22}^{(0)}\rangle = \kappa, \quad (6.48)$$

where

$$\kappa = \frac{\sqrt{\pi R}}{2}\frac{\mu_1^2}{2(\lambda_{11}+\lambda_{12})+\widetilde{\lambda}_{11}+\widetilde{\lambda}_{12}}. \quad (6.49)$$

Consequently, we can see that $2(\lambda_{11}+\lambda_{12})+\widetilde{\lambda}_{11}+\widetilde{\lambda}_{12} \neq 0$ must hold for an extremum. Actually, the VEV also should not be close to this pole in order to be physical.

We thus conclude that the brane–localized potential $V_{B\text{eff}}$ aligns the VEV of $X^{(0)}$ such that it is proportional to the identity matrix, *i.e.*,

$$\langle X^{(0)}\rangle = \kappa_X \cdot \mathrm{diag}(1,1). \quad (6.50)$$

The presence of the operator $V_{B\text{eff}}(X)$ therefore completely fixes the structure of the VEVs. In order to check whether this potential really has a minimum for this VEVs, we will next calculate the Hessian matrix for the total potential.

6.5 Minimum of the Total Potential

In order to discuss the minimum of the total potential $V_{\text{eff}}^{\text{total}} = (V'_{\text{eff}} + V_{B\text{eff}})$, we will start with the minimum of $V_{B\text{eff}}$. We identify 208 structurally different second derivatives. From Eqs. (B.21) and (B.22), we can see that there is no mixing between real and imaginary parts due to Hermiticity, *i.e.*,

$$\frac{\partial^2 V_{B\text{eff}}(X)}{\partial R_{ab}^{(0)}\partial I_{cd}^{(0)}} = \frac{\partial^2 V_{B\text{eff}}(X)}{\partial R_{ab}^{(0)}\partial I_{cd}^{(n)}} = \frac{\partial^2 V_{B\text{eff}}(X)}{\partial R_{ab}^{(n)}\partial I_{cd}^{(0)}} = \frac{\partial^2 V_{B\text{eff}}(X)}{\partial R_{ab}^{(n)}\partial I_{cd}^{(n)}} = \frac{\partial^2 V_{B\text{eff}}(X)}{\partial R_{ab}^{(n)}\partial I_{cd}^{(m)}} = 0, \quad (6.51)$$

where $a,b,c,d = 1,2$. Furthermore, there is no mixing between diagonal and off-diagonal elements:

$$\begin{aligned}\frac{\partial^2 V_{B\text{eff}}(X)}{\partial R_{aa}^{(0)}\partial R_{cd}^{(0)}} = \frac{\partial^2 V_{B\text{eff}}(X)}{\partial I_{aa}^{(0)}\partial I_{cd}^{(0)}} = \frac{\partial^2 V_{B\text{eff}}(X)}{\partial R_{aa}^{(0)}\partial R_{cd}^{(n)}} = \frac{\partial^2 V_{B\text{eff}}(X)}{\partial I_{aa}^{(0)}\partial I_{cd}^{(n)}} = \frac{\partial^2 V_{B\text{eff}}(X)}{\partial R_{aa}^{(n)}\partial R_{cd}^{(0)}} &= \\ \frac{\partial^2 V_{B\text{eff}}(X)}{\partial I_{aa}^{(n)}\partial I_{cd}^{(0)}} = \frac{\partial^2 V_{B\text{eff}}(X)}{\partial R_{aa}^{(n)}\partial R_{cd}^{(n)}} = \frac{\partial^2 V_{B\text{eff}}(X)}{\partial I_{aa}^{(n)}\partial I_{cd}^{(n)}} = \frac{\partial^2 V_{B\text{eff}}(X)}{\partial R_{aa}^{(n)}\partial R_{cd}^{(m)}} = \frac{\partial^2 V_{B\text{eff}}(X)}{\partial I_{aa}^{(n)}\partial I_{cd}^{(m)}} &= 0.\end{aligned} \quad (6.52)$$

The detailed expressions for the remaining 2nd order derivatives are given in Appendix B.3. Taking all of them together, we find the associated Hessian matrix

$$H\big(V_{B\text{eff}}\big) = \left(\frac{\partial^2 V'_{\text{eff}}}{\partial A_a^{(n)} \partial A_c^{(m)}}\right) \tag{6.53}$$

belonging to the operator potential $V_{B\text{eff}}$. This matrix can be written as

$$H\big(V_{B\text{eff}}\big) = \begin{pmatrix} H^{(0)(0)} & H^{(0)(1)} & \dots & H^{(0)(n)} & \dots \\ H^{(1)(0)} & H^{(1)(1)} & \dots & H^{(1)(n)} & \dots \\ \vdots & \vdots & \ddots & & \\ H^{(n)(0)} & H^{(n)(1)} & & H^{(n)(n)} & \\ \vdots & \vdots & & & \ddots \end{pmatrix}, \tag{6.54}$$

where the sub–matrices $H^{(i)(j)}$ $(i, j = 0, 1, 2, \infty)$ are defined by

$$H^{(i)(j)} = \begin{pmatrix} H_R^{(i)(j)} & 0 \\ 0 & H_I^{(i)(j)} \end{pmatrix}, \tag{6.55}$$

where

$$H_R^{(0)(0)} = \frac{4}{\pi R} \begin{pmatrix} \lambda_{11} + \lambda_{12} + \widetilde{\lambda}_{11} & 0 & 0 & \lambda_{11} + \lambda_{12} + \widetilde{\lambda}_{12} \\ 0 & -\widetilde{\lambda}_{12} & \widetilde{\lambda}_{11} & 0 \\ 0 & \widetilde{\lambda}_{11} & -\widetilde{\lambda}_{12} & 0 \\ \lambda_{11} + \lambda_{12} + \widetilde{\lambda}_{12} & 0 & 0 & \lambda_{11} + \lambda_{12} + \widetilde{\lambda}_{11} \end{pmatrix}, \tag{6.56}$$

$$H_I^{(0)(0)} = -\frac{4}{\pi R} \begin{pmatrix} \lambda_{11} - \lambda_{12} - \widetilde{\lambda}_{11} & 0 & 0 & \lambda_{11} - \lambda_{12} - \widetilde{\lambda}_{12} \\ 0 & \widetilde{\lambda}_{12} & \widetilde{\lambda}_{11} & 0 \\ 0 & \widetilde{\lambda}_{11} & \widetilde{\lambda}_{12} & 0 \\ \lambda_{11} - \lambda_{12} - \widetilde{\lambda}_{12} & 0 & 0 & \lambda_{11} - \lambda_{12} - \widetilde{\lambda}_{11} \end{pmatrix}, \tag{6.57}$$

and

$$\begin{gathered} H_{R,I}^{(n)(n)} = 2H_{R,I}^{(0)(0)}, \quad H_{R,I}^{(0)(n)} = \sqrt{2}\cos(n\pi) H_{R,I}^{(0)(0)}, \\ H_{R,I}^{(n)(m)} = 2\cos(n\pi)\cos(m\pi) H_{R,I}^{(0)(0)}. \end{gathered} \tag{6.58}$$

The sum $H = H\big(V'_{\text{eff}}\big) + H\big(V_{B\text{eff}}\big)$ of both potentials reads

$$H = \begin{pmatrix} H^{(0)} + H^{(0)(0)} & -\sqrt{2}H^{(0)(0)} & \sqrt{2}H^{(0)(0)} & \dots & \sqrt{2}c_n H^{(0)(0)} & \dots \\ -\sqrt{2}H^{(0)(0)} & H^{(1)} + 2H^{(0)(0)} & -2H^{(0)(0)} & \dots & -2c_n H^{(0)(0)} & \dots \\ \sqrt{2}H^{(0)(0)} & -2H^{(0)(0)} & H^{(2)} + 2H^{(0)(0)} & & & \\ \vdots & \vdots & & \ddots & & \\ \sqrt{2}c_n H^{(0)(0)} & -2c_n H^{(0)(0)} & & & H^{(n)} + 2H^{(0)(0)} & \\ \vdots & \vdots & & & & \ddots \end{pmatrix}, \tag{6.59}$$

where $c_n = \cos(n\pi)$. In order to get rid of the periodic minus signs, we can perform a field–redefinition for the scalars $X^{(n)} \to X'^{(n)} = (-1)^n X^{(n)}$. This leads to $\cos(n\pi)X^{(n)} = X'^{(n)}$.

The total mass matrix in Eq. (6.59) can be discussed in terms of time–independent perturbation theory [137]. This is a valid Ansatz under the assumption that the matrix $H^{(0)(0)}$ can be understood as a sufficiently small perturbation, *i.e.*, for

$$\kappa^2\lambda_{ijkl}, \kappa^2\widetilde{\lambda}_{ijkl} \gg \lambda_{ij}, \widetilde{\lambda}_{ij}. \tag{6.60}$$

In perturbation theory, we consider an operator H, which is the sum an operator $H\big(V'_{\rm eff}\big) = H_0$ and a sufficiently small perturbation $H\big(V_{B\rm eff}\big) = H'$, *i.e.*,

$$H = H_0 + H'. \tag{6.61}$$

The eigenvalues of H_0 are $\rho_1^{(m)0}$, $\rho_2^{(m)0}$, $\ldots$, $\rho_n^{(m)0}$, $\ldots$, where $m = 0, 1, 2, \ldots$ The eigenvalues $\rho_n^{(m)0}$ are associated with a complete orthonormal set of eigenvectors $|v_n^0\alpha\rangle$, where the label α distinguishes in the case of degenerate eigenvalues the eigenvectors belonging to $\rho_n^{(m)0}$, *i.e.*, $H_0|v_n^0\alpha\rangle = \rho_n^{(m)0}|v_n^0\alpha\rangle$. We want to solve the perturbed eigenvalue equation $H|v_n\alpha\rangle = \rho_n^{(m)}|v_n^0\alpha\rangle$. The common procedure is to calculate the eigenvectors up to first order and the eigenvalues up to second order in perturbation theory. For non–degenerate perturbation theory, we have the relations

$$\rho_n^{(m)} \approx \rho_n^{(m)0} + \langle v_n^0|H'|v_n^0\rangle + \sum_{i\neq n}\sum_{\alpha}\frac{|\langle v_i^0\alpha|H'|v_n^0\rangle|^2}{\rho_n^{(m)0} - \rho_i^{(m)0}}, \tag{6.62a}$$

$$|v_n\rangle \approx |v_n^0\rangle + \sum_{i\neq n}\sum_{\alpha}\frac{\langle v_i^0\alpha|H'|v_n^0\rangle}{\rho_n^{(m)0} - \rho_i^{(m)0}}|v_i^0\alpha\rangle. \tag{6.62b}$$

Let us first concentrate on the eigenvalues of the higher KK modes, *i.e.*, $n \geq 1$. The first important point is that these eigenvalues are non–degenerate. Moreover, the block–diagonal 8×8 sub–matrices of the unperturbed and the perturbation matrix are structurally similar. We therefore find that $\langle v_i^0\alpha|H^{(0)(0)}|v_n^0\rangle = 0$, for $i \neq n$, and consequently $|v_n\rangle = |v_n^0\rangle$. The perturbed eigenvalues are

$$\begin{array}{lllllll}
\rho_1^{(n)} &=& a^{(n)} + b^{(n)} + \delta_1, & \rho_2^{(n)} &=& c^{(n)} + e^{(n)} + \delta_2, \\
\rho_3^{(n)} &=& c^{(n)} - e^{(n)} + \delta_3, & \rho_4^{(n)} &=& a^{(n)} - b^{(n)} + \delta_2, \\
\rho_5^{(n)} &=& d^{(n)} + f^{(n)} - \delta_4, & \rho_6^{(n)} &=& c^{(n)} - e^{(n)} + \delta_3, \\
\rho_7^{(n)} &=& c^{(n)} + e^{(n)} + \delta_2, & \rho_8^{(n)} &=& d^{(n)} - f^{(n)} + \delta_2,
\end{array} \tag{6.63}$$

where $\delta_1 = \frac{8}{\pi R}[2(\lambda_{11} + \lambda_{12}) + \widetilde{\lambda}_{11} + \widetilde{\lambda}_{12}]$, $\delta_2 = \frac{8}{\pi R}(\widetilde{\lambda}_{11} - \widetilde{\lambda}_{12})$, $\delta_3 = \frac{8}{\pi R}(-\widetilde{\lambda}_{11} - \widetilde{\lambda}_{12})$ and $\delta_4 = \frac{8}{\pi R}[2(\lambda_{11} - \lambda_{12}) - \widetilde{\lambda}_{11} - \widetilde{\lambda}_{12}]$. The discussion of the zero mode is more difficult, since some eigenvalues are degenerate. For the non–degenerate eigenvalues, we find

$$\rho_1^{(0)} = a^{(0)} + b^{(0)} + \frac{1}{2}\delta_1, \quad \rho_4^{(0)} = a^{(0)} - b^{(0)} + \frac{1}{2}\delta_2, \quad \rho_5^{(0)} = 2d^{(0)} - \frac{1}{2}\delta_4. \tag{6.64}$$

The possible values of $\rho_n^{(0)}$ are given by the eigenvalues of the $g_n \times g_n$ matrix

$$H'_{\alpha\beta} = \langle v_n^0 \beta | H' | v_n^0 \alpha \rangle. \tag{6.65}$$

For $\rho_2^{(0)} = \rho_7^{(0)} = 2c^{(0)}$, we have $H'_{\alpha\beta} = \frac{1}{2}\mathrm{diag}(\delta_2, \delta_2)$, and for $\rho_3^{(0)} = \rho_6^{(0)} = \rho_8^{(0)} = 0$, it follows that $H'_{\alpha\beta} = \frac{1}{2}\mathrm{diag}(\delta_3, \delta_3, \delta_2)$. The second order corrections are

$$V_{\gamma\beta} = \langle v_n^0 \gamma | H' | \sum_{i \neq n} \frac{\sum_\alpha |v_i^0 \alpha\rangle\langle v_i^0 \alpha|}{\rho_n^{(m)0} - \rho_i^{(m)0}} | H' | v_n^0 \beta \rangle. \tag{6.66}$$

However, due to the fact that $\langle v_i^0 \alpha | H^{(0)(0)} | v_n^0 \beta \rangle = 0$, for $i \neq n$, we can see that the second order corrections are all zero, *i.e.*, $V_{\gamma\beta} = 0$. Thus, we get up to second order

$$\begin{array}{lllllll} \rho_2^{(0)} & = & 2c^{(0)} + \frac{1}{2}\delta_2, & \rho_3^{(0)} & = & \frac{1}{2}\delta_3, & \rho_6^{(0)} = \frac{1}{2}\delta_3, \\ \rho_7^{(0)} & = & 2c^{(0)} + \frac{1}{2}\delta_2, & \rho_8^{(0)} & = & \frac{1}{2}\delta_2. & \end{array} \tag{6.67}$$

The Hessian of the total potential V'_{eff} and $V_{B\mathrm{eff}}$ is therefore positive semi–definite when the parameters satisfy the conditions

$$\widetilde{\lambda}_{12} \leq 0 \quad \text{and} \quad |\widetilde{\lambda}_{11}| \leq -\widetilde{\lambda}_{12}. \tag{6.68}$$

Thus, for a G_{LR} bi–doublet propagating on an interval in 5D flat space, we can always find a minimum for a suitable choice of parameter after dimensional reduction in the 4D effective theory. The VEVs in Eq. (6.19) lead to conditions for the parameters given in Eqs. (6.30), (6.38) and (6.41). The remaining freedom of a unitary transformation of the VEVs can be fixed by a brain localized term (*cf.*. Eq. (6.43)). Regarding this term as small perturbation of the scalar potential, the minimum is maintained if Eqs. (6.68) are satisfied.

Chapter 7

The Model

In this Chapter, we will discuss a new model for Dirac leptogenesis. This Dirac leptogenesis scenario is formulated in a geometry with three 5D throats and a LR symmetric gauge group in the bulk.

7.1 Geometry with Three Throats

Let us consider a 5D model defined on three intervals that are glued together at a single point as shown in Fig. 7.1. We will occasionally denote the intervals as throats (for a discussion, see Sec. 4.2). The coordinates on the three throats are respectively $z_1^M = (x^\mu, y_1), z_2^M = (x^\mu, y_2)$, and $z_3^M = (x^\mu, y_3)$, where the 5D Lorentz indices are denoted by capital Roman letters $M = 0, 1, 2, 3, 5$, while the usual 4D Lorentz indices are symbolized by Greek letters $\mu = 0, 1, 2, 3$, and the coordinates y_1, y_2, and y_3, describe the 5th dimension for the three throats. The physical space is thus defined by three bulks with $0 \leq y_1 \leq \pi R_1, 0 \leq y_2 \leq \pi R_2$, and $0 \leq y_3 \leq \pi R_3$, where R_1, R_2, and R_3, denote the size of the three bulks. We will call the intersection point at $y_1 = y_2 = y_3 = 0$ the UV brane, and denote the endpoints of the intervals at $z_1 = \pi R_1, z_2 = \pi R_2$, and $z_3 = \pi R_3$ as IR branes. Although this vocabulary is usually used for warped spacetime, we will throughout work in flat space. It is also useful to characterize this geometry by elements of the symmetric group S_3 that include Z_2 reflection symmetries interchanging the 1st and 2nd as well as the 2nd and 3rd throat (see Fig. 7.1). We will comment on these symmetries and how they are broken below.

The gauge group on the three intervals is that of the LR symmetric model $G_{LR} = SU(2)_L \times SU(2)_R \times U(1)_{B-L}$ (for a discussion see 4.1). The LR gauge bosons propagate freely in all three throats. The 5D lepton multiplets are in the G_{LR} representations

$$\psi_L = \begin{pmatrix} \nu_L \\ e_L \end{pmatrix} \; : \; (\tfrac{1}{2}, 0, -1), \qquad \psi_R = \begin{pmatrix} \nu_R \\ e_R \end{pmatrix} \; : \; (0, \tfrac{1}{2}, -1). \tag{7.1a}$$

We will assume here that the fermion fields are all localized at the UV brane. The

scalar sector contains three 5D Higgs multiplets χ, ϕ, and ξ, in the G_{LR} representations

$$\chi, \phi, \xi \,:\, (\tfrac{1}{2}, \tfrac{1}{2}, 0). \tag{7.1b}$$

They have the charge–decomposition

$$X = (X_u, X_d) = \begin{pmatrix} X_1^0 & X_1^+ \\ X_2^- & X_2^0 \end{pmatrix}, \quad \widetilde{X} = \epsilon X^* \epsilon = -\epsilon (X_d^*, X_u^*) = \begin{pmatrix} X_2^{0*} & -X_2^+ \\ -X_1^- & X_1^{0*} \end{pmatrix}, \tag{7.2}$$

where $X = \chi, \phi, \xi$, and ϵ is the antisymmetric 2×2 tensor. In Eq. (7.2), the up– and down–type Higgs doublets X_u and X_d are given by $X_u = (X_1^0, X_2^-)^T$, $X_d = (X_1^+, X_2^0)^T$, which transform under G_{LR} as $X_u, X_d \sim (\frac{1}{2}, 0, 0)$, and under $G_{\rm SM}$ as $X_u \sim (\frac{1}{2}, -1)$ and $X_d \sim (\frac{1}{2}, +1)$. In our setup, it is important that the three bi–doublets live on separate throats: χ propagates in the first, ϕ in the second, and ξ in the third throat.

The action of the gauge fields for the three bulks is given by

$$\mathcal{S}_{\rm gauge} = \int d^4x \sum_{i=1}^{3} \int_0^{\pi R_i} dy_i \, \mathcal{L}^i_{\rm gauge} + \text{h.c.}, \tag{7.3}$$

where $\mathcal{L}^i_{\rm gauge}$ is the 5D bulk Lagrangian in the ith throat. The gauge kinetic terms read

$$\mathcal{L}^i_{\rm gauge} = -\frac{M_L}{4} (F_L^a)_{MN} (F_L^a)^{MN} - \frac{M_R}{4} (F_R^a)_{MN} (F_R^a)^{MN} - \frac{M_B}{4} B_{MN} B^{MN}, \tag{7.4}$$

with field strengths $(F^a_{L,R})_{MN} = \partial_M A^a_{L,RN} - \partial_N A^a_{L,RM} + f^{abc} A^b_{L,RM} A^c_{L,RN}$ (f^{abc} is the structure constant and $a, b, c = 1, 2, 3$), $B_{MN} = \partial_M B_N - \partial_N B_M$. In Eq. (7.4), the quantities M_L, M_R, and M_B, have mass dimension +1, and the gauge fields A^a_{LM}, A^a_{RM}, and B_M, have mass dimension +1. We assume that at the IR brane in the first throat $y_1 = \pi R_1$, G_{LR} is broken to the SM gauge group $G_{LR} \to G_{\rm SM}$. Following Refs. [123, 124, 138], G_{LR} is broken by BCs to $G_{\rm SM}$ at the IR brane $y_1 = \pi R_1$ of the 1st throat. The BCs to achieve this symmetry breaking are

$$\text{at } y_1 = \pi R_1 \quad : \quad \partial_{y_1} A^{La}_\mu = 0, \; \partial_{y_1} A^{Ra}_\mu = 0, \; \partial_{y_1} B_\mu = 0, \; B_\mu - A^{R3}_\mu = 0, \tag{7.5}$$

where $A^{\pm a}_M$ is defined as $A^{\pm a}_M = \frac{1}{\sqrt{2}} (A^{La}_M \pm A^{Ra}_M)$. When χ acquires in the first throat a VEV $\langle \chi \rangle \sim \text{diag}(1, 1)$, G_{LR} is spontaneously broken as $G_{LR} \to SU(2)_D \times U(1)_{B-L}$. Together with the symmetry breaking via BCs [see Eq. (7.5)], the total surviving gauge group is then $U(1)_Q$ of electromagnetism. We will comment on the SSB via the Higgs VEV of χ in some more detail later in Sec. 7.2.

The kinetic terms of the fermions and scalars are given by

$$\mathcal{S}^{\rm kin}_{\rm fermion} = \int d^4x \sum_{i=1}^{3} \int_0^{\pi R_i} dy_i \, \mathcal{L}^i_{\rm fermion}, \tag{7.6a}$$

$$\mathcal{S}^{\rm kin}_{\rm scalar} = \int d^4x \Big(\int_0^{\pi R_1} dy_1 \, \mathcal{L}^{\rm kin}_{\chi,1} + \int_0^{\pi R_2} dy_2 \, \mathcal{L}^{\rm kin}_{\phi,2} + \int_0^{\pi R_3} dy_3 \, \mathcal{L}^{\rm kin}_{\xi,3} \Big), \tag{7.6b}$$

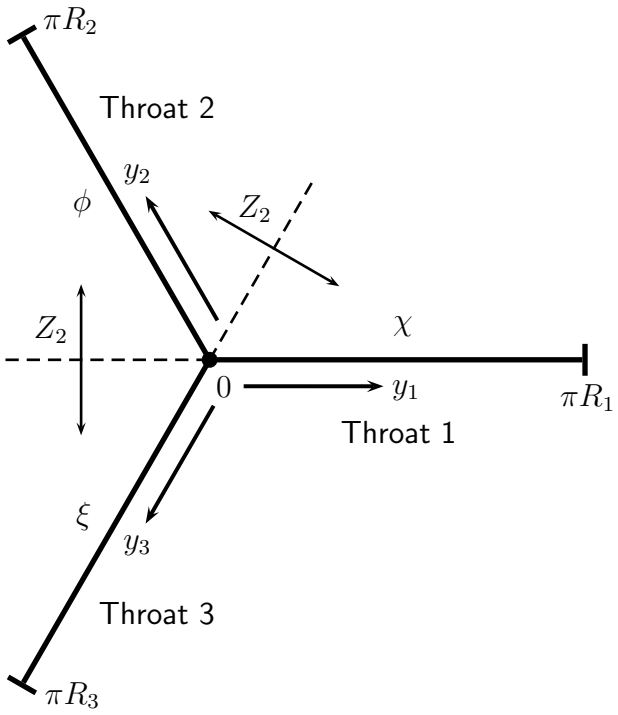

Figure 7.1: Geometry of the three throats (*cf.* Fig. 4.3). The throats are described by intervals with coordinates y_1, y_2, and y_3, and intersect in the UV brane at $y_1 = y_2 = y_3 = 0$. The scalar bi–doublets χ, ϕ, and ξ, are separately living on the 1st, 2nd, and 3rd throat, respectively. At the IR brane $y_1 = \pi R_1$, G_{LR} is broken to $G_{\rm SM}$ by BCs. The SM fermions are localized at the UV brane, whereas the LR gauge bosons propagate freely throughout the three throats. The throats are characterized by Z_2 reflection symmetries (see main text).

where the 5D Lagrangian densities are

$$\mathcal{L}^i_{\rm fermion} = \frac{1}{3}C\delta(y_i)\mathrm{i}(\overline{\psi}_L\Gamma^\mu D_\mu\psi_L + \overline{\psi}_R\Gamma^\mu D_\mu\psi_R) + \text{h.c.}, \tag{7.7a}$$

$$\mathcal{L}^{\rm kin}_{X,i} = [K_X + K'_X\delta(y_i)]\,\mathrm{tr}\,(D_M X)^\dagger D^M X, \tag{7.7b}$$

for $(X,i) = (\chi,1),(\phi,2),(\xi,3)$, and D_M is the covariant derivative with $D_M\psi_{L,R} = \partial_M\psi_{L,R} - \frac{1}{2}\mathrm{i}\sigma^a A^a_{L,RM}\psi_{L,R}$ and $D_M X = \partial_M X - \frac{1}{2}\mathrm{i}(\sigma^a A^a_{LM}X - X\sigma^a A^a_{RM})$. In Eq. (7.7), K_X is a dimensionless bulk kinetic parameter and K'_X and C are gauge kinetic parameters of 4D brane kinetic terms localized at $y_1 = 0$ and $y_1 = \pi R_1$ that have mass dimension -1. The scalars X have in Eq. (7.7) mass dimension $+3/2$, and the fermion doublets ψ_L and ψ_R, have mass dimension $+2$. Note also that we have absorbed in the covariant derivatives the dimensionful gauge coupling into a redefinition of the gauge fields.

From Eq. (7.6), one sees that χ,ϕ, and ξ propagate in the 1st, 2nd, and 3rd throat, respectively, while ψ_L and ψ_R are localized at the UV brane $y_1 = y_2 = y_3 = 0$. The 5D Yukawa couplings of the fermions to the scalars in the three throats read

$$\mathcal{S}_Y = \int d^4x\Big(\int_0^{\pi R_1} dy_1\,\mathcal{L}^Y_{\chi,1} + \int_0^{\pi R_2} dy_2\,\mathcal{L}^Y_{\phi,2} + \int_0^{\pi R_3} dy_3\,\mathcal{L}^Y_{\xi,3}\Big) + \text{h.c.}, \tag{7.8}$$

in which the 5D Yukawa coupling Lagrangians $\mathcal{L}^Y_{X,i}$ are defined as

$$\mathcal{L}^Y_{X,i} = \delta(y_i)\overline{\psi}_L(Y_X X + \widetilde{Y}_X\widetilde{X})\psi_R, \tag{7.9}$$

where Y_X and $\widetilde{Y}_X$ are the complex Yukawa couplings to X and $\widetilde{X}$, with $(X,i) = (\chi,1),(\phi,2),(\xi,3)$.

It is useful to discuss our model in terms of discrete symmetries acting on the scalar bi–doublets X. First of all, we assume the symmetry

$$D_1 \;:\; \chi \leftrightarrow \phi, \quad \text{throat } 1 \leftrightarrow \text{throat } 2. \tag{7.10}$$

The symmetry D_1 establishes among the Yukawa couplings the identities $Y_\chi = Y_\phi$ and $\widetilde{Y}_\chi = \widetilde{Y}_\phi$. Also, D_1 implies that $R_1 = R_2$. In the effective theory, however, D_1 is broken by the scalar masses as a consequence of choosing different BCs for χ and ϕ. These BCs and the scalar masses will be discussed in some more detail in Sec. 7.2.

In addition, we assume that the scalar sector is invariant under the Z_2 exchange symmetry

$$D_2 \;:\; \phi \leftrightarrow \xi, \quad \text{throat } 2 \leftrightarrow \text{throat } 3, \tag{7.11}$$

which corresponds in Fig. 7.1 to the Z_2 reflection symmetry with respect to the dashed line between the throats 2 and 3. The symmetry D_2 implies in Eq. (7.7b) for the scalars equal bulk kinetic terms

$$K_\phi = K_\xi \equiv K. \tag{7.12}$$

This symmetry is responsible for establishing a resonant decay amplitude of the scalars in leptogenesis. In particular, it implies that $R_2 = R_3$, *i.e.*, the 2nd and 3rd throat have equal size. Different from the symmetry D_1, however, D_2 remains almost completely intact in the scalar sector. The symmetry D_2 is broken at the UV brane $y_i = 0$ by the Yukawa couplings $Y_\phi \neq Y_\xi$ and $\widetilde{Y}_\phi \neq \widetilde{Y}_\xi$. Moreover, D_2 is broken by the brane kinetic terms $K'_\phi \neq K'_\xi$, which induces in the effective theory a tiny splitting between the 4D scalar degrees of freedom of ϕ and ξ, which is important for the value of the resonant decay amplitude of these fields. Although D_2 is broken by the Yukawa couplings, we will, in the following, require that the Yukawa couplings to ϕ and ξ are still roughly of the same order, *i.e.*, besides having already established $Y_\chi = Y_\phi$ and $\widetilde{Y}_\chi = \widetilde{Y}_\phi$ via the symmetry D_1, we assume that $Y_\phi \sim Y_\xi$ and $\widetilde{Y}_\phi \sim \widetilde{Y}_\xi$. We will outline a possible model building realization of this later, when discussing the origin of the Dirac Yukawa couplings in Sec. 7.3. The discrete symmetries and their breakings are summarized in Tab. 7.1.

In the following, we will, for simplicity, take the Yukawa couplings in Eq. (7.9) to be

symmetry	broken by
D_1	scalar masses (BCs)
D_2	brane kinetic terms, Yukawa couplings

Table 7.1: Discrete symmetries and the types of symmetry breaking terms.

of the type

$$\mathcal{L}^Y_{X,i} = \delta(y_i) Y_X \overline{\psi}_L (X + e^{\mathrm{i}\alpha_i} \widetilde{X}) \psi_R + \text{h.c.}, \tag{7.13}$$

where $\alpha_1 = \alpha_2 = \alpha, \alpha_3 = \beta$, and $Y_\chi = Y_\phi$. These Yukawa couplings are consistent with the discrete symmetry $D_3 : \ \chi \leftrightarrow e^{\mathrm{i}\alpha}\widetilde{\chi},\ \phi \leftrightarrow e^{\mathrm{i}\alpha}\widetilde{\phi},\ \xi \to e^{\mathrm{i}\beta}\widetilde{\xi}$. This discrete symmetry just serves here to simplify the discussion, but is, however, not important for the general features of our model. In a G_{SM}–invariant notation, the Yukawa couplings in Eq. (7.13) can be rewritten as

$$\mathcal{L}^Y_{X,i} = \delta(y_i) Y_X \left[\overline{\psi}_L (X_u - e^{\mathrm{i}\alpha_i} X^c_d)\nu_R + \overline{\psi}_L (X_d - e^{\mathrm{i}\alpha_i} X^c_u) e_R\right] + \text{h.c.}, \tag{7.14}$$

where the $SU(2)_L$ doublets ϕ_i and ξ_i $(i = 1, 2)$, are defined as in Eq. (7.2), and, in this notation, we have introduced $X^c_u = \epsilon X^*_u$ and $X^c_d = \epsilon X^*_d$. Like in Eq. (7.13), the symmetry D_1 implies in Eq. (7.14) that $Y_\chi = Y_\phi$.

In general, there can be a non–zero $X_u - X^c_d$ (and $X^c_u - X_d$) mixing between the doublets belonging to the same representation X, and we can write in the notation of Eq. (7.2) for each pair of doublets X_u and X_d the corresponding mass eigenstates $\widehat{X}_1$ and $\widehat{X}_2$ as

$$\begin{pmatrix} \widehat{X}_1 \\ \widehat{X}_2 \end{pmatrix} = V_X \begin{pmatrix} X_u \\ X^c_d \end{pmatrix} = \begin{pmatrix} c_X & -s_X \\ s_X & c_X \end{pmatrix} \begin{pmatrix} X_u \\ X^c_d \end{pmatrix} \quad \text{and} \quad \begin{pmatrix} \widehat{X}^c_1 \\ \widehat{X}^c_2 \end{pmatrix} = V_X \begin{pmatrix} X^c_u \\ X_d \end{pmatrix} \tag{7.15}$$

where $c_X = \cos(\alpha_X)$, $s_X = \sin(\alpha_X)$, and α_X is the mixing angle between X_u and X_d^c. We denote the mass of $\widehat{X}_1$ by M_{X_1} and the mass of $\widehat{X}_2$ by M_{X_2}, and suppose, like in the standard two–Higgs doublet model, that the mass splitting between M_{X_1} and M_{X_2} is, say, of the order of the EW scale. That means, $|M_{X_1} - M_{X_2}| \sim 1\,\text{TeV}$. Consequently, in terms of the Higgs doublet mass eigenstates, Eq. (7.14) reads

$$\begin{aligned}\mathcal{L}^Y_{X,i} &= \delta(y_i) Y_X \Big\{ \overline{\psi}_L \big[(c_X + e^{\mathrm{i}\alpha_i} s_X) \widehat{X}_1 - (e^{\mathrm{i}\alpha_i} c_X - s_X) \widehat{X}_2 \big] \nu_R \\ &- \overline{\psi}_L \big[(e^{\mathrm{i}\alpha_i} c_X + s_X) \widehat{X}_1^c - (c_X - e^{\mathrm{i}\alpha_i} s_X) \widehat{X}_2^c \big] e_R \Big\} + \text{h.c.}, \end{aligned} \tag{7.16}$$

where we have used the orthogonality of V_X, *i.e.*, $V_X^T V_X = 0$. Since the exact value of this splitting is not of particular importance for our considerations, we can assume that the mixing angles α_X are all very small, and will in the following always approximately identify the field $\widehat{X}_1$ with X_u and $\widehat{X}_2$ with X_d^c.

7.2 VEVs and Scalar Masses

One advantage of our multi–throat geometry is that the scalar fields are separated on different throats. We can thus write the total scalar potential of χ, ϕ, and ξ, as a sum

$$V_{\text{total}} = \sum_{X=\chi,\phi,\xi} V(X), \tag{7.17}$$

where $V(X)$ is a potential of the general form for a single scalar bi–doublet as given in Eq. (6.3). The important point is here that the mixing among the scalars vanishes. The scalar bi–doublets in the three throats are subject to the BCs

$$\text{at the UV brane} \;:\; \partial_{y_1}\chi\big|_{y_1=0} = 0, \quad \partial_{y_2}\phi\big|_{y_2=0} = 0, \quad \partial_{y_3}\xi\big|_{y_3=0} = 0, \tag{7.18a}$$

$$\text{at the IR branes} \;:\; \partial_{y_1}\chi\big|_{y_1=\pi R_1} = 0, \quad \phi\big|_{y_2=\pi R_2} = 0, \quad \xi\big|_{y_3=\pi R_3} = 0. \tag{7.18b}$$

Note that we have for the field χ in the first throat Neumann BCs at both endpoints, whereas the fields ϕ and ξ have Neumann BCs at the UV brane and Dirichlet BCs at the IR branes. For χ, the most general flat space KK expansions of the scalars, consistent with the BCs in Eqs. (7.18a) are given by

$$\chi(x_\mu, y_1) = \frac{1}{\sqrt{\pi R_1}} \Big[\chi^{(0)}(x_\mu) + \sqrt{2} \sum_{n=1}^{+\infty} \chi^{(n)}(x_\mu) \cos\Big(\frac{n y_1}{R_1}\Big) \Big], \tag{7.19}$$

while the KK expansion for the fields ϕ and ξ read

$$X(x_\mu, y_i) = \sqrt{\frac{2}{\pi R_i}} \sum_{n=1}^{+\infty} X^{(n)}(x_\mu) \cos\Big(\frac{(2n-1) y_i}{2R_i}\Big), \tag{7.20}$$

where $(X,i) = (\phi,2),(\xi,3)$. Note the important fact that the Dirichlet BCs at the IR branes have projected out the zero modes of ϕ and ξ, such that only χ will have a zero mode. At the same time, the Neumann BCs at the UV brane ensure that χ,ϕ, and ξ, are non–vanishing there, such that the wave functions of all the scalars χ,ϕ, and ξ, will have a non–zero overlap with the fermions localized at the UV brane.

As we have already studied in detail in Chapter 6, the potential of the scalar bi–doublet ϕ with a KK expansion as given in Eq. (7.19) has for a wide range of parameters a local minimum for the VEVs

$$\langle\chi^{(0)}\rangle = \kappa_\chi \cdot \mathrm{diag}(1,1), \quad \langle\chi^{(n)}\rangle = 0, \tag{7.21}$$

where κ_χ is real parameter with mass dimension +1 and $n = 1,2,\ldots$. In other words, only the zero mode $\chi^{(0)}$ acquires a non–zero VEV while all higher KK excitations have zero VEVs. Qualitatively, this is because only the zero mode has a negative mass–squared (coming from the potential), while the higher KK excitations have, for a sufficiently large compactification scale, always positive mass-squares. Similarly, since the zero modes of ϕ and ξ have been projected out by the Dirichlet BCs, we will assume for the potentials of ϕ and ξ the VEVs

$$\langle\phi^{(n)}\rangle = \langle\xi^{(n)}\rangle = 0, \tag{7.22}$$

where $n = 1,2,\ldots$, *i.e.*, the VEVs of all KK excitations of ϕ and ξ vanish. As one can see from Eq. (6.3), these VEVs lead indeed to a minimum of the potential, since all first order derivatives vanish, while the second derivatives give

$$-2\sum_{i,j}\mu^2_{X_{i,j}} + \Big(\frac{n}{\pi R_1}\Big)^2 > 0. \tag{7.23}$$

Therefore, only $\chi^{(0)}$ with the VEV as given in Eq. (7.21) will be responsible for spontaneously breaking $G_{\rm SM} \to SU(2)_D \times U(1)_{B-L}$. Moreover, only the zero mode $\chi^{(0)}$ will generate non–zero mass terms for the fermions from the Yukawa interactions in Eq. (7.9).

Next, let us have a closer look at the masses of the scalar KK excitations. For this purpose, we denote by $M_n^2(X)$ the mass squares of the nth KK state $X^{(n)}$ of X. As demonstrated in Chapter 6, after canonically normalizing the kinetic terms of the scalars in Eq. (7.7b), we arrive for χ at the masses of the KK states

$$M_n^2(\chi) = \Big[-\mu_\chi^2 + \Big(\frac{n}{\pi R_1}\Big)^2\Big]\Big[1 - \frac{K'_X}{\pi R_1} + \ldots\Big], \tag{7.24}$$

where $n = 0,1,2\ldots$, the tachyonic mass–squared $-\mu_\chi^2$ is determined by the coefficients μ_{ij}^2 in Eq. (6.3) applied to the field $X \to \chi$, and the dots denote higher powers of $K'/\pi R_1$. By the same argument, we obtain for the KK excitations of ϕ in canonical normalization the masses

$$M_n^2(\phi) = \Big[-\mu_\phi^2 + \Big(\frac{2n-1}{2\pi R_2}\Big)^2\Big]\Big[1 - \frac{K'_\phi}{\pi R_2} + \ldots\Big], \tag{7.25}$$

where $n = 1, 2, \ldots$, and the mass–square μ_ϕ^2 is determined by the coefficients μ_{ij}^2 in Eq. (6.3) specialized for the field $X \to \phi$. The field ξ has KK states with masses

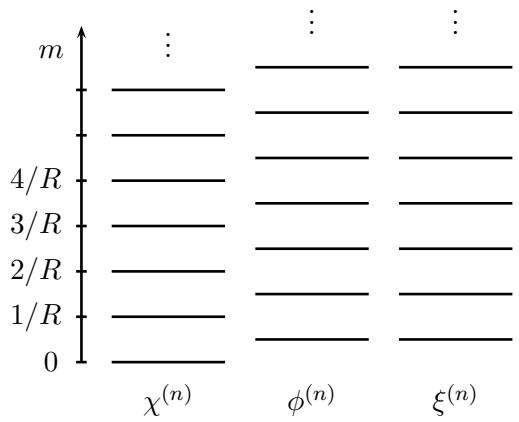

Figure 7.2: Masses of the KK states of χ, ϕ and ξ. The masses of $\phi^{(n)}$ and $\xi^{(n)}$ are practically degenerate.

$M_n^2(\xi)$ that are obtained from $M_n^2(\phi)$ by setting in Eq. (7.25) $\mu_\phi^2 \to \mu_\xi^2$, $K'_\phi \to K'_\xi$, and $R_2 \to R_3$. Now, the discrete symmetry D_2 in Eq. (7.11) establishes $\mu_\phi^2 = \mu_\xi^2$ as well as $R_2 = R_3$ but is broken by $K'_\phi \neq K'_\xi$. The mass squares $M_n^2(\phi)$ and $M_n^2(\xi)$ will therefore be practically degenerate, up to corrections of the order $K'_\phi/(\pi R_2) \sim K'_\xi/(\pi R_3)$. We thus find that under order one variations of the brane kinetic terms K'_X the mass splittings are of the order

$$\frac{M_n^2(\phi) - M_n^2(\xi)}{M_n^2(\phi)} \sim \frac{K'_X}{\pi R_2}, \tag{7.26}$$

where K'_X is of the same order as K'_χ, K'_ϕ, and K'_ξ. Since K'_X has mass dimension -1 in five dimensions, we expect K'_X to be of the order $K'_X \sim 1/M_*$, where M_* is the fundamental higher–dimensional Planck scale. Recall that for a number of δ flat extra dimensions with common compactification radius R, we have $M_{\rm Pl}^2 = M_*^{2+\delta} R^\delta$, where $M_{\rm Pl} \approx 10^{18}\,\text{GeV}$ is the usual 4D Planck scale (see Sec. 4.2.2). In δ such extra dimensions, K'_X has mass dimension $-\delta$ and the mass–squared splitting in Eq. (7.26) generalizes to $[M_n^2(\phi) - M_n^2(\xi)]/M_n^2(\phi) \sim (M_*/M_{\rm Pl})^2$, independent from the number of extra dimensions δ. If, for example, the fundamental scale is $M_* \sim 10^{12}\,\text{GeV}$, we arrive in Eq. (7.26) at a tiny mass splitting

$$[M_n^2(\phi) - M_n^2(\xi)]/M_n^2(\phi) \sim 10^{-14}. \tag{7.27}$$

This small relative mass–squared splitting between the KK states arises from the hierarchy between M_* and $M_{\rm Pl}$. It is interesting to observe that, instead of explicitly using higher-dimension operators, this splitting becomes small as a consequence of rescaling the scalar fields when going to canonical normalization.

7.3 Fermion Masses

After integrating out the extra dimensions, we obtain from Eq. (7.14) in the 4D effective theory for the Yukawa couplings

$$\begin{aligned}\mathcal{L}_Y^{\rm eff} &= \int_0^{\pi R_1} dy_1\, \mathcal{L}_{\chi,1}^Y + \int_0^{\pi R_2} dy_1\, \mathcal{L}_{\phi,2}^Y + \int_0^{\pi R_3} dy_1\, \mathcal{L}_{\xi,3}^Y \qquad (7.28)\\ &= \frac{1}{\sqrt{\pi R_1}}\mathcal{L}_{\chi,1}^{Y(0)} + \sqrt{2}\sum_{n=1}^{\infty}\Big(\frac{1}{\sqrt{\pi R_1}}\mathcal{L}_{\chi,1}^{Y(n)} + \frac{1}{\sqrt{\pi R_2}}\mathcal{L}_{\phi,2}^{Y(n)} + \frac{1}{\sqrt{\pi R_3}}\mathcal{L}_{\xi,3}^{Y(n)}\Big),\end{aligned}$$

where the 4D Yukawa couplings to the 0th and nth KK modes $\mathcal{L}_{X,i}^{Y(n)}$ are

$$\begin{aligned}\mathcal{L}_{\chi,1}^{Y(0)} &= Y_\ell\overline{\psi}_L(\chi_u^{(0)} - e^{{\rm i}\alpha}\chi_d^{c(0)})\nu_R + Y_\ell\overline{\psi}_L(\chi_d^{(0)} - e^{{\rm i}\alpha}\chi_u^{c(0)})e_R + \text{h.c.}, \qquad (7.29a)\\ \mathcal{L}_{\chi,1}^{Y(n)} &= Y_\ell\overline{\psi}_L(\chi_u^{(n)} - e^{{\rm i}\alpha}\chi_d^{c(n)})\nu_R + Y_\ell\overline{\psi}_L(\chi_d^{(n)} - e^{{\rm i}\alpha}\chi_u^{c(n)})e_R + \text{h.c.}, \qquad (7.29b)\\ \mathcal{L}_{\phi,2}^{Y(n)} &= Y_\ell\overline{\psi}_L(\phi_u^{(n)} - e^{{\rm i}\alpha}\phi_d^{c(n)})\nu_R + Y_\ell\overline{\psi}_L(\phi_d^{(n)} - e^{{\rm i}\alpha}\phi_u^{c(n)})e_R + \text{h.c.}, \qquad (7.29c)\\ \mathcal{L}_{\xi,3}^{Y(n)} &= Y'_\ell\overline{\psi}_L(\xi_u^{(n)} - e^{{\rm i}\beta}\xi_d^{c(n)})\nu_R + Y'_\ell\overline{\psi}_L(\xi_d^{(n)} - e^{{\rm i}\beta}\xi_u^{c(n)})e_R + \text{h.c.}, \qquad (7.29d)\end{aligned}$$

where $n = 1, 2, \ldots$, and we have identified $Y_\ell = Y_\chi = Y_\phi$ and $Y'_\ell = Y_\xi$. In more than five dimensions, the normalization factors $\sqrt{\pi R_i}$ in the above expressions will be replaced with $\sqrt{\pi R_i} \to \sqrt{V_\delta}$, where V_δ is the extra-dimensional volume. Note that the only contribution to $\mathcal{L}_Y^{\rm eff}$ from zero modes is provided by $\mathcal{L}_{\chi,1}^{Y(0)}$ in Eq. (7.29a). In the 4D effective theory, the discrete symmetry D_1 in Eq. (7.10) interchanges $\mathcal{L}_{\chi,1}^{Y(n)} \leftrightarrow \mathcal{L}_{\phi,2}^{Y(n)}$ for $n \geq 1$, but it is broken by the Yukawa couplings $\mathcal{L}_{\chi,1}^{Y(0)}$ to the zeromodes. Since only the zero modes $\chi_u^{(0)}$ and $\chi_d^{(0)}$ acquire nonzero VEVs, Dirac neutrino masses are generated only from $\mathcal{L}_{\chi,1}^{Y(0)}$. To reproduce Dirac neutrino masses of the order $\sim 10^{-2}$ eV, we need Dirac Yukawa couplings of the order $\sim 10^{-12}$. In our model, such small Yukawa couplings will originate (i) from a volume suppression mechanism and (ii) from higher-dimension operators as proposed in Ref. [76].

To estimate the volume suppression of the Yukawa couplings, consider a generalization of our 5D throat model to δ flat extra dimensions with common compactification radius R (*cf.* Sec. 4.2.2). Having $1/R \gtrsim 1\,\text{TeV}$ requires at least two extra dimensions $\delta \geq 2$, and for $\delta = 2$, the compactification scale would then be $1/R \sim 100\,\text{TeV}$. In such a scenario, the Yukawa couplings in Eqs. (7.29) have mass dimension $-\delta/2$ and are of the order $\sim M_*^{-\delta/2}$. For $\delta = 2$ and $M_* \sim 10^{12}\,\text{GeV}$, as assumed to obtain the tiny mass–squared splitting in Eq. (7.27), we then have in the 4D effective theory a suppression of the Dirac Yukawa couplings by a volume factor of the order $\sim 1/(M_*R) \sim 10^{-7}$. This volume suppression alone would therefore produce in the low energy effective theory Dirac Yukawa couplings of the order $\sim 10^{-7}$, which, though small, are still by roughly 5 orders of magnitude too large to account for the observed neutrino masses.

In our model, the suppression of the Yukawa couplings by additional 5 orders of magnitude shall be implemented through higher dimension operators similar to the discussion in Ref. [76]. Let us briefly sketch one way how this mechanism could be realized here. For this purpose, we assume two additional complex SM singlet scalars s_1 and s_2. The scalars are charged under an extra $U(1) \times U(1)$ product gauge group as $s_1 \sim (+1, 0)$ and $s_2 \sim (0, +1)$. We also assign the scalar bi–doublets χ, ϕ, and ξ, under this group the charges $\chi \sim (-1, 0), \phi \sim (-1, 0)$, and $\xi \sim (0, -1)$. Note that this $U(1)$ charge assignment respects the symmetry D_1 but breaks D_2. We thus see that in the 4D effective theory, the Yukawa couplings in Eqs. (7.29) become dimension–five operators as shown in Fig. 7.3 which are suppressed by a factor $\sim \langle s_i \rangle / M_*$. The dimension–five operators are shown in Fig.7.3. In analogy with Eq. (7.17), we can

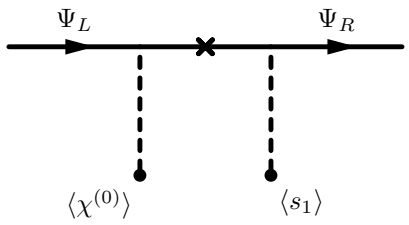

Figure 7.3: Dimension-five operator suppressing the Dirac Yukawa couplings.

assume for the scalars a potential $V(s_1, s_2) = \lambda_1(v_1^2 - |s_1|^2) + \lambda_2(v_2^2 - |s_2|^2)^2$, where $\lambda_1 \sim \lambda_2$ and $v_1 \sim v_2$. For $\lambda_{1,2} > 0$, this potential has a minimum at $|s_1| = v_1$ and $|s_2| = v_2$. As a consequence, the effective Yukawa couplings of the leptons to χ and ϕ in Eqs. (7.29b) and (7.29c) will be degenerate and of the same order as the effective Yukawa coupling to ξ in Eq. (7.29d). Taking $v_{1,2} \sim 10^5\,\mathrm{GeV}$, we obtain, in combination with the volume suppression factor $\sim 10^{-5}$ discussed above, Dirac Yukawa couplings of the order $\sim 10^{-12}$, giving Dirac neutrino masses of the order $\sim 10^{-2}\,\mathrm{eV}$ in perfect agreement with observation.

In this model, all Dirac Yukawa couplings, including those of the charged leptons, are of the order $\sim 10^{-12}$, which would give too small charged lepton masses. Realistic charged lepton masses can, however, be generated by 4D Dirac mass terms of the type $\sim C\overline{e}_L e_R$ (C is some mass and e_L and e_R are 4D LH and RH charged leptons) that are localized at the IR brane of an extra throat with only $U(1)_Q$ gauge invariance (a similar mass term for the neutrinos can, for example, be forbidden by requiring that ν_R is not propagating in this extra throat or by assuming a symmetry that acts in the extra throat on ψ_L, ν_R, and e_R). The same argumentation can also be applied to reproduce the quark masses.

Chapter 8

Dirac Leptogenesis

Due to the smallness of the Yukawa couplings in the model introduced in Chapter 7, we have to consider resonantly enhanced leptogenesis. In this Chapter, we thus turn to the discussion of leptogenesis in the throats 2 and 3, where the 4D scalar degrees of freedom of ϕ and ξ exhibit a tiny mass splitting induced by brane kinetic terms. We are neglecting the possible contribution of χ, which is not in resonance with ϕ and ξ. Since, in this model, the neutrinos are Dirac particles, we will assume that the baryon asymmetry is generated via Dirac leptogenesis [27, 76, 129, 130]. Furthermore, we consider the limit in which the $\phi_u - \phi_d^c$ and $\xi_u - \xi_d^c$ mixings are small. For $Y_\ell \sim Y'_\ell$ and $Y_\ell, Y'_\ell \lesssim 10^{-12}$, a mass splitting of the order $|M_n^2(\phi_u) - M_n(\xi_u)^2|/|M_n^2(\phi_u)| \sim 10^{-14}$ is responsible for an enhanced generation of baryon asymmetry.

8.1 CP–Asymmetry

In our leptogenesis model, the quarks also contribute to the asymmetry, since their Yukawa couplings Y_q are of the same order as Y_ℓ. We are therefore actually talking about a scenario of combined baryogenesis and leptogenesis in the sense that a LR asymmetry is not only generated in the lepton but also in the quark sector. The 4D Yukawa couplings to the 0th and nth KK modes in the quark sector are analogous to the leptonic couplings in Eq. (7.29) with the following replacements: $Y_\ell \leftrightarrow Y_q$, $Y'_\ell \leftrightarrow Y'_q$, $\psi_L \leftrightarrow Q_L$, $\nu_R \leftrightarrow u_R$, and $e_R \leftrightarrow d_R$. Consequently, we would have to take further Feynman diagrams into account. We find the same diagrams as for leptons, where we just have to replace leptons by quarks. Additionally, quarks are allowed as intermediate states in the wave–function correction, for a decay into leptons and vice versa, since the net amount of color charge remains zero throughout the whole process. Vertex diagrams with leptons as final (intermediate) and quarks as intermediate (final) states are forbidden due to conservation of color charge. Here, we are considering the decays of massive scalar KK excitations far above the EW scale, for which the loop calculations in Chapter 5 in the limit of neglegible quark masses also holds.

Let us start with the discussion of the lepton asymmetry ε^v in terms of KK modes.

The CP–violation induced by the vertex–correction for the nth KK mode of ϕ_u takes the form

$$\begin{aligned}\varepsilon^{v(n)}_{\phi_u} &= \frac{\Gamma(\phi_u^{(n)} \to \overline{\psi}_L \ell_R) - \Gamma(\overline{\phi}_u^{(n)} \to \psi_L \overline{\ell}_R)}{\Gamma^{(n)}_{\phi_u} + \Gamma^{(n)}_{\overline{\phi}_u}} \\ &= \frac{\mathrm{Im}\,[e^{\mathrm{i}(\alpha-\beta)}\mathrm{tr}(Y_\ell Y_\ell'^\dagger)^2]}{16\pi(\mathrm{tr}(Y_\ell^\dagger Y_\ell) + 3\mathrm{tr}(Y_q^\dagger Y_q))} \sum_{k=1}^{k_{\max}} f(M_k^2(\xi_u)/M_n^2(\phi_u)), \end{aligned} \tag{8.1}$$

where the function $f(x)$ is given by $f(x) = 1 - x\ln(1+1/x)$ and the total decay width $\Gamma^{(n)}_{\phi_u}$ of ϕ_u has been extended by the decay width into quarks. This contribution of the quarks has the same form as the decay widths in Eq. (5.9), where we only have to replace the leptons by quarks and take color factors into account. Note that there is also the diagram with ξ_d as an intermediate state, for which the following argumentation applies correspondingly. For the decays of $\xi_u^{(n)}$ with $\phi_u^{(n)}$ as intermediate an state, we have

$$\varepsilon^{v(n)}_{\xi_u} = \frac{-\mathrm{Im}\,[e^{\mathrm{i}(\alpha-\beta)}\mathrm{tr}(Y_\ell Y_\ell'^\dagger)^2]}{16\pi\,(\mathrm{tr}(Y_\ell'^\dagger Y_\ell') + 3\mathrm{tr}(Y_q'^\dagger Y_q'))} \sum_{k=1}^{k_{\max}} f(M_k^2(\phi_u)/M_n^2(\xi_u)). \tag{8.2}$$

We can combine Eqs. (8.1) and (8.2) into

$$\begin{aligned}\varepsilon^{v(n)}_{\phi_u+\xi_u} &= \frac{\mathrm{Im}\,[e^{\mathrm{i}(\alpha-\beta)}\mathrm{tr}(Y_\ell Y_\ell'^\dagger)^2]}{16\pi\,(\mathrm{tr}(Y_\ell^\dagger Y_\ell) + 3\mathrm{tr}(Y_q^\dagger Y_q))} \\ &\times \sum_{k=1}^{k_{\max}} [f(M_k^2(\xi_u)/M_n^2(\phi_u)) - f(M_k^2(\phi_u)/M_n^2(\xi_u))]. \end{aligned} \tag{8.3}$$

The splitting between the scalars $\phi_x^{(n)}$ and $\xi_x^{(n)}$ as well as $\phi_x^{(n+1)}$ and $\xi_x^{(n+1)}$, where $x = u, d$, is illustrated in Fig. 8.1. Defining the quantities $\Delta M^{(n)} = M_{n+1}(X_i) - M_n(X_i)$ $(i = 1, 2)$, $m^{(n)} = 1/2[M_n(X_1) + M_n(X_2)]$, and $\Delta m^{(n)} = M_n(X_2) - M_n(X_1)$, Eq. (8.3) can be approximated as follows: Since $f(M_k^2(X_2)/M_n^2(X_1)) \approx f(M_k^2(X_1)/M_n^2(X_2))$, we can write

$$f\left(\frac{M_k^2(X_2)}{M_n^2(X_1)}\right) - f\left(\frac{M_k^2(X_1)}{M_n^2(X_2)}\right) = df = f'dx, \tag{8.4}$$

where $f'(x) = 1/(1+x) - \ln(1+1/x)$ denotes the derivative of the function $f(x)$ with

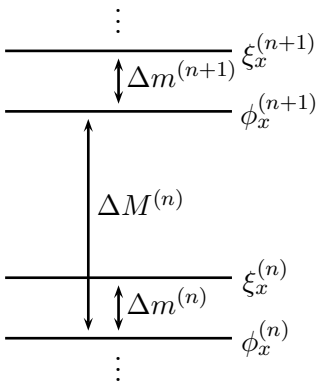

Figure 8.1: The splitting between the scalars $\phi_x^{(n)}$ and $\xi_x^{(n)}$ as well as $\phi_x^{(n+1)}$ and $\xi_x^{(n+1)}$, where $x = u, d$ (*cf.* Ref [139]).

respect to x and

$$\begin{aligned} dx &= \frac{M_k^2(X_2)}{M_n^2(X_1)} - \frac{M_k^2(X_1)}{M_n^2(X_2)} \\ &\approx \frac{m^{(k)2} + \Delta m^{(k)} m^{(k)}}{m^{(n)2} - \Delta m^{(n)} m^{(n)}} - \frac{m^{(k)2} - \Delta m^{(k)} m^{(k)}}{m^{(n)2} + \Delta m^{(n)} m^{(n)}} \\ &= 2\frac{m^{(k)2}}{m^{(n)2}} \frac{\Delta m^{(n)}/m^{(n)} + \Delta m^{(k)}/m^{(k)}}{1 - (\Delta m^{(n)}/m^{(n)})^2} \\ &\approx 2\frac{m^{(k)2}}{m^{(n)2}} \left(\frac{\Delta m^{(n)}}{m^{(n)}} + \frac{\Delta m^{(k)}}{m^{(k)}} \right), \end{aligned} \tag{8.5}$$

here we have used

$$M_n^2(X_1) = (m^{(n)} + 1/2\Delta m^{(n)})^2 \approx m^{(n)2} + \Delta m^{(n)} m^{(n)}, \tag{8.6a}$$
$$M_n^2(X_2) = (m^{(n)} - 1/2\Delta m^{(n)})^2 \approx m^{(n)2} - \Delta m^{(n)} m^{(n)}. \tag{8.6b}$$

Thus, we end up with a CP–violation induced by the vertex–correction that is given by

$$\varepsilon^{v(n)} \approx \frac{\mathrm{Im}\left[e^{\mathrm{i}(\alpha-\beta)} \mathrm{tr}(Y_\ell Y_\ell'^\dagger)^2\right]}{8\pi \left(\mathrm{tr}(Y_\ell^\dagger Y_\ell) + 3\mathrm{tr}(Y_q^\dagger Y_q)\right)} \sum_{k=1}^{k_{\max}} \left(\frac{\Delta m^{(n)}}{m^{(n)}} + \frac{\Delta m^{(k)}}{m^{(k)}} \right) \frac{m^{(k)2}}{m^{(n)2}} f'\left(\frac{m^{(k)2}}{m^{(n)2}} \right), \tag{8.7}$$

since $M_k^2(X_2)/M_n^2(X_1) \lesseqgtr m^{(k)2}/m^{(n)2} \lesseqgtr M_k^2(X_1)/M_n^2(X_2)$. The function $xf'(x)$ has in the parameter range $x \in [0, \infty[$ a global minimum $x_{\max} f'(x_{\max}) = -0.216$ at $x_{\max} = 0.462$ and the asymptotic behavior $\lim_{x\to 0} xf'(x) = 0$ and $\lim_{x\to\infty} xf'(x) = 0$. From Eq. (8.7), it can be easily seen that every summand which contributes to $\varepsilon^{v(n)}$ is suppressed by a factor $\Delta m^{(n)}/m^{(n)}$ or $\Delta m^{(k)}/m^{(k)}$. In the resonant limit,

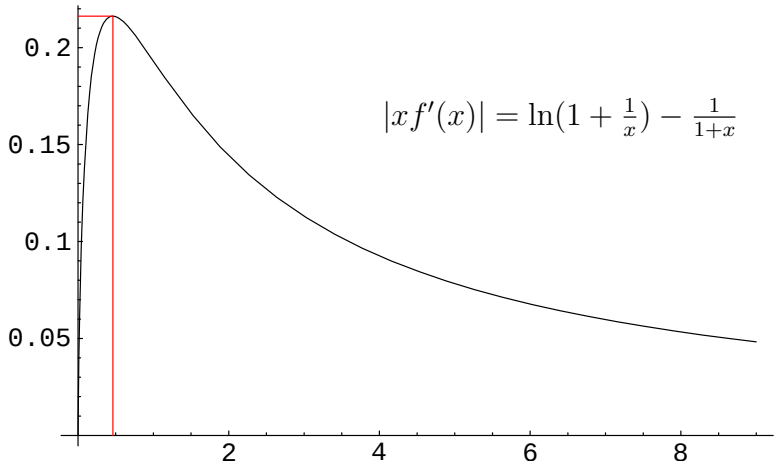

Figure 8.2: The function $|xf'(x)| = x(\ln(1+1/x) - 1/(1+x))$ in the range $[0,9]$. It is obvious that the contribution is small over the whole interval $[0,\infty[$.

$\Delta m^{(n)}/m^{(n)}$ or $\Delta m^{(k)}/m^{(k)}$ and become very small. The vertex contribution to the total L asymmetry is than negligible. Now, we focus on the ε^w-type contribution induced by wave–function corrections. Taking the smallness of the splitting between $M_n(X_1)$ and $M_n(X_2)$ into account, we can perform a similar estimate as in the case of the vertex corrections. We start with the asymmetry

$$\begin{aligned}\varepsilon^{w(n)}_{\phi_u} &= \frac{\Gamma(\phi_u^{(n)} \to \overline{\psi}_L \ell_R) - \Gamma(\overline{\phi}_u^{(n)} \to \psi_L \overline{\ell}_R)}{\Gamma^{(n)}_{\phi_u} + \Gamma^{(n)}_{\overline{\phi}_u}} \\ &= -\frac{\mathrm{Im}\,[e^{\mathrm{i}(\alpha-\beta)}\mathrm{tr}(Y_\ell Y_\ell'^\dagger)^2]}{16\pi\,(\mathrm{tr}(Y_\ell^\dagger Y_\ell) + 3\mathrm{tr}(Y_q^\dagger Y_q))} \sum_{k=1}^{k_{\max}} g(M_k^2(\xi_u)/M_n^2(\phi_u)),\end{aligned} \tag{8.8}$$

and get for the combined asymmetry of ϕ_u and ξ_u

$$\varepsilon^{w(n)}_{\phi_u+\xi_u} \approx -\frac{\mathrm{Im}\,[e^{\mathrm{i}(\alpha-\beta)}\mathrm{tr}(Y_\ell Y_\ell'^\dagger)^2]}{16\pi\,(\mathrm{tr}(Y_\ell^\dagger Y_\ell) + 3\mathrm{tr}(Y_q^\dagger Y_q))} \sum_{k=1}^{k_{\max}} \left[g\left(\frac{M_k^2(\xi_u)}{M_n^2(\phi_u)}\right) - g\left(\frac{M_k^2(\phi_u)}{M_n^2(\xi_u)}\right)\right], \tag{8.9}$$

where $g(x)$ has been defined as $g(x) = 1/(1-x)$. For $k = n$, the summand in Eq. (8.9) becomes

$$-\frac{\mathrm{Im}\,[e^{\mathrm{i}(\alpha-\beta)}\mathrm{tr}(Y_\ell Y_\ell'^\dagger)^2]}{16\pi\,(\mathrm{tr}(Y_\ell^\dagger Y_\ell) + 3\mathrm{tr}(Y_q^\dagger Y_q))} \frac{M_n^2(\phi_u) + M_n^2(\xi_u)}{M_n^2(\phi_u) - M_n^2(\xi_u)}. \tag{8.10}$$

The remaining sum in Eq. (8.9) can be further approximated as

$$\varepsilon^{w(n)} \approx -\frac{\mathrm{Im}\,[e^{\mathrm{i}(\alpha-\beta)}\mathrm{tr}(Y_\ell Y_\ell'^\dagger)^2]}{8\pi\,(\mathrm{tr}(Y_\ell^\dagger Y_\ell) + 3\mathrm{tr}(Y_q^\dagger Y_q))} \sum_{k=1,k\neq n}^{k_{\max}} \left(\frac{\Delta m^{(n)}}{m^{(n)}} + \frac{\Delta m^{(k)}}{m^{(k)}}\right) \frac{m^{(k)2}}{m^{(n)2}}\, g'\left(\frac{m^{(k)2}}{m^{(n)2}}\right), \tag{8.11}$$

where $g'(x) = -1/(1-x)^2$ is the derivative of the function $g(x)$ with respect to x. Fig. (8.3) shows the function $xg'(x)$, which has the asymptotic behavior $\lim_{x\to 0} xg'(x) =$

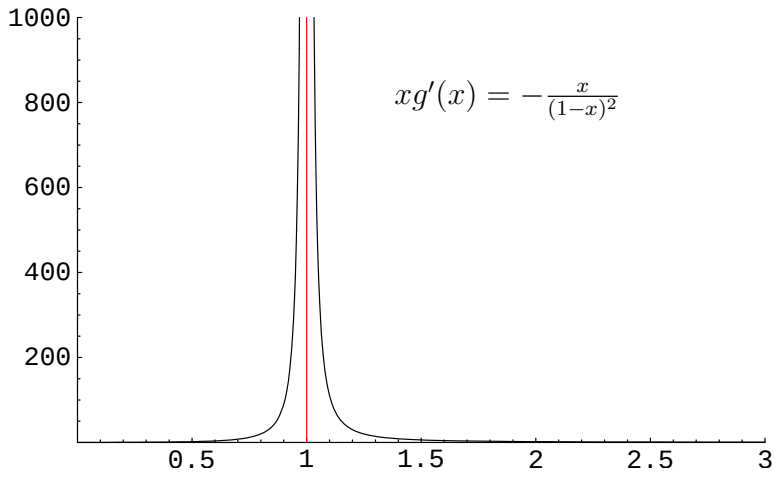

Figure 8.3: The function $xg'(x) = -x/((1-x)^2)$ in the range $[0,3]$. It is obvious that the resonant contribution is dominant over the whole range $[0,\infty[$.

0, $\lim_{x\to\infty} xg'(x) = 0$, and $\lim_{x\to 1} xg'(x) = \infty$. We see that the wave–function corrections contribute constructive and the corrections with $k = n$ dominates.

In the following, we will therefore concentrate on the asymmetries generated by the resonantly enhanced wave–function corrections. Since there is no constraint on the mass ratio of up–type and down–type fields, we will consider resonant splittings only for scalar fields of the same type. As a consequence, we end up with

$$\begin{aligned}
\varepsilon^{(n)}_{\overline{X}^{(n)}_u \to \nu_R} \approx & -\left[\frac{\mathrm{Im}\left\{e^{\mathrm{i}(\alpha-\beta)}[\mathrm{tr}(Y_\ell'^\dagger Y_\ell)^2 + 3\mathrm{tr}(Y_\ell'^\dagger Y_\ell)\mathrm{tr}(Y_q'^\dagger Y_q)]\right\}}{M_n(\phi_u)^2 - M_n(\xi_u)^2}\right. \\
& \left. + \frac{3\mathrm{Im}[\mathrm{tr}(Y_\ell'^\dagger Y_\ell)\mathrm{tr}(Y_q' Y_q^\dagger)]}{M_n(\phi_u)^2 - M_n(\xi_u)^2}\right]\left(\frac{M_n(\phi_u)^2}{16\pi(\mathrm{tr}(Y_\ell^\dagger Y_\ell) + 3\mathrm{tr}(Y_q^\dagger Y_q))}\right. \\
& \left. + \frac{M_n(\xi_u)^2}{16\pi(\mathrm{tr}(Y_\ell'^\dagger Y_\ell') + 3\mathrm{tr}(Y_q'^\dagger Y_q'))}\right) = \varepsilon^{(n)}_\ell, \qquad (8.12) \\
\varepsilon^{(n)}_{\overline{X}^{(n)}_u \to \overline{e}_R} \approx & -\varepsilon^{(n)}_\ell, \qquad (8.13)
\end{aligned}$$

where we have used that $\mathrm{tr}(AB^T) = \mathrm{tr}(A^T B)$ for any two $n \times n$ matrices A and B, since $\mathrm{tr}(A) = \mathrm{tr}(A^T)$ and $\mathrm{tr}(AB) = \mathrm{tr}(BA)$. Due to the similar structure of lepton and quark Yukawa couplings in our scenario, we have to take similar asymmetries for the decays to quarks into account, *i.e.*, $\varepsilon^{(n)}_{\overline{X}^{(n)}_u \to u_R} = -\varepsilon^{(n)}_{\overline{X}^{(n)}_u \to \overline{d}_R} = \varepsilon^{(n)}_q$. Where $\varepsilon^{(n)}_\ell$ and $\varepsilon^{(n)}_q$ differ in the Yukawa couplings and in the color factor for the wave–function

correction with quarks in the intermediate as well as in the final states. Exactly the same equations hold also for the resonant decays of $\phi_d^{(n)}$ and $\xi_d^{(n)}$.

In order to analyze the resulting asymmetry, let us a go to the limit where we will replace all Yukawa coupling matrices by values of the order $Y_\ell \approx Y'_\ell \approx Y_q \approx Y'_q \sim 10^{-12}$ and assume order one values for the combinations of α, β, and the relative phases between Y_ℓ and Y'_ℓ, as well as between Y_q and Y'_q, *i.e.*,

$$\varepsilon_\ell^{(n)} \approx \varepsilon_q^{(n)} \approx 10^{-10}. \tag{8.14}$$

These values are of the same order as the observed η_B. So, we have to see to which extent this LR asymmetry is converted into a B asymmetry by sphaleron processes.

8.2 Conversion of LR Asymmetry into B Asymmetry

The leptogenesis in our model proceeds along the same lines as the Dirac leptogenesis scenario presented in Sec. 3.4.2. However, due to the fact that in our model all Yukawa couplings are very small, we have to take all RH fermions into account to find η_B. We assume all Yukawa couplings to be of the same order of magnitude $\sim 10^{-12}$. But in principle, the smallest couplings determine the asymmetry. For the analysis of the conversion of the LR asymmetry into a B asymmetry, we refer to chemical potentials, the convenient way to treat particle asymmetries [70, 140]. A brief summary of this topic and the basic equations is given in Appendix C. Here, we will denote with $\mu_{X_i^{0(0)}}$ and $\mu_{X_i^{-(0)}}$ the potentials of the two scalar fields $\chi_u^{(0)}$ and $\chi_d^{(0)c}$. The LH particles should be in equilibrium, due to the gauge couplings, *i.e.*, their reactions occur rapidly compared to the expansion rate of the Universe. All RH particles, because they are not thermalized by Higgs interactions, carry an asymmetry

$$\sum_{i=1}^{3} \mu_{\nu_{iR}} \neq 0, \qquad \sum_{i=1}^{3} \mu_{e_{iR}} \neq 0, \qquad \mu_{u_R} \neq 0, \qquad \mu_{d_R} \neq 0. \tag{8.15a}$$

These asymmetries are generated by the out–of–equilibrium decays of higher KK-modes ($n \geq 1$) of the heavy bulk scalars. The chemical potentials in equilibrium obey the following relations:

$$\begin{aligned} W^- \leftrightarrow X_i^{0(0)} + X_i^{-(0)} : &\qquad \mu_{W^-} = \mu_{X_i^{0(0)}} + \mu_{X_i^{-(0)}}, \\ W^- \leftrightarrow \overline{u}_L + d_L : &\qquad \mu_{W^-} = \mu_{d_L} - \mu_{u_L}, \\ W^- \leftrightarrow \overline{\nu}_{iL} + e_{iL} : &\qquad \mu_{W^-} = \mu_{e_{iL}} - \mu_{\nu_{iL}}. \end{aligned} \tag{8.16}$$

With the help of these relations, we can reduce the number of chemical potentials from $5+4N+2M$ to $4+3N+M$, where N denotes the number of fermion generations and M is the number of Higgs doublets (*cf.* Chapter C). Since the chemical potential for

the third component of weak isospin T_3 [*cf.* Eq.(C.6a)] has to vanish, we find $\mu_{W^-} = 0$. The interaction of the Higgs particles with $W^\pm$ only implies that

$$\sum_{i=1}^{M} \mu_{X_i^{0(0)}} = \sum_{i=1}^{M} \mu_{X_i^{+(0)}}. \tag{8.17}$$

We can consider the zero mode of χ as being decoupled for temperatures $T > T_c$, since all other interactions are strongly suppressed by the small Yukawa couplings. Thus, this zero mode will conserve an initial asymmetry. When there are no processes above the EW scale which could cause an asymmetry, we find:

$$\sum_{i=1}^{M} \mu_{X_i^{0(0)}} = \sum_{i=1}^{M} \mu_{X_i^{-(0)}} = 0. \tag{8.18}$$

Using Eqs. (8.16), (C.8), and (C.9), we obtain

$$\mu_{d_L} = -\frac{1}{3N} \sum_{i=1}^{N} \mu_{\nu_{iL}} \quad \text{and} \quad \mu_{u_R} = -\frac{2}{3N} \sum_{i=1}^{N} \mu_{\nu_{iL}} - \mu_{d_R}, \tag{8.19}$$

and, thus, for a vanishing chemical potential of the electric charge $\mu_Q = 0$ [*cf.* Eq. (C.6b)] above T_c, it follows that

$$\sum_{i=1}^{N} \mu_{\nu_{iL}} = -\frac{3}{8}\Big(3N\mu_{d_R} + \sum_{i=1}^{N} \mu_{e_{iR}}\Big). \tag{8.20}$$

This leads to

$$\mu_B = -\frac{4}{3} \sum_{i=1}^{N} \mu_{\nu_{iL}} = \frac{1}{2}\Big(3N\mu_{d_R} + \sum_{i=1}^{N} \mu_{e_{iR}}\Big) \tag{8.21}$$

and

$$\mu_L = \frac{1}{4} \sum_{i=1}^{N} \mu_{e_{iR}} + \sum_{i=1}^{N} \mu_{\nu_{iR}} - \frac{9N}{4}\mu_{d_R}. \tag{8.22}$$

For $N = 3$, the net baryon number is then

$$\mu_B = \frac{9}{2}\mu_{d_R} + \frac{1}{2} \sum_{i=1}^{N} \mu_{e_{iR}}. \tag{8.23}$$

So, we can see that the asymmetry in the RH sector leads to the creation of a baryon asymmetry. Since we expect the LR asymmetry for all fermions to be approximately equal, the final baryon asymmetry will thus be of the same order of magnitude as the LR asymmetry generated by out–of–equilibrium decays.

8.3 LR–Equilibration and Wash–Out

Now, we discuss the total amount of B asymmetry which is generated in out–of–equilibrium decays of the heavy bulk scalars $\phi_u^{(n)}$ and $\xi_u^{(n)}$. The contribution from $\phi_d^{(n)c}$ and $\xi_d^{(n)c}$ is assumed to be of the same order of magnitude and thus does not change the result significantly. For the rest of this discussion we will therefore give our results only in terms of the up–type fields $\phi_u^{(n)}$ and $\xi_u^{(n)}$. Furthermore, we use the results from the previous sections, *i.e.*, we concentrate on the reconant terms and take the LR asymmetry to be equal to the B asymmetry.

The ratio of neutrino number to entropy produced in out–of–equilibrium decays can be approximated in the "drift and decay limit" [51], *i.e.*, $n_{X^{(n)_i}} = n_{\overline{X}^{(n)_i}} \sim n_\gamma$ by

$$\frac{\Delta n_{\nu_R}}{s} \sim \frac{\Delta n_{e_R}}{s} \sim \frac{\sum_{n=1}^{n_{\max}} (\varepsilon_\nu^{(n)} - \varepsilon_{\overline{\nu}}^{(n)}) \cdot n_\gamma}{g_* n_\gamma} = \frac{2 \sum_{n=1}^{n_{\max}} \varepsilon_\ell^{(n)}}{g_*}, \tag{8.24a}$$

$$\frac{\Delta n_{u_R}}{s} \sim \frac{\Delta n_{d_R}}{s} \sim \frac{2 \sum_{n=1}^{n_{\max}} \varepsilon_q^{(n)}}{g_*}, \tag{8.24b}$$

where n_γ is the number density of photons and $g_* \sim \mathcal{O}(100)$ is the total number of relativistic degrees of freedom at low energies. In Eqs. (8.24a) and (8.24b), we have neglected usual possible annihilation effects of the scalars, since these are proportional to the scalar number density and thus self–quenching. However, going to high energies, we have to take a possibly large number of accessible KK modes into account, which would change g_* [139]. The number of relevant relativistic degrees of freedom increases with the temperature T due to the presence of the KK tower. For δ extra dimensions, the numbers of relativistic KK excitations $N_T(X_i)$ and $N_T(Y_i)$ of the scalar fields X_i and Y_i below T are

$$N_T(X) = \text{int}[(T - M_0(X_i))R_i]^\delta \quad \text{and} \quad N_T(Y_i) = \text{int}[TR_i]^\delta, \tag{8.25}$$

where Y_i in contrast to X_i has no zero mode and int$[x]$ denotes the rounded down integer value of x. The number of active degrees of freedom for one extra dimension as a function of T is approximately given by

$$\begin{aligned} g(T) \approx g_* + g_N &= g_* + 2\Big\{ \sum_i \theta(T - M_0(X_i)) \text{int}\big[(T - M_0(X_i))R_i\big]^\delta \\ &+ \sum_j \text{int}\big[(TR_j)\big]^\delta \Big\}, \end{aligned} \tag{8.26}$$

where the factor 2 accounts for the fact that we have scalar bi–doublets in our model. Obviously, the KK modes can change the number of relativistic degrees of freedom for $T > M_0(X_i)$ significantly, unless M_* is very high. The dominant contribution to the LR asymmetry η_{LR} is generated by the nth pair of KK modes $\phi_u^{(n)}$ and $\xi_u^{(n)}$ around the energy at which they drop out of thermal equilibrium, *i.e.*, at $T \approx M_n(\phi_u) \approx M_n(\xi_u)$:

$$\eta_{LR} = \sum_{n=1}^{n_{\max}} \eta_{LR}^{(n)} \approx \sum_{n=1}^{n_{\max}} \frac{\varepsilon_{X_u}^{(n)}}{g\big(M_n(X_u)\big)}. \tag{8.27}$$

The asymmetry $\varepsilon_{\phi_u}^{(n)}$ is independent of n, since the relative mass splitting between $\phi_u^{(n)}$ and $\xi_u^{(n)}$ remains constant with n. The remaining sum over $1/g\big(M_n(\phi_u)\big)$ can be written in form of an integral

$$\sum_{g_N(T_{\rm min})}^{g_N(T_{\rm max})} \frac{1}{g_* + g_N(T)} = \sum_{g_N(T_{\rm min})}^{g_N(T_{\rm max})} \frac{d\Big[\ln\big(1+\frac{g_N(T)}{g_*}\big)\Big]}{d\, g_N(T)} \sim \ln\left(\frac{g_* + g_N(T_{\rm max})}{g_* + g_N(T_{\rm min})}\right). \tag{8.28}$$

Here, a plausible energy range for leptogenesis is given by $T_{\rm min} \sim 100\,{\rm GeV}$ and $T_{\rm max} \sim 10^9\,{\rm GeV}$, where the upper bound is motivated by the gravitino problem (*cf.* Sec. 3.4.3). For $\delta = 2$, as used in Sec.. 7.3, Eqs. (8.26) and (8.28) lead to a factor of just about 6. The total baryonic asymmetry is consequently given by

$$\eta_B \approx \sum_{n=1}^{n_{\rm max}} \eta_{LR}^{(n)} \approx 10^{-10}. \tag{8.29}$$

We thus see that for a reasonable range of parameters, the amount of baryon asymmetry that is generated in our model is in good agreement with the observed value. Note, however, that in Eq. (8.29), we have assumed that sphaleron processes were fully active in converting the lepton asymmetry into a baryon asymmetry. This requires, of course, that the lepton asymmetry is produced early enough, at temperatures not much below $T_c \sim 100\,{\rm GeV}$, where sphalerons are still in thermal equilibrium. Considering the energy range of leptogenesis given above with KK masses between 10^9GeV and 10^5GeV, we can estimate the time scale for the heavy scalar decays to be of the order $t_D \simeq 10^{-10}$sec. The scalar lifetime has to be short compared to this time scale, *i.e.*, $t_D > \tau = 1/\Gamma_{X_i}^{(n)}$. To ensure that this is indeed the case, it might be necessary to have Yukawa couplings of the leptons to the higher KK states $\phi^{(n)}$ and $\xi^{(n)}$ $(n \geq 1)$ which are larger than $\sim 10^{-12}$ by a few (up to five) orders of magnitude. This would require, however, additional studies, which are beyond the scope of this thesis, but deserve further considerations.

Compared to the original model of Dirac leptogenesis [27], in our model, the smallness of the Dirac Yukawa couplings to the higher KK states $\phi^{(n)}$ and $\xi^{(n)}$ $(n \geq 1)$ has the clear advantage that the mass scale of the decaying scalar KK resonances can be very small ($\sim 100\,{\rm TeV}$) compared to the GUT scale. The reason is that we are in the weak wash–out regime: the quantity r [*cf.* Eq. (3.16)], determining the effectiveness of the inverse decays, is always much smaller than one, *i.e.*,

$$r = \frac{\Gamma_{\phi_u}^{(n)}}{H(M_n(\phi_u))} \sim \frac{{\rm tr}(Y_\ell Y_\ell^\dagger)}{g(M_n(\phi_u))^{1/2}} \frac{M_{\rm Pl}}{M_n(\phi_u)} \ll 1, \tag{8.30}$$

while keeping simultaneously the baryon asymmetry at the observed value $\eta_B \approx 10^{-10}$. This is only possible in our model, where we can use the resonant enhancement of η_B to compensate for the small Yukawa couplings Y_ℓ. As a consequence, this allows us to avoid the problems associated with GUT scale baryogenesis, such as the gravitino problem (see Sec. 3.4.3) which is generally an advantage of low–scale leptogenesis.

Chapter 9

Summary and Conclusions

From the present experimental and theoretical point of view, Dirac and Majorana neutrinos can both be implemented in our picture of particle physics. The seesaw mechanism predicts Majorana neutrinos, which could be tested at low energies in neutrinoless double beta decay experiments. However, there is no evidence for Majorana neutrinos so far. In fact, current neutrino oscillation data is in perfect agreement with neutrinos being Dirac particles. For Majorana neutrinos, the standard leptogenesis scenario and its implications have been much appreciated in the literature. Despite the popularity of Majorana neutrinos, however, it is also possible to generate sufficient baryon asymmetry with Dirac neutrinos, which is known as Dirac leptogenesis.

In this thesis, we have discussed Dirac leptogenesis for a LR–symmetric model in extra dimensions. The main intention of this model is to overcome the drawbacks of the original formulation of Dirac leptogenesis. The model

- provides scalar KK modes as an attractive origin of the heavy decaying particles that produce the baryon asymmetry,
- establishes a connection between low–energy observables and the parameters entering leptogenesis through discrete symmetries, and
- circumvents the necessity for GUT scale baryogenesis by a resonant enhancement of CP–violation.

These aspects are realized in an extra–dimensional geometry with three throats in the flat limit. Multi–throat backgrounds are motivated by string theory and offer a number of advantages for model building. In our model, the KK excitations can have masses as low as roughly 100 TeV up to the fundamental Planck scale. Discrete exchange symmetries between the throats link the low–energy Dirac neutrino Yukawa couplings with those to the heavy KK resonances. An important aspect is that GUT scale baryogenesis is avoided by small Yukawa couplings that are mainly suppressed by the extra–dimensional bulk volume. Otherwise, for large Yukawa couplings, we would have strong wash–out effects. The smallness of these Yukawa couplings becomes compatible with the observed baryon asymmetry only in connection with the

aid of resonant leptogenesis, which is established here in a natural way as a consequence of the discrete symmetries acting on the throats. Such a low–scale leptogenesis avoids the general problem with a low reheating temperature of the order of 10^9 GeV (gravitino problem), as predicted in generic inflationary supergravity models. A further interesting feature of this model is that the discrete symmetries can be broken by brane–localized kinetic terms and BCs.

We have considered in detail the CP–asymmetry generated in the decays of the heavy scalar KK modes into fermions. For this purpose, we have applied and compared different techniques. First, we have performed a standard calculation for the CP–violation in Dirac leptogenesis and found a disagreement with the result stated in the literature. The main difference is here how the complex conjugation has been applied to the Yukawa couplings. Next, we have transferred a resummation approach for unstable particles from resonant Majorana leptogenesis to the case of Dirac leptogenesis. As another main point in this thesis, we have explicitly minimized the scalar potential of a scalar bi–doublet within the LR–symmetric model in the 5D bulk. We have shown that, after dimensional reduction, the VEV of the scalar zero mode breaks in the 4D effective theory $SU(2)_L \times SU(2)_R$ down to the diagonal subgroup $SU(2)_D$. At the same time, the VEVs of the higher KK scalars are all zero. This allows for EWSB in connection with BCs at the IR brane. We have performed a corresponding analysis to describe the effect of brane–localized terms on the vacuum alignment. This is particularly useful for SSB in the presence of several 5D scalar bi–doublets. Finally, we have calculated the baryon asymmetry generated in our model including the contribution from the whole tower of KK states. Our results show that, under these circumstances, one can obtain a baryon asymmetry in agreement with observation.

In a more comprehensive analysis, one should include the effect of annihilation processes on the generation of the baryon asymmetry in detail. Also, explicit evaluations of Boltzmann equations might lead to a better understanding of the underlying dynamical processes. A possible danger for BBN, which should be checked in this scenario, is the overproduction of KK gravitons in extra dimensions. On the side of model building, one open question is how to obtain non–universal Yukawa couplings to the scalar KK states which might be important to avoid too late decays. This could for example, be achieved by altering the spectrum with dominant brane kinetic terms, by delocalizing also the fermions in the extra dimensions, or by switching on nonzero warp factors in the throats.

It would be interesting to investigate further possibilities of generating the mass splitting relevant for leptogenesis, such as mass splittings induced by loop corrections. This could be connected, *e.g.*, with TeV–scale supersymmetry. The fact that our model describes a low–scale leptogenesis scenario offers the appealing possibility to work out ample implications for collider physics. It would also be attractive to study the connection of our multi–throat setup to cosmology in the context of inflation and dark matter.

Appendix A

Decay Rate

Here, we derive the explicit expression for a $1 \to 2$ decay of an unstable particle as needed in Chapter (5). The general decay rate of an unstable particle to a given final state has the form

$$\Gamma = \frac{1}{2M_i}\Big(\int \prod_f \frac{d^3p_f}{(2\pi)^3}\frac{1}{2E_f}\Big)|\mathcal{M}(M_i \to p_f)|^2(2\pi)^4\delta^{(4)}(p_i - \sum_f p_f). \tag{A.1}$$

Considering the special case of one massive initial particle k and a massless two-particle final state $p+q$, *i.e.* $E_p = p^0 = |\mathbf{p}|$ and $E_q = q^0 = |\mathbf{q}|$, the Lorentz-invariant phase space takes the simple form

$$\begin{aligned} I_{Lips} &= \int \frac{d^3p}{(2\pi)^2}\frac{1}{2|\mathbf{p}|}\int d^3q\frac{1}{2|\mathbf{q}|}\delta^{(4)}(k-p-q)|\mathcal{M}|^2 \\ &= \int \frac{d^3p}{(2\pi)^2}\frac{1}{2|\mathbf{p}|}\frac{1}{2|\mathbf{k}-\mathbf{p}|}\,\delta\Big(k^0 - |\mathbf{p}| - |\mathbf{k}-\mathbf{p}|\Big)|\mathcal{M}|^2 \\ &= \frac{1}{8\pi}\int_{|\mathbf{p}|_{-1}}^{|\mathbf{p}|_{+1}} d|\mathbf{p}|\int_{-1}^{1} d\cos\vartheta\frac{1}{|\mathbf{k}|}\,\delta\Big(\cos\vartheta - \frac{k^0}{|\mathbf{k}|} + \frac{k^2}{2|\mathbf{k}||\mathbf{p}|}\Big)|\mathcal{M}|^2, \end{aligned} \tag{A.2}$$

where we are using spherical coordinates $d^3p = |\mathbf{p}|^2\, d\varphi\, d\cos\vartheta\, d|\mathbf{p}|$ to integrate over the δ-distribution for which

$$\delta\Big(k^0 - |\mathbf{p}| - |\mathbf{k}-\mathbf{p}|\Big) = \frac{|\mathbf{k}-\mathbf{p}|}{|\mathbf{k}||\mathbf{p}|}\,\delta\Big(\cos\vartheta - \frac{k^0}{|\mathbf{k}|} + \frac{k^2}{2|\mathbf{k}||\mathbf{p}|}\Big) \tag{A.3}$$

holds if $|\mathbf{k}|$, $|\mathbf{p}| > 0$ since $\delta(f(x)) = \delta(x)/f'(x)$. The angle ϑ denotes the angle between $\mathbf{k}$ and $\mathbf{p}$, *i.e.*, $\mathbf{k}\cdot\mathbf{p} = |\mathbf{k}||\mathbf{p}|\cos\vartheta$. Due to the δ-distribution and the fact that $-1 \le \cos\vartheta \le 1$ we can see that $|\mathbf{p}|_{-1} = \frac{1}{2}(k^0 - |\mathbf{k}|) \le |\mathbf{p}| \le \frac{1}{2}(k^0 + |\mathbf{k}|) = |\mathbf{p}|_{+1}$. Thus the final result takes the form

$$I_{Lips} = \frac{1}{8\pi}|\mathcal{M}|^2. \tag{A.4}$$

It is obvious that we can understand Eq. (5.8) in terms of the absolute–value squares of the amplitudes, since

$$\Gamma = \frac{1}{16\pi^2 M_i} |\mathcal{M}(M_i \to p_1 p_2)|^2. \tag{A.5}$$

This is the form of the decay rate used for the discussion of heavy scalar decays in this work.

Appendix B

Minimization Equations for the Total Potential

In this Appendix, we present the explicit expressions for the minimization of the total potential $V_{\text{eff}}^{\text{total}} = V'_{\text{eff}} + V_{B\text{eff}}$ introduced in Chapter 6.

B.1 Minimization Equations for the Potential

Let us first analyze the exact extremizing conditions of the bulk potential V'_{eff} in Eq. (6.18). We can use similar arguments as in Sec. 6.2 to discuss the $10 \cdot 4^2 = 160$ structurally different second derivatives of $V'_{\text{eff}}(X)$:

$$\begin{gathered}
\left.\frac{\partial^2 V'_{\text{eff}}(X)}{\partial R^{(0)}_{ab}\partial R^{(0)}_{cd}}\right|_{\text{VEVs}}, \quad \left.\frac{\partial^2 V'_{\text{eff}}(X)}{\partial I^{(0)}_{ab}\partial I^{(0)}_{cd}}\right|_{\text{VEVs}}, \quad \left.\frac{\partial^2 V'_{\text{eff}}(X)}{\partial R^{(0)}_{ab}\partial I^{(0)}_{cd}}\right|_{\text{VEVs}}, \\
\left.\frac{\partial^2 V'_{\text{eff}}(X)}{\partial R^{(0)}_{ab}\partial R^{(r)}_{cd}}\right|_{\text{VEVs}}, \quad \left.\frac{\partial^2 V'_{\text{eff}}(X)}{\partial I^{(0)}_{ab}\partial I^{(r)}_{cd}}\right|_{\text{VEVs}}, \quad \left.\frac{\partial^2 V'_{\text{eff}}(X)}{\partial R^{(r)}_{ab}\partial I^{(0)}_{cd}}\right|_{\text{VEVs}}, \quad \left.\frac{\partial^2 V'_{\text{eff}}(X)}{\partial R^{(0)}_{ab}\partial I^{(r)}_{cd}}\right|_{\text{VEVs}}, \\
\left.\frac{\partial^2 V'_{\text{eff}}(X)}{\partial R^{(r)}_{ab}\partial R^{(s)}_{cd}}\right|_{\text{VEVs}}, \quad \left.\frac{\partial^2 V'_{\text{eff}}(X)}{\partial I^{(r)}_{ab}\partial I^{(s)}_{cd}}\right|_{\text{VEVs}}, \quad \left.\frac{\partial^2 V'_{\text{eff}}(X)}{\partial R^{(r)}_{ab}\partial I^{(s)}_{cd}}\right|_{\text{VEVs}},
\end{gathered} \tag{B.1}$$

where the summation indices run over $a, b, c, d = 1, 2$, and $r, s = 1, \ldots, \infty$. Except for the zero mode, all higher KK modes acquire zero VEVs. Therefore, all linear derivatives for $R^{(r)}_{ab}$ or $I^{(r)}_{ab}$ have to be zero:

$$\left.\frac{\partial^2 V'_{\text{eff}}(X)}{\partial R^{(0)}_{ab}\partial R^{(r)}_{cd}}\right|_{\text{VEVs}} = \left.\frac{\partial^2 V'_{\text{eff}}(X)}{\partial I^{(0)}_{ab}\partial I^{(r)}_{cd}}\right|_{\text{VEVs}} = \left.\frac{\partial^2 V'_{\text{eff}}(X)}{\partial R^{(0)}_{ab}\partial I^{(r)}_{cd}}\right|_{\text{VEVs}} = \left.\frac{\partial^2 V'_{\text{eff}}(X)}{\partial R^{(r)}_{ab}\partial I^{(0)}_{cd}}\right|_{\text{VEVs}} = 0. \tag{B.2}$$

Furthermore, only squared terms in the higher KK-modes could lead to a nonzero result when differentiating with respect to $R^{(r)}_{ab}R^{(s)}_{ab}$, $I^{(r)}_{ab}I^{(s)}_{ab}$, or $R^{(r)}_{ab}I^{(s)}_{ab}$. Since Δ_{mn}

appears in the squared terms, all derivatives with $r \neq s$ are already zero:

$$\left.\frac{\partial^2 V'_{\rm eff}(X)}{\partial R^{(r)}_{ab}\partial R^{(s)}_{cd}}\right|_{\rm VEVs} = \left.\frac{\partial^2 V'_{\rm eff}(X)}{\partial I^{(r)}_{ab}\partial I^{(s)}_{cd}}\right|_{\rm VEVs} = \left.\frac{\partial^2 V'_{\rm eff}(X)}{\partial R^{(r)}_{ab}\partial I^{(s)}_{cd}}\right|_{\rm VEVs} = 0. \tag{B.3}$$

In Eq. (B.1), we will, as before, replace $V'_{\rm eff}$ by ${V'}^0_{\rm eff}$ and introduce

$$\begin{aligned} {V'}^r_{\rm eff}(X) = \; & - \sum_{i,j} \mu^2_{ij}\,{\rm tr}\, X^{(r)\dagger}_i X^{(r)}_j + K\Big(\frac{n}{\pi R}\Big)^2 {\rm tr}\, X^{(n)\dagger}_1 X^{(n)}_1 \\ & + \frac{1}{\pi R}\sum_{i,j,k,l,r}\Big\{\lambda_{ijkl}\Big[{\rm tr}\, X^{(0)\dagger}_i X^{(0)}_j\,{\rm tr}\, X^{(r)\dagger}_k X^{(r)}_l + \text{all permutations}\Big] \\ & + \widetilde{\lambda}_{ijkl}\Big[{\rm tr}\, X^{(0)\dagger}_i X^{(0)}_j X^{(r)\dagger}_k X^{(r)}_l + \text{all permutations}\Big]\Big\}. \end{aligned} \tag{B.4}$$

With all these considerations in mind, the non–trivial second derivatives are

$$\left.\frac{\partial^2 {V'}^0_{\rm eff}(X)}{\partial R^{(0)}_{ab}\partial I^{(0)}_{cd}}\right|_{\rm VEVs} = 0, \tag{B.5}$$

$$\begin{aligned} \left.\frac{\partial^2 {V'}^0_{\rm eff}(X)}{\partial R^{(0)}_{11}\partial R^{(0)}_{12}}\right|_{\rm VEVs} &= \left.\frac{\partial^2 {V'}^0_{\rm eff}(X)}{\partial R^{(0)}_{11}\partial R^{(0)}_{21}}\right|_{\rm VEVs} = \left.\frac{\partial^2 {V'}^0_{\rm eff}(X)}{\partial R^{(0)}_{12}\partial R^{(0)}_{22}}\right|_{\rm VEVs} = \left.\frac{\partial^2 {V'}^0_{\rm eff}(X)}{\partial R^{(0)}_{21}\partial R^{(0)}_{22}}\right|_{\rm VEVs} \\ &= \left.\frac{\partial^2 {V'}^0_{\rm eff}(X)}{\partial I^{(0)}_{11}\partial I^{(0)}_{12}}\right|_{\rm VEVs} = \left.\frac{\partial^2 {V'}^0_{\rm eff}(X)}{\partial I^{(0)}_{11}\partial I^{(0)}_{21}}\right|_{\rm VEVs} = \left.\frac{\partial^2 {V'}^0_{\rm eff}(X)}{\partial I^{(0)}_{12}\partial I^{(0)}_{22}}\right|_{\rm VEVs} \\ &= \left.\frac{\partial^2 {V'}^0_{\rm eff}(X)}{\partial I^{(0)}_{21}\partial I^{(0)}_{22}}\right|_{\rm VEVs} = 0, \end{aligned} \tag{B.6}$$

$$\begin{aligned} \left.\frac{\partial^2 {V'}^0_{\rm eff}(X)}{\partial R^{(0)}_{11}\partial R^{(0)}_{11}}\right|_{\rm VEVs} &= \left.\frac{\partial^2 {V'}^0_{\rm eff}(X)}{\partial R^{(0)}_{22}\partial R^{(0)}_{22}}\right|_{\rm VEVs} \\ &= -2(\mu^2_{11}+\mu^2_{22}) + \frac{4}{(\pi R)}[2(2\lambda_{1111}+3\lambda_{1112}+4\lambda_{1122}+3\lambda_{1211} \\ &\quad +2\lambda_{1212}+2\lambda_{1221}+3\lambda_{1222}+3\lambda_{2212}+2\lambda_{2222}) \\ &\quad +(3\widetilde{\lambda}_{1111}+6\widetilde{\lambda}_{1112}+4\widetilde{\lambda}_{1122}+2\widetilde{\lambda}_{1212}+6\widetilde{\lambda}_{1222} \\ &\quad +3\widetilde{\lambda}_{2222})]\kappa^2 = a^0, \end{aligned} \tag{B.7}$$

$$\begin{aligned} \left.\frac{\partial^2 {V'}^0_{\rm eff}(X)}{\partial R^{(0)}_{11}\partial R^{(0)}_{22}}\right|_{\rm VEVs} &= 2(\mu^2_{11}+\mu^2_{22}) + \frac{4}{(\pi R)}[2(\lambda_{1112}+\lambda_{1211}+2\lambda_{1212}+2\lambda_{1221} \\ &\quad +\lambda_{1222}+\lambda_{2212}) - (\widetilde{\lambda}_{1111}-2\widetilde{\lambda}_{1112}-4\widetilde{\lambda}_{1122}-2\widetilde{\lambda}_{1212} \\ &\quad -2\widetilde{\lambda}_{1222}+\widetilde{\lambda}_{2222})]\kappa^2 = b^0, \end{aligned} \tag{B.8}$$

$$\begin{aligned}
\left.\frac{\partial^2 V'^0_{\rm eff}(X)}{\partial R^{(0)}_{12}\partial R^{(0)}_{12}}\right|_{\rm VEVs} &= \left.\frac{\partial^2 V'^0_{\rm eff}(X)}{\partial R^{(0)}_{12}\partial R^{(0)}_{21}}\right|_{\rm VEVs} = \left.\frac{\partial^2 V'^0_{\rm eff}(X)}{\partial R^{(0)}_{21}\partial R^{(0)}_{21}}\right|_{\rm VEVs} = \left.\frac{\partial^2 V'^0_{\rm eff}(X)}{\partial I^{(0)}_{12}\partial I^{(0)}_{12}}\right|_{\rm VEVs} \\
&= -\left.\frac{\partial^2 V'^0_{\rm eff}(X)}{\partial I^{(0)}_{12}\partial I^{(0)}_{21}}\right|_{\rm VEVs} = \left.\frac{\partial^2 V'^0_{\rm eff}(X)}{\partial I^{(0)}_{21}\partial I^{(0)}_{21}}\right|_{\rm VEVs} \\
&= -2(\mu^2_{11}+\mu^2_{22}) + \frac{8}{(\pi R)}[(\lambda_{1111}+\lambda_{1112}+2\lambda_{1122}+\lambda_{1211} \\
&\quad +\lambda_{1222}+\lambda_{2212}+\lambda_{2222}) + (\widetilde{\lambda}_{1111}+2\widetilde{\lambda}_{1112}+\widetilde{\lambda}_{1222} \\
&\quad +\widetilde{\lambda}_{2222})]\kappa^2 = c^0, \qquad \text{(B.9)} \\
\left.\frac{\partial^2 V'^0_{\rm eff}(X)}{\partial I^{(0)}_{11}\partial I^{(0)}_{11}}\right|_{\rm VEVs} &= \left.\frac{\partial^2 V'^0_{\rm eff}(X)}{\partial I^{(0)}_{11}\partial I^{(0)}_{22}}\right|_{\rm VEVs} = \left.\frac{\partial^2 V'^0_{\rm eff}(X)}{\partial I^{(0)}_{22}\partial I^{(0)}_{22}}\right|_{\rm VEVs} \\
&= -2(\mu^2_{11}+\mu^2_{22}) + \frac{4}{(\pi R)}[2(\lambda_{1111}+\lambda_{1112}+2\lambda_{1122}+\lambda_{1211} \\
&\quad -2\lambda_{1212}+2\lambda_{1221}+\lambda_{1222}+\lambda_{2212}+\lambda_{2222}) \\
&\quad +(\widetilde{\lambda}_{1111}+2\widetilde{\lambda}_{1112}+4\widetilde{\lambda}_{1122}-2\widetilde{\lambda}_{1212}+2\widetilde{\lambda}_{1222} \\
&\quad +\widetilde{\lambda}_{2222})]\kappa^2 = d^0. \qquad \text{(B.10)}
\end{aligned}$$

In order to simplify the expressions, we have used here the extremizing condition to substitute μ^2_{12} by

$$\begin{aligned}
\mu^2_{12} &= -\frac{1}{2}(\mu^2_{11}+\mu^2_{22}) + \frac{1}{(\pi R)}[2(\lambda_{1111}+2\lambda_{1112}+2\lambda_{1122}+2\lambda_{1211} \\
&\quad +2\lambda_{1212}+2\lambda_{1221}+2\lambda_{1222}+2\lambda_{2212}+\lambda_{2222}) \\
&\quad +(\widetilde{\lambda}_{1111}+4\widetilde{\lambda}_{1112}+4\widetilde{\lambda}_{1122}+2\widetilde{\lambda}_{1212}+4\widetilde{\lambda}_{1222}+\widetilde{\lambda}_{2222})]\kappa^2, \qquad \text{(B.11)}
\end{aligned}$$

It is easily seen that the non–trivial second derivatives of $V'^r_{\rm eff}$ take the same values as the corresponding second derivatives of $V'^0_{\rm eff}$, except for a factor $(n/(\pi R))^2$ from the bulk kinetic term:

$$\begin{aligned}
\left.\frac{\partial^2 V'^0_{\rm eff}(X)}{\partial R^{(r)}_{ab}\partial I^{(r)}_{cd}}\right|_{\rm VEVs} &= 0, \qquad \text{(B.12)} \\
\left.\frac{\partial^2 V'^0_{\rm eff}(X)}{\partial R^{(r)}_{11}\partial R^{(r)}_{12}}\right|_{\rm VEVs} &= \left.\frac{\partial^2 V'^0_{\rm eff}(X)}{\partial R^{(r)}_{11}\partial R^{(r)}_{21}}\right|_{\rm VEVs} = \left.\frac{\partial^2 V'^0_{\rm eff}(X)}{\partial R^{(r)}_{12}\partial R^{(r)}_{22}}\right|_{\rm VEVs} = \left.\frac{\partial^2 V'^0_{\rm eff}(X)}{\partial R^{(r)}_{21}\partial R^{(r)}_{22}}\right|_{\rm VEVs} \\
&= \left.\frac{\partial^2 V'^0_{\rm eff}(X)}{\partial I^{(r)}_{11}\partial I^{(r)}_{12}}\right|_{\rm VEVs} = \left.\frac{\partial^2 V'^0_{\rm eff}(X)}{\partial I^{(r)}_{11}\partial I^{(r)}_{21}}\right|_{\rm VEVs} = \left.\frac{\partial^2 V'^0_{\rm eff}(X)}{\partial I^{(r)}_{12}\partial I^{(r)}_{22}}\right|_{\rm VEVs} \\
&= \left.\frac{\partial^2 V'^0_{\rm eff}(X)}{\partial I^{(r)}_{21}\partial I^{(r)}_{22}}\right|_{\rm VEVs} = 0, \qquad \text{(B.13)}
\end{aligned}$$

$$\left.\frac{\partial^2 V'^0_{\text{eff}}(X)}{\partial R_{11}^{(r)}\partial R_{11}^{(r)}}\right|_{\text{VEVs}} = \left.\frac{\partial^2 V'^0_{\text{eff}}(X)}{\partial R_{22}^{(r)}\partial R_{22}^{(r)}}\right|_{\text{VEVs}} = a^0 + 2K\Big(\frac{r}{\pi R}\Big) = a^r, \tag{B.14}$$

$$\left.\frac{\partial^2 V'^0_{\text{eff}}(X)}{\partial R_{11}^{(r)}\partial R_{22}^{(r)}}\right|_{\text{VEVs}} = b^0 = b^r, \tag{B.15}$$

$$\begin{aligned}\left.\frac{\partial^2 V'^0_{\text{eff}}(X)}{\partial R_{12}^{(r)}\partial R_{12}^{(r)}}\right|_{\text{VEVs}} &= \left.\frac{\partial^2 V'^0_{\text{eff}}(X)}{\partial R_{21}^{(r)}\partial R_{21}^{(r)}}\right|_{\text{VEVs}} = \left.\frac{\partial^2 V'^0_{\text{eff}}(X)}{\partial I_{12}^{(r)}\partial I_{12}^{(r)}}\right|_{\text{VEVs}} = \left.\frac{\partial^2 V'^0_{\text{eff}}(X)}{\partial I_{21}^{(r)}\partial I_{21}^{(r)}}\right|_{\text{VEVs}} \\ &= c^0 + 2K\Big(\frac{r}{\pi R}\Big) = c^r,\end{aligned} \tag{B.16}$$

$$\left.\frac{\partial^2 V'^0_{\text{eff}}(X)}{\partial I_{11}^{(r)}\partial I_{11}^{(r)}}\right|_{\text{VEVs}} = \left.\frac{\partial^2 V'^0_{\text{eff}}(X)}{\partial I_{22}^{(r)}\partial I_{22}^{(r)}}\right|_{\text{VEVs}} = d^0 + 2K\Big(\frac{r}{\pi R}\Big) = d^r, \tag{B.17}$$

$$\left.\frac{\partial^2 V'^0_{\text{eff}}(X)}{\partial R_{12}^{(r)}\partial R_{21}^{(r)}}\right|_{\text{VEVs}} = -\left.\frac{\partial^2 V'^0_{\text{eff}}(X)}{\partial I_{12}^{(r)}\partial I_{21}^{(r)}}\right|_{\text{VEVs}} = c^0 = e^r, \tag{B.18}$$

$$\left.\frac{\partial^2 V'^0_{\text{eff}}(X)}{\partial I_{11}^{(r)}\partial I_{22}^{(r)}}\right|_{\text{VEVs}} = d^0 = f^r. \tag{B.19}$$

$$\tag{B.20}$$

To whether there is a range of the parameters μ_{ij}, λ_{ijkl}, and $\widetilde{\lambda}_{ijkl}$ where V'_{eff} has a local minimum, we have to check whether the Hessian matrix $H\big(V'_{\text{eff}}\big)$ of V'_{eff} in Eq. (6.31) is positive semi–definite. In Sec. B.1 we show that there indeed exist such a local minimum.

B.2 Extremization Equations for the Brane–Localized Term

The brane–localized term $V_B(X)$ in Eq. 6.43 can be splitted into $V_B(X) = A_B(X) + B_B(X)$, where $B_B(X)$ only consists of mixed terms in X and $\widetilde{X}$, while $A_B(X)$ contains all the remaining terms. The 4D effective operator $V_{B\text{eff}}(X) = A_{B\text{eff}}(X) + B_{B\text{eff}}(X)$ can be calculated by integrating over the extra dimension y. The two parts $A_{B\text{eff}}(X) =$

$\int_0^{\pi R} dy A_B(X)$ and $B_{B\text{eff}}(X) = \int_0^{\pi R} dy B_B(X)$ of $V_{B\text{eff}}(X)$ have the form

$$
\begin{aligned}
A_{B\text{eff}}(X) &= -\mu_1^2 \frac{1}{\sqrt{\pi R}} \Big[(X_1^{(0)})^{(0)} + (X_2^{(0)})^{(0)} + \sqrt{2} \sum_{n=1}^{\infty} \cos(n\pi) \Big[(X_1^{(0)})^{(n)} + (X_2^{(0)})^{(n)} \Big] \Big] \\
&+ \lambda_{11} \frac{1}{\pi R} \Big[(X_1^{(0)})^{(0)} + (X_2^{(0)})^{(0)} + \sqrt{2} \sum_{n=1}^{\infty} \cos(n\pi) \Big[(X_1^{(0)})^{(n)} + (X_2^{(0)})^{(n)} \Big] \Big]^2 \\
&+ \widetilde{\lambda}_{11} \frac{1}{\pi R} \Big[\Big[(X_1^{(0)})^{(0)2} + 2 (X_1^{+})^{(0)} (X_2^{-})^{(0)} + (X_2^{(0)})^{(0)2} \Big] \\
&+ 2 \sum_{n=1}^{\infty} \Big[(X_1^{(0)})^{(n)2} + 2 (X_1^{+})^{(n)} (X_2^{-})^{(n)} + (X_2^{(0)})^{(n)2} \Big] \\
&+ 2\sqrt{2} \sum_{n=1}^{\infty} \cos(n\pi) \Big[(X_1^{(0)})^{(0)} (X_1^{(0)})^{(n)} + (X_1^{+})^{(0)} (X_2^{-})^{(n)} \\
&+ (X_2^{-})^{(0)} (X_1^{+})^{(n)} + (X_2^{(0)})^{(0)} (X_2^{(0)})^{(n)} \Big] \\
&+ 2 \sum_{\substack{n,m=1 \\ n \neq m}}^{\infty} \cos(n\pi) \cos(m\pi) \Big[(X_1^{(0)})^{(n)} (X_1^{(0)})^{(m)} + (X_1^{+})^{(n)} (X_2^{-})^{(m)} \\
&+ (X_2^{-})^{(n)} (X_1^{+})^{(m)} + (X_2^{(0)})^{(n)} (X_2^{(0)})^{(m)} \Big] \Big] + \text{h.c.}, \qquad \text{(B.21)}
\end{aligned}
$$

$$
\begin{aligned}
B_{B\text{eff}}(X) &= \lambda_{12} \frac{1}{\pi R} \Big[(X_1^{(0)})^{(0)} + (X_2^{(0)})^{(0)} + \sqrt{2} \sum_{n=1}^{\infty} \cos(n\pi) \Big[(X_1^{(0)})^{(n)} + (X_2^{(0)})^{(n)} \Big] \Big] \\
&\quad \Big[(X_1^{0*})^{(0)} + (X_2^{0*})^{(0)} + \sqrt{2} \sum_{n=1}^{\infty} \cos(n\pi) \Big[(X_1^{0*})^{(n)} + (X_2^{0*})^{(n)} \Big] \Big] \\
&+ \widetilde{\lambda}_{12} \frac{1}{\pi R} \Big[\Big[(X_1^{(0)})^{(0)} (X_2^{0*})^{(0)} - (X_1^{+})^{(0)} (X_1^{-})^{(0)} - (X_2^{+})^{(0)} (X_2^{-})^{(0)} \\
&+ (X_2^{(0)})^{(0)} (X_1^{0*})^{(0)} \Big] + 2 \sum_{n=1}^{\infty} \Big[(X_1^{(0)})^{(n)} (X_2^{0*})^{(n)} - (X_1^{+})^{(n)} (X_1^{-})^{(n)} \\
&- (X_2^{+})^{(n)} (X_2^{-})^{(n)} + (X_2^{(0)})^{(n)} (X_1^{0*})^{(n)} \Big] \\
&+ \sqrt{2} \sum_{n=1}^{\infty} \cos(n\pi) \Big[(X_1^{(0)})^{(0)} (X_2^{0*})^{(n)} + (X_1^{(0)})^{(n)} (X_2^{0*})^{(0)} \\
&- (X_1^{+})^{(0)} (X_1^{-})^{(n)} - (X_1^{+})^{(n)} (X_1^{-})^{(0)} - (X_2^{+})^{(0)} (X_2^{-})^{(n)} \\
&- (X_2^{+})^{(n)} (X_2^{-})^{(0)} + (X_2^{(0)})^{(0)} (X_1^{0*})^{(n)} + (X_2^{(0)})^{(n)} (X_1^{0*})^{(0)} \Big] \\
&+ 2 \sum_{\substack{n,m=1 \\ n \neq m}}^{\infty} \cos(n\pi) \cos(m\pi) \Big[(X_1^{(0)})^{(n)} (X_2^{0*})^{(m)} + (X_1^{(0)})^{(m)} (X_2^{0*})^{(n)} \\
&- (X_1^{+})^{(n)} (X_1^{-})^{(m)} - (X_2^{+})^{(n)} (X_2^{-})^{(m)} + (X_2^{(0)})^{(n)} (X_1^{0*})^{(m)} \Big] \Big] + \text{h.c.}
\end{aligned}
$$

(B.22)

The calculation of the extremizing equations for $A_{B\text{eff}}(X)$ and $B_{B\text{eff}}(X)$ is significantly simplified by noting that both terms are real. Since $z + z^* = 2\text{Re}(z)$, we will in our further calculations only have to consider two times the real part of X. The local extrema of $V_{B\text{eff}}(X)$ satisfy the following extremum conditions:

$$\begin{aligned}
\left.\frac{\partial V_{B\text{eff}}(X)}{\partial R_{11}^{(0)}}\right|_{\text{VEVs}} &= -\mu_1^2\frac{2}{\sqrt{\pi R}} \\
&+ (\lambda_{11}+\lambda_{12})\frac{4}{\pi R}\Big[\big\langle R_{11}^{(0)}\big\rangle + \big\langle R_{22}^{(0)}\big\rangle + \sqrt{2}\sum_{n=1}^{\infty}\cos(n\pi)\Big(\big\langle R_{11}^{(n)}\big\rangle + \big\langle R_{22}^{(n)}\big\rangle\Big)\Big] \\
&+ \widetilde{\lambda}_{11}\frac{4}{\pi R}\Big[\big\langle R_{11}^{(0)}\big\rangle + \sqrt{2}\sum_{n=1}^{\infty}\cos(n\pi)\big\langle R_{11}^{(n)}\big\rangle\Big] \\
&+ \widetilde{\lambda}_{12}\frac{4}{\pi R}\Big[\big\langle R_{22}^{(0)}\big\rangle + \sqrt{2}\sum_{n=1}^{\infty}\cos(n\pi)\big\langle R_{22}^{(n)}\big\rangle\Big] = 0, \qquad \text{(B.23a)} \\
\left.\frac{\partial V_{B\text{eff}}(X)}{\partial R_{22}^{(0)}}\right|_{\text{VEVs}} &= -\mu_1^2\frac{2}{\sqrt{\pi R}} \\
&+ (\lambda_{11}+\lambda_{12})\frac{4}{\pi R}\Big[\big\langle R_{22}^{(0)}\big\rangle + \big\langle R_{11}^{(0)}\big\rangle + \sqrt{2}\sum_{n=1}^{\infty}\cos(n\pi)\Big(\big\langle R_{22}^{(n)}\big\rangle + \big\langle R_{11}^{(n)}\big\rangle\Big)\Big] \\
&+ \widetilde{\lambda}_{11}\frac{4}{\pi R}\Big[\big\langle R_{22}^{(0)}\big\rangle + \sqrt{2}\sum_{n=1}^{\infty}\cos(n\pi)\big\langle R_{22}^{(n)}\big\rangle\Big] \\
&+ \widetilde{\lambda}_{12}\frac{4}{\pi R}\Big[\big\langle R_{11}^{(0)}\big\rangle + \sqrt{2}\sum_{n=1}^{\infty}\cos(n\pi)\big\langle R_{11}^{(n)}\big\rangle\Big] = 0, \qquad \text{(B.23b)} \\
\left.\frac{\partial V_{B\text{eff}}(X)}{\partial I_{11}^{(0)}}\right|_{\text{VEVs}} &= -(\lambda_{11}-\lambda_{12})\frac{4}{\pi R}\Big[\big\langle I_{11}^{(0)}\big\rangle + \big\langle I_{22}^{(0)}\big\rangle + \sqrt{2}\sum_{n=1}^{\infty}\cos(n\pi)\Big(\big\langle I_{11}^{(n)}\big\rangle + \big\langle I_{22}^{(n)}\big\rangle\Big)\Big] \\
&- \widetilde{\lambda}_{11}\frac{4}{\pi R}\Big[\big\langle I_{11}^{(0)}\big\rangle + \sqrt{2}\sum_{n=1}^{\infty}\cos(n\pi)\big\langle I_{11}^{(n)}\big\rangle\Big] \\
&+ \widetilde{\lambda}_{12}\frac{4}{\pi R}\Big[\big\langle I_{22}^{(0)}\big\rangle + \sqrt{2}\sum_{n=1}^{\infty}\cos(n\pi)\big\langle I_{22}^{(n)}\big\rangle\Big] = 0, \qquad \text{(B.23c)} \\
\left.\frac{\partial V_{B\text{eff}}(X)}{\partial I_{22}^{(0)}}\right|_{\text{VEVs}} &= -(\lambda_{11}-\lambda_{12})\frac{4}{\pi R}\Big[\big\langle I_{22}^{(0)}\big\rangle + \big\langle I_{11}^{(0)}\big\rangle + \sqrt{2}\sum_{n=1}^{\infty}\cos(n\pi)\Big(\big\langle I_{22}^{(n)}\big\rangle + \big\langle I_{11}^{(n)}\big\rangle\Big)\Big] \\
&- \widetilde{\lambda}_{11}\frac{4}{\pi R}\Big[\big\langle I_{22}^{(0)}\big\rangle + \sqrt{2}\sum_{n=1}^{\infty}\cos(n\pi)\big\langle I_{22}^{(n)}\big\rangle\Big] \\
&+ \widetilde{\lambda}_{12}\frac{4}{\pi R}\Big[\big\langle I_{11}^{(0)}\big\rangle + \sqrt{2}\sum_{n=1}^{\infty}\cos(n\pi)\big\langle I_{11}^{(n)}\big\rangle\Big] = 0, \qquad \text{(B.23d)}
\end{aligned}$$

$$\left.\frac{\partial V_{B\text{eff}}(X)}{\partial R_{12}^{(0)}}\right|_{\text{VEVs}} = \widetilde{\lambda}_{11}\frac{4}{\pi R}\Big[\big\langle R_{21}^{(0)}\big\rangle + \sqrt{2}\sum_{n=1}^{\infty}\cos(n\pi)\big\langle R_{21}^{(n)}\big\rangle\Big]$$
$$- \widetilde{\lambda}_{12}\frac{4}{\pi R}\Big[\big\langle R_{12}^{(0)}\big\rangle + \sqrt{2}\sum_{n=1}^{\infty}\cos(n\pi)\big\langle R_{12}^{(n)}\big\rangle\Big] = 0, \tag{B.23e}$$

$$\left.\frac{\partial V_{B\text{eff}}(X)}{\partial R_{21}^{(0)}}\right|_{\text{VEVs}} = \widetilde{\lambda}_{11}\frac{4}{\pi R}\Big[\big\langle R_{12}^{(0)}\big\rangle + \sqrt{2}\sum_{n=1}^{\infty}\cos(n\pi)\big\langle R_{12}^{(n)}\big\rangle\Big]$$
$$- \widetilde{\lambda}_{12}\frac{4}{\pi R}\Big[\big\langle R_{21}^{(0)}\big\rangle + \sqrt{2}\sum_{n=1}^{\infty}\cos(n\pi)\big\langle R_{21}^{(n)}\big\rangle\Big] = 0, \tag{B.23f}$$

$$\left.\frac{\partial V_{B\text{eff}}(X)}{\partial I_{12}^{(0)}}\right|_{\text{VEVs}} = -\widetilde{\lambda}_{11}\frac{4}{\pi R}\Big[\big\langle I_{21}^{(0)}\big\rangle + \sqrt{2}\sum_{n=1}^{\infty}\cos(n\pi)\big\langle I_{21}^{(n)}\big\rangle\Big]$$
$$- \widetilde{\lambda}_{12}\frac{4}{\pi R}\Big[\big\langle I_{12}^{(0)}\big\rangle + \sqrt{2}\sum_{n=1}^{\infty}\cos(n\pi)\big\langle I_{12}^{(n)}\big\rangle\Big] = 0, \tag{B.23g}$$

$$\left.\frac{\partial V_{B\text{eff}}(X)}{\partial I_{21}^{(0)}}\right|_{\text{VEVs}} = -\widetilde{\lambda}_{11}\frac{4}{\pi R}\Big[\big\langle I_{12}^{(0)}\big\rangle + \sqrt{2}\sum_{n=1}^{\infty}\cos(n\pi)\big\langle I_{12}^{(n)}\big\rangle\Big]$$
$$- \widetilde{\lambda}_{12}\frac{4}{\pi R}\Big[\big\langle I_{21}^{(0)}\big\rangle + \sqrt{2}\sum_{n=1}^{\infty}\cos(n\pi)\big\langle I_{21}^{(n)}\big\rangle\Big] = 0, \tag{B.23h}$$

$$\left.\frac{\partial V_{B\text{eff}}(X)}{\partial R_{11}^{(n)}}\right|_{\text{VEVs}} = -\mu_1^2\frac{2\sqrt{2}}{\sqrt{\pi R}}\cos(n\pi) + (\lambda_{11}+\lambda_{12})\frac{4\sqrt{2}}{\pi R}\Big[\cos(n\pi)\big\langle R_{11}^{(0)}\big\rangle + \cos(n\pi)\big\langle R_{22}^{(0)}\big\rangle$$
$$+ \sqrt{2}\Big(\big\langle R_{11}^{(n)}\big\rangle + \big\langle R_{22}^{(n)}\big\rangle\Big) + \sqrt{2}\sum_{\substack{m=1\\m\neq n}}^{\infty}\cos(n\pi)\cos(m\pi)\Big(\big\langle R_{11}^{(m)}\big\rangle + \big\langle R_{22}^{(m)}\big\rangle\Big)\Big]$$
$$+ \widetilde{\lambda}_{11}\frac{4\sqrt{2}}{\pi R}\Big[\sqrt{2}\big\langle R_{11}^{(n)}\big\rangle + \cos(n\pi)\big\langle R_{11}^{(0)}\big\rangle + \sqrt{2}\sum_{\substack{m=1\\m\neq n}}^{\infty}\cos(n\pi)\cos(m\pi)\big\langle R_{11}^{(m)}\big\rangle\Big]$$
$$+ \widetilde{\lambda}_{12}\frac{4\sqrt{2}}{\pi R}\Big[\sqrt{2}\big\langle R_{22}^{(n)}\big\rangle + \cos(n\pi)\big\langle R_{22}^{(0)}\big\rangle + \sqrt{2}\sum_{\substack{m=1\\m\neq n}}^{\infty}\cos(n\pi)\cos(m\pi)\big\langle R_{22}^{(m)}\big\rangle\Big]$$
$$= 0, \tag{B.23i}$$

$$\left.\frac{\partial V_{B\text{eff}}(X)}{\partial R_{22}^{(n)}}\right|_{\text{VEVs}} = -\mu_1^2\frac{2\sqrt{2}}{\sqrt{\pi R}}\cos(n\pi) + (\lambda_{11}+\lambda_{12})\frac{4\sqrt{2}}{\pi R}\Big[\cos(n\pi)\big\langle R_{22}^{(0)}\big\rangle + \cos(n\pi)\big\langle R_{11}^{(0)}\big\rangle$$
$$+ \sqrt{2}\Big(\big\langle R_{22}^{(n)}\big\rangle + \big\langle R_{11}^{(n)}\big\rangle\Big) + \sqrt{2}\sum_{\substack{m=1\\m\neq n}}^{\infty}\cos(n\pi)\cos(m\pi)\Big(\big\langle R_{22}^{(m)}\big\rangle + \big\langle R_{11}^{(m)}\big\rangle\Big)\Big]$$
$$+ \widetilde{\lambda}_{11}\frac{4\sqrt{2}}{\pi R}\Big[\sqrt{2}\big\langle R_{22}^{(n)}\big\rangle + \cos(n\pi)\big\langle R_{22}^{(0)}\big\rangle + \sqrt{2}\sum_{\substack{m=1\\m\neq n}}^{\infty}\cos(n\pi)\cos(m\pi)\big\langle R_{22}^{(m)}\big\rangle\Big]$$
$$+ \widetilde{\lambda}_{12}\frac{4\sqrt{2}}{\pi R}\Big[\sqrt{2}\big\langle R_{11}^{(n)}\big\rangle + \cos(n\pi)\big\langle R_{11}^{(0)}\big\rangle + \sqrt{2}\sum_{\substack{m=1\\m\neq n}}^{\infty}\cos(n\pi)\cos(m\pi)\big\langle R_{11}^{(m)}\big\rangle\Big]$$
$$= 0, \tag{B.23j}$$

$$\begin{aligned}
\left.\frac{\partial V_{B\text{eff}}(X)}{\partial I_{11}^{(n)}}\right|_{\text{VEVs}} &= -(\lambda_{11}-\lambda_{12})\frac{4\sqrt{2}}{\pi R}\Big[\cos(n\pi)\big\langle I_{11}^{(0)}\big\rangle + \cos(n\pi)\big\langle I_{22}^{(0)}\big\rangle \\
&+ \sqrt{2}\Big(\big\langle I_{11}^{(n)}\big\rangle + \big\langle I_{22}^{(n)}\big\rangle\Big) + \sqrt{2}\sum_{\substack{m=1\\m\neq n}}^{\infty}\cos(n\pi)\cos(m\pi)\Big(\big\langle I_{11}^{(m)}\big\rangle + \big\langle I_{22}^{(m)}\big\rangle\Big)\Big] \\
&- \widetilde{\lambda}_{11}\frac{4\sqrt{2}}{\pi R}\Big[\sqrt{2}\big\langle I_{11}^{(n)}\big\rangle + \cos(n\pi)\big\langle I_{11}^{(0)}\big\rangle + \sqrt{2}\sum_{\substack{m=1\\m\neq n}}^{\infty}\cos(n\pi)\cos(m\pi)\big\langle I_{11}^{(m)}\big\rangle\Big] \\
&+ \widetilde{\lambda}_{12}\frac{4\sqrt{2}}{\pi R}\Big[\sqrt{2}\big\langle I_{22}^{(n)}\big\rangle + \cos(n\pi)\big\langle I_{22}^{(0)}\big\rangle + \sqrt{2}\sum_{\substack{m=1\\m\neq n}}^{\infty}\cos(n\pi)\cos(m\pi)\big\langle I_{22}^{(m)}\big\rangle\Big] \\
&= 0, \qquad \text{(B.23k)}
\end{aligned}$$

$$\begin{aligned}
\left.\frac{\partial V_{B\text{eff}}(X)}{\partial I_{22}^{(n)}}\right|_{\text{VEVs}} &= -(\lambda_{11}-\lambda_{12})\frac{4\sqrt{2}}{\pi R}\Big[\cos(n\pi)\big\langle I_{22}^{(0)}\big\rangle + \cos(n\pi)\big\langle I_{11}^{(0)}\big\rangle \\
&+ \sqrt{2}\Big(\big\langle I_{22}^{(n)}\big\rangle + \big\langle I_{11}^{(n)}\big\rangle\Big) + \sqrt{2}\sum_{\substack{m=1\\m\neq n}}^{\infty}\cos(n\pi)\cos(m\pi)\Big(\big\langle I_{22}^{(m)}\big\rangle + \big\langle I_{11}^{(m)}\big\rangle\Big)\Big] \\
&- \widetilde{\lambda}_{11}\frac{4\sqrt{2}}{\pi R}\Big[\sqrt{2}\big\langle I_{22}^{(n)}\big\rangle + \cos(n\pi)\big\langle I_{22}^{(0)}\big\rangle + \sqrt{2}\sum_{\substack{m=1\\m\neq n}}^{\infty}\cos(n\pi)\cos(m\pi)\big\langle I_{22}^{(m)}\big\rangle\Big] \\
&+ \widetilde{\lambda}_{12}\frac{4\sqrt{2}}{\pi R}\Big[\sqrt{2}\big\langle I_{11}^{(n)}\big\rangle + \cos(n\pi)\big\langle I_{11}^{(0)}\big\rangle + \sqrt{2}\sum_{\substack{m=1\\m\neq n}}^{\infty}\cos(n\pi)\cos(m\pi)\big\langle I_{11}^{(m)}\big\rangle\Big] \\
&= 0, \qquad \text{(B.23l)}
\end{aligned}$$

$$\begin{aligned}
\left.\frac{\partial V_{B\text{eff}}(X)}{\partial R_{12}^{(n)}}\right|_{\text{VEVs}} &= \widetilde{\lambda}_{11}\frac{4}{\pi R}\Big[2\big\langle R_{21}^{(n)}\big\rangle + \sqrt{2}\cos(n\pi)\big\langle R_{21}^{(0)}\big\rangle + 2\sum_{\substack{m=1\\m\neq n}}^{\infty}\cos(n\pi)\cos(m\pi)\big\langle R_{21}^{(m)}\big\rangle\Big] \\
&- \widetilde{\lambda}_{12}\frac{4}{\pi R}\Big[2\big\langle R_{12}^{(n)}\big\rangle + \sqrt{2}\cos(n\pi)\big\langle R_{12}^{(0)}\big\rangle + 2\sum_{\substack{m=1\\m\neq n}}^{\infty}\cos(n\pi)\cos(m\pi)\big\langle R_{12}^{(m)}\big\rangle\Big] \\
&= 0, \qquad \text{(B.23m)}
\end{aligned}$$

$$\begin{aligned}
\left.\frac{\partial V_{B\text{eff}}(X)}{\partial R_{21}^{(n)}}\right|_{\text{VEVs}} &= \widetilde{\lambda}_{11}\frac{4}{\pi R}\Big[2\big\langle R_{12}^{(n)}\big\rangle + \sqrt{2}\cos(n\pi)\big\langle R_{12}^{(0)}\big\rangle + 2\sum_{\substack{m=1\\m\neq n}}^{\infty}\cos(n\pi)\cos(m\pi)\big\langle R_{12}^{(m)}\big\rangle\Big] \\
&- \widetilde{\lambda}_{12}\frac{4}{\pi R}\Big[2\big\langle R_{21}^{(n)}\big\rangle + \sqrt{2}\cos(n\pi)\big\langle R_{21}^{(0)}\big\rangle + 2\sum_{\substack{m=1\\m\neq n}}^{\infty}\cos(n\pi)\cos(m\pi)\big\langle R_{21}^{(m)}\big\rangle\Big] \\
&= 0, \qquad \text{(B.23n)}
\end{aligned}$$

$$\left.\frac{\partial V_{B\text{eff}}(X)}{\partial I_{12}^{(n)}}\right|_{\text{VEVs}} = -\widetilde{\lambda}_{11}\frac{4}{\pi R}\Big[2\big\langle I_{21}^{(n)}\big\rangle + \sqrt{2}\cos(n\pi)\big\langle I_{21}^{(0)}\big\rangle + 2\sum_{\substack{m=1\\m\neq n}}^{\infty}\cos(n\pi)\cos(m\pi)\big\langle I_{21}^{(m)}\big\rangle\Big]$$
$$- \widetilde{\lambda}_{12}\frac{4}{\pi R}\Big[2\big\langle I_{12}^{(n)}\big\rangle + \sqrt{2}\cos(n\pi)\big\langle I_{12}^{(0)}\big\rangle + 2\sum_{\substack{m=1\\m\neq n}}^{\infty}\cos(n\pi)\cos(m\pi)\big\langle I_{12}^{(m)}\big\rangle\Big]$$
$$= 0, \tag{B.23o}$$

$$\left.\frac{\partial V_{B\text{eff}}(X)}{\partial I_{21}^{(n)}}\right|_{\text{VEVs}} = -\widetilde{\lambda}_{11}\frac{4}{\pi R}\Big[2\big\langle I_{12}^{(n)}\big\rangle + \sqrt{2}\cos(n\pi)\big\langle I_{12}^{(0)}\big\rangle + 2\sum_{\substack{m=1\\m\neq n}}^{\infty}\cos(n\pi)\cos(m\pi)\big\langle I_{12}^{(m)}\big\rangle\Big]$$
$$- \widetilde{\lambda}_{12}\frac{4}{\pi R}\Big[2\big\langle I_{21}^{(n)}\big\rangle + \sqrt{2}\cos(n\pi)\big\langle I_{21}^{(0)}\big\rangle + 2\sum_{\substack{m=1\\m\neq n}}^{\infty}\cos(n\pi)\cos(m\pi)\big\langle I_{21}^{(m)}\big\rangle\Big]$$
$$= 0. \tag{B.23p}$$

From these conditions we see that if the only the zero mode acquires a VEV, these VEVs must must have the form given in Eq. (6.50).

B.3 Minimization Equations for the Brane–Localized Term

In this Section, we will list the exact expressions for all the nonzero 2nd order derivatives of the potential V_{Beff} in Eq. (6.43). We find

$$\frac{\partial^2 V_{B\text{eff}}(X)}{\partial R_{aa}^{(0)2}} = \frac{4}{\pi R}(\lambda_{11}+\lambda_{12}+\widetilde{\lambda}_{11}), \tag{B.24a}$$
$$\frac{\partial^2 V_{B\text{eff}}(X)}{\partial I_{aa}^{(0)2}} = -\frac{4}{\pi R}(\lambda_{11}-\lambda_{12}+\widetilde{\lambda}_{11}), \tag{B.24b}$$
$$\frac{\partial^2 V_{B\text{eff}}(X)}{\partial R_{aa}^{(n)2}} = \frac{8}{\pi R}(\lambda_{11}+\lambda_{12}+\widetilde{\lambda}_{11}), \tag{B.24c}$$
$$\frac{\partial^2 V_{B\text{eff}}(X)}{\partial I_{aa}^{(n)2}} = -\frac{4}{\pi R}(\lambda_{11}-\lambda_{12}+\widetilde{\lambda}_{11}), \tag{B.24d}$$

and

$$\left.\frac{\partial^2 V_{B\text{eff}}(X)}{\partial R^{(0)}_{aa}\partial R^{(n)}_{aa}}\right|_{\text{VEVs}} = \frac{4\sqrt{2}}{\pi R}\cos(n\pi)(\lambda_{11}+\lambda_{12}+\widetilde{\lambda}_{11}), \tag{B.24e}$$

$$\left.\frac{\partial^2 V_{B\text{eff}}(X)}{\partial I^{(0)}_{aa}\partial I^{(n)}_{aa}}\right|_{\text{VEVs}} = -\frac{4\sqrt{2}}{\pi R}\cos(n\pi)(\lambda_{11}-\lambda_{12}+\widetilde{\lambda}_{11}), \tag{B.24f}$$

$$\left.\frac{\partial^2 V_{B\text{eff}}(X)}{\partial R^{(n)}_{aa}\partial R^{(m)}_{aa}}\right|_{\text{VEVs}} = \frac{8}{\pi R}\cos(n\pi)\cos(m\pi)(\lambda_{11}+\lambda_{12}+\widetilde{\lambda}_{11}), \tag{B.24g}$$

$$\left.\frac{\partial^2 V_{B\text{eff}}(X)}{\partial I^{(n)}_{aa}\partial I^{(m)}_{aa}}\right|_{\text{VEVs}} = -\frac{8}{\pi R}\cos(n\pi)\cos(m\pi)(\lambda_{11}-\lambda_{12}+\widetilde{\lambda}_{11}), \tag{B.24h}$$

while the 2nd derivatives with respect to off-diagonal elements, *i.e.*, for $a \neq b$, are

$$\left.\frac{\partial^2 V_{B\text{eff}}(X)}{\partial R^{(0)2}_{ab}}\right|_{\text{VEVs}} = \left.\frac{\partial^2 V_{B\text{eff}}(X)}{\partial I^{(0)2}_{ab}}\right|_{\text{VEVs}} = -\frac{4}{\pi R}\lambda_{12}, \tag{B.24i}$$

$$\left.\frac{\partial^2 V_{B\text{eff}}(X)}{\partial R^{(n)2}_{ab}}\right|_{\text{VEVs}} = \left.\frac{\partial^2 V_{B\text{eff}}(X)}{\partial I^{(n)2}_{ab}}\right|_{\text{VEVs}} = -\frac{8}{\pi R}\lambda_{12}. \tag{B.24j}$$

For $a \neq b$, we find

$$\left.\frac{\partial^2 V_{B\text{eff}}(X)}{\partial R^{(0)}_{aa}\partial R^{(0)}_{bb}}\right|_{\text{VEVs}} = (\lambda_{11}+\lambda_{12}+\widetilde{\lambda}_{12})\frac{4}{\pi R}, \tag{B.24k}$$

$$\left.\frac{\partial^2 V_{B\text{eff}}(X)}{\partial I^{(0)}_{aa}\partial I^{(0)}_{bb}}\right|_{\text{VEVs}} = -(\lambda_{11}-\lambda_{12}-\widetilde{\lambda}_{12})\frac{4}{\pi R}, \tag{B.24l}$$

$$\left.\frac{\partial^2 V_{B\text{eff}}(X)}{\partial R^{(0)}_{aa}\partial R^{(n)}_{bb}}\right|_{\text{VEVs}} = (\lambda_{11}+\lambda_{12}+\widetilde{\lambda}_{12})\frac{4\sqrt{2}}{\pi R}\cos(n\pi), \tag{B.24m}$$

$$\left.\frac{\partial^2 V_{B\text{eff}}(X)}{\partial I^{(0)}_{aa}\partial I^{(n)}_{bb}}\right|_{\text{VEVs}} = -(\lambda_{11}-\lambda_{12}-\widetilde{\lambda}_{12})\frac{4\sqrt{2}}{\pi R}\cos(n\pi), \tag{B.24n}$$

$$\left.\frac{\partial^2 V_{B\text{eff}}(X)}{\partial R^{(n)}_{aa}\partial R^{(n)}_{bb}}\right|_{\text{VEVs}} = (\lambda_{11}+\lambda_{12}+\widetilde{\lambda_{12}})\frac{8}{\pi R}, \tag{B.24o}$$

$$\left.\frac{\partial^2 V_{B\text{eff}}}{\partial I^{(n)}_{aa}\partial I^{(n)}_{bb}}\right|_{\text{VEVs}} = -(\lambda_{11}-\lambda_{12}-\widetilde{\lambda_{12}})\frac{8}{\pi R}, \tag{B.24p}$$

$$\left.\frac{\partial^2 V_{B\text{eff}}(X)}{\partial R^{(n)}_{aa}\partial R^{(m)}_{bb}}\right|_{\text{VEVs}} = (\lambda_{11}+\lambda_{12}+\widetilde{\lambda}_{12})\frac{8}{\pi R}\cos(n\pi)\cos(m\pi), \tag{B.24q}$$

$$\left.\frac{\partial^2 V_{B\text{eff}}(X)}{\partial I^{(n)}_{aa}\partial I^{(m)}_{bb}}\right|_{\text{VEVs}} = -(\lambda_{11}-\lambda_{12}-\widetilde{\lambda}_{12})\frac{8}{\pi R}\cos(n\pi)\cos(m\pi), \tag{B.24r}$$

and for purely off-diagonal derivatives, *i.e.*, $ab \neq cd$, $a \neq b$ and $c \neq d$:

$$\left.\frac{\partial^2 V_{B\text{eff}}(X)}{\partial R^{(0)}_{ab}\partial R^{(0)}_{cd}}\right|_{\text{VEVs}} = -\left.\frac{\partial^2 V_{B\text{eff}(X)}}{\partial I^{(0)}_{ab}\partial I^{(0)}_{cd}}\right|_{\text{VEVs}} = \widetilde{\lambda}_{11}\frac{4}{\pi R}, \tag{B.24s}$$

$$\left.\frac{\partial^2 V_{B\text{eff}}(X)}{\partial R^{(0)}_{ab}\partial R^{(n)}_{cd}}\right|_{\text{VEVs}} = -\left.\frac{\partial^2 V_{B\text{eff}}(X)}{\partial I^{(0)}_{ab}\partial I^{(n)}_{cd}}\right|_{\text{VEVs}} = \widetilde{\lambda}_{11}\frac{4\sqrt{2}}{\pi R}\cos(n\pi), \tag{B.24t}$$

$$\left.\frac{\partial^2 V_{B\text{eff}}(X)}{\partial R^{(n)}_{ab}\partial R^{(n)}_{cd}}\right|_{\text{VEVs}} = -\left.\frac{\partial^2 V_{B\text{eff}}(X)}{\partial I^{(n)}_{ab}\partial I^{(n)}_{cd}}\right|_{\text{VEVs}} = \widetilde{\lambda}_{11}\frac{8}{\pi R}, \tag{B.24u}$$

$$\left.\frac{\partial^2 V_{B\text{eff}}(X)}{\partial R^{(n)}_{ab}\partial R^{(m)}_{cd}}\right|_{\text{VEVs}} = -\left.\frac{\partial^2 V_{B\text{eff}}(X)}{\partial I^{(n)}_{ab}\partial I^{(m)}_{cd}}\right|_{\text{VEVs}} = \widetilde{\lambda}_{11}\frac{8}{\pi R}\cos(n\pi)\cos(m\pi). \tag{B.24v}$$

The implications of these results for the minimum of the total potential $V_{\text{eff}}^{\text{total}}$ are discussed in Sec. 6.5.

Appendix C

Chemical Potentials

In Sec. 8.2, we discuss the convertion of the asymmetry generated by the heavy scalar decays into an B asymmetry. In this context, it is convenient to use chemical potentials. Here, we give a short summary of the basic concept of chemical potentials [70, 140].

The number density n for a weakly interacting gas of particles is given by

$$n = \frac{g}{(2\pi)^3} \int f(\mathbf{p}) \mathrm{d}^3 p, \tag{C.1}$$

where g counts the internal degrees of freedom and $f(\mathbf{p})$ (the phase space distribution function for the kinetic equilibrium) is the familiar Dirac or Bose-Einstein distribution:

$$\frac{1}{\exp[(E(\mathbf{p}) - \mu)/T] \pm 1}. \tag{C.2}$$

Here, as in general, holds $E = (m^2 + \mathbf{p}^2)^{1/2}$ and μ denotes the chemical potential of the particles. For antiparticles, the sign of μ flips. In contrast to the kinetic equilibrium, the chemical equilibrium describes a state where all the chemical potentials of the interacting particles are related to each other. The net number density is

$$\begin{aligned} n - \overline{n} &= \frac{g}{2\pi^2} \int_m^\infty \sqrt{E^2 - m^2}\, \mathrm{d}E \\ &\times \left(\frac{1}{\exp[(E(\mathbf{p}) - \mu)/T] \pm 1} - \frac{1}{\exp[(E(\mathbf{p}) + \mu)/T] \pm 1} \right) \\ &= \begin{cases} \frac{gT^3}{6} \frac{\mu}{T} \left[1 + \frac{1}{\pi^2} \frac{\mu}{T}^2 + \ldots \right] & \text{for bosons,} \\ \frac{gT^3}{3} \frac{\mu}{T} \left[1 + \frac{1}{\pi^2} \frac{\mu}{T}^2 + \ldots \right] & \text{for fermions,} \end{cases} \end{aligned} \tag{C.3}$$

for $T \gg m$. Here, we are considering all SM particles in the ultrarelativistic limit ($\mathbf{p} \gg m$). This should be a good approximation at temperatures $T > T_C \sim 100\,\mathrm{GeV}$, *i.e.*, above EW phase transition. To characterize the asymmetry between matter and

antimatter, we can use the particle-to-entropy ratio

$$\frac{n-\overline{n}}{s} = \frac{15g}{2\pi^2 g_*}\frac{\mu}{T} \qquad \text{for bosons and} \tag{C.4a}$$

$$\frac{n-\overline{n}}{s} = \frac{15g}{4\pi^2 g_*}\frac{\mu}{T} \qquad \text{for fermions,} \tag{C.4b}$$

where g_* counts the total number of effectively massless degrees of freedom, *i.e.*,

$$g_* = \sum_{i=\text{bosons}} g_i \left(\frac{T_i}{T}\right)^3 + \frac{7}{8}\sum_{i=\text{fermions}} g_i \left(\frac{T_i}{T}\right)^3, \tag{C.5}$$

where $s = (\rho + p)/T = 2\pi^2 g_* T^3/45$ is the entropy density, T_i denotes the temperature and g_i the internal degrees of freedom of the ith particle species. At temperatures far above the EWSB scale g_* takes the value $g_* = 106.75$ in the SM and $g_* = 228.75$ in the minimal supersymmetric model. Furthermore, it is assumed that $|\mu/T| \ll 1$, since baryon and lepton chemical potentials are expected to be of the order $|\mu| \sim 10^{-10}T$. We suppose that no Bose-Einstein condensation takes place, *i.e.*, $|\mu| < m$ where m is the mass of the particle.

For N generations of quarks and leptons and M complex Higgs doublets, the relevant fields are: N left–handed quark doublets q_{iL} $(i = 1, \ldots, N)$, N left–handed lepton doublets ψ_{iL}, $2N$ right–handed quark singlets u_{iR} and d_{iR}, $2N$ right–handed lepton singlets ν_{iR} and e_{iR}, one right–handed charged gauge boson field $W^{\pm}$, as well as M complex scalar doublets $X_i^{(0)}$. Here, the eight gluon fields as well as the fields W_μ^3 and B_μ are neglected since their chemical potentials vanish. Above the EW phase transition, the chemical potentials for fields in the same EW multiplet are equal, *i.e.*, $W^{\pm}$ also acquires a zero chemical potential. In what follows, μ_{W^-} will denote the chemical potential of W^-, $\mu_{\nu_{iL}}$ ($\mu_{\nu_{iR}}$) will stand for all the left–handed (right–handed) neutrino fields, and $\mu_{e_{iL}}$ ($\mu_{e_{iR}}$) will be used for all the left–handed (right–handed) charged lepton fields. Since the Cabbibo mixing ensures the equality of the chemical potentials for all the up–quark states as well as the equality of the chemical potentials for all down–quarks states, we can assign μ_{u_L} (μ_{u_R}) and μ_{d_L} (μ_{d_R}) to all the left–handed (right–handed) up– and down–quark fields, respectively. The chemical potentials μ_{T_3}, μ_Q, μ_B and μ_L of the third component of the weak isospin, the electric charge, baryon and the lepton number density, respectively, are given by

$$\mu_{T_3} = \frac{3N}{2}(\mu_{u_L} - \mu_{d_L}) + \frac{1}{2}\sum_{i=1}^{N}(\mu_{\nu_{iL}} - \mu_{e_{iL}}) - 4\mu_{W^-} - \sum_{i=1}^{M}(\mu_{X_i^{0(0)}} + \mu_{X_i^{-(0)}}), \tag{C.6a}$$

$$\mu_Q = 2N(\mu_{u_L} + \mu_{u_R}) - N(\mu_{d_L} + \mu_{d_R}) - \sum_{i=1}^{N}(\mu_{e_{iL}} + \mu_{e_{iR}}) - 4\mu_{W^-} - \sum_{i=1}^{M}\mu_{X_i^{-(0)}}, \tag{C.6b}$$

$$\mu_B = N(\mu_{u_L} + \mu_{u_R}) + N(\mu_{d_L} + \mu_{d_R}), \tag{C.6c}$$

$$\mu_L = \sum_{i=1}^{N} (\mu_{\nu_{iL}} + \mu_{e_{iL}} + \mu_{\nu_{iR}} + \mu_{e_{iR}}). \tag{C.6d}$$

For $T \gtrsim T_{\rm sphal}$, the sphaleronic interactions

$$S \leftrightarrow d_L + u_L + d_L + \nu_L \quad \text{and} \quad S \leftrightarrow u_L + d_L + u_L + e_L \tag{C.7}$$

provide the two additional relation:

$$N(\mu_{u_L} + 2\mu_{d_L}) + \sum_{i=1}^{N} \mu_{\nu_{iL}} = 0, \quad \text{and} \quad N(\mu_{d_L} + 2\mu_{u_L}) + \sum_{i=1}^{N} \mu_{e_{iL}} = 0. \tag{C.8}$$

For our discussion, we assume that possible sphaleronic processes due to the RH gauge fields in the LR symmetric model are exponentially suppressed by a high LR–symmetry breaking scale. As pointed out in Ref. [70], there are also QCD sphaleron–like transitions to be taken into account. These processes enforce

$$\mu_{u_L} + \mu_{d_L} = \mu_{u_R} + \mu_{d_R}. \tag{C.9}$$

For $T \gtrsim T_c \gtrsim T_{\rm sphal}$, the third component of weak isospin T_3 as well as the electromagnetic charge Q have to vanish, *i.e.*, $\mu_{T_3} = \mu_Q = 0$. Using the equations given in this Appendix and considering the relevant interactions which are in chemical equilibrium [for our model *cf.* Eqs. (8.16)], one can derive the B asymmetry as done in Sec. 8.2.

Acknowledgments

Finally, I would like to thank everybody, who has supported me during the elaboration of this thesis. The presented work would not have been possible in the present form without their generous support. I sincerely thank

- Dr. Gerhart Seidl, for his dedicated support, for being scintillatingly witty, for patiently proofreading this thesis and last but not least for all that I have learned from him,
- Prof. Dr. Reinhold Rückl, for the opportunity for this thesis,
- Bo In Oh, for all the love she gives me,
- Julian and Lukas, for all the joy they radiate,
- my parents and family, for their selfless support throughout my life,
- Florian Plentinger, for keeping me smiling as well as proofreading this thesis,
- and all the other persons at the Lehrstuhl für Theoretische Physik II, for the pleasant work climate.

Figure on the front page:

Generic Calabi-Yau manifold with three throats. (taken from [125])

Bibliography

[1] W. M. Yao *et al.* (Particle Data Group), J. Phys. **G33**, 1 (2006).

[2] R. H. Cyburt, Phys. Rev. **D70**, 023505 (2004), astro-ph/0401091.

[3] A. D. Sakharov, Pisma Zh. Eksp. Teor. Fiz. **5**, 32 (1967).

[4] M. Fukugita and T. Yanagida, Phys. Lett. **B174**, 45 (1986).

[5] M. A. Luty, Phys. Rev. **D45**, 455 (1992).

[6] W. Buchmuller and M. Plumacher, Phys. Lett. **B389**, 73 (1996), hep-ph/9608308.

[7] M. Plumacher, Z. Phys. **C74**, 549 (1997), hep-ph/9604229.

[8] G. 't Hooft, Phys. Rev. Lett. **37**, 8 (1976).

[9] V. A. Kuzmin, V. A. Rubakov, and M. E. Shaposhnikov, Phys. Lett. **B155**, 36 (1985).

[10] P. Minkowski, Phys. Lett. **B67**, 421 (1977).

[11] T. Yanagida In Proceedings of the Workshop on the Baryon Number of the Universe and Unified Theories, Tsukuba, Japan, 13-14 Feb 1979.

[12] M. Gell-Mann, P. Ramond, and R. Slansky Print-80-0576 (CERN).

[13] S. L. Glashow, NATO Adv. Study Inst. Ser. B Phys. **59**, 687 (1979).

[14] G. Bellini *et al.*, Eur. Phys. J. **C19**, 43 (2001), nucl-ex/0007012.

[15] C. Arnaboldi *et al.* (CUORE), Nucl. Instrum. Meth. **A518**, 775 (2004), hep-ex/0212053.

[16] K. Wamba (EXO) (2002), hep-ph/0210186.

[17] I. Abt *et al.* (2004), hep-ex/0404039.

[18] H. V. Klapdor-Kleingrothaus, L. Baudis, G. Heusser, B. Majorovits, and H. Pas (GENIUS) (1999), hep-ph/9910205.

[19] C. E. Aalseth *et al.* (Majorana) (2002), hep-ex/0201021.

[20] R. Hazama *et al.*, AIP Conf. Proc. **610**, 959 (2002).

[21] R. Arnold *et al.*, Nucl. Instrum. Meth. **A536**, 79 (2005), physics/0402115.

[22] R. N. Mohapatra and J. C. Pati, Phys. Rev. **D11**, 566 (1975).

[23] R. N. Mohapatra and J. C. Pati, Phys. Rev. **D11**, 2558 (1975).

[24] G. Senjanovic and R. N. Mohapatra, Phys. Rev. **D12**, 1502 (1975).

[25] J. C. Pati and A. Salam, Phys. Rev. **D10**, 275 (1974).

[26] S. Rajpoot, Phys. Rev. **D22**, 2244 (1980).

[27] K. Dick, M. Lindner, M. Ratz, and D. Wright, Phys. Rev. Lett. **84**, 4039 (2000), hep-ph/9907562.

[28] I. R. Klebanov and M. J. Strassler, JHEP **08**, 052 (2000), hep-th/0007191.

[29] H. L. Verlinde, Nucl. Phys. **B580**, 264 (2000), hep-th/9906182.

[30] S. B. Giddings, S. Kachru, and J. Polchinski, Phys. Rev. **D66**, 106006 (2002), hep-th/0105097.

[31] S. Fukuda *et al.* (Super-Kamiokande), Phys. Lett. **B539**, 179 (2002), hep-ex/0205075.

[32] Q. R. Ahmad *et al.* (SNO), Phys. Rev. Lett. **89**, 011302 (2002), nucl-ex/0204009.

[33] Y. Fukuda *et al.* (Super-Kamiokande), Phys. Rev. Lett. **81**, 1562 (1998), hep-ex/9807003.

[34] T. Araki *et al.* (KamLAND), Phys. Rev. Lett. **94**, 081801 (2005), hep-ex/0406035.

[35] M. Apollonio *et al.* (CHOOZ), Eur. Phys. J. **C27**, 331 (2003), hep-ex/0301017.

[36] E. Aliu *et al.* (K2K), Phys. Rev. Lett. **94**, 081802 (2005), hep-ex/0411038.

[37] D. Bailin and A. Love Bristol, UK: IOP (1994) 322 p. (Graduate student series in physics).

[38] T. Schwetz, Phys. Scripta **T127**, 1 (2006), hep-ph/0606060.

[39] K. Symanzik, Commun. Math. Phys. **34**, 7 (1973).

[40] T. Appelquist and J. Carazzone, Phys. Rev. **D11**, 2856 (1975).

[41] S. Weinberg, Phys. Rev. Lett. **43**, 1566 (1979).

[42] R. N. Mohapatra and G. Senjanovic, Phys. Rev. Lett. **44**, 912 (1980).

[43] J. Schechter and J. W. F. Valle, Phys. Rev. **D22**, 2227 (1980).

[44] G. Lazarides, Q. Shafi, and C. Wetterich, Nucl. Phys. **B181**, 287 (1981).

[45] S. M. Barr, Phys. Rev. Lett. **92**, 101601 (2004), `hep-ph/0309152`.

[46] K. S. Babu and C. N. Leung, Nucl. Phys. **B619**, 667 (2001), `hep-ph/0106054`.

[47] A. Zee, Phys. Lett. **B93**, 389 (1980).

[48] K. S. Babu, Phys. Lett. **B203**, 132 (1988).

[49] N. Arkani-Hamed, S. Dimopoulos, G. R. Dvali, and J. March-Russell, Phys. Rev. **D65**, 024032 (2002), `hep-ph/9811448`.

[50] Y. Grossman and M. Neubert, Phys. Lett. **B474**, 361 (2000), `hep-ph/9912408`.

[51] E. W. Kolb and M. S. Turner, Front. Phys. **69**, 1 (1990).

[52] S. Dimopoulos and L. Susskind, Phys. Rev. **D18**, 4500 (1978).

[53] S. Dimopoulos and L. Susskind, Phys. Lett. **B81**, 416 (1979).

[54] S. Weinberg, Phys. Rev. Lett. **42**, 850 (1979).

[55] M. Yoshimura, Phys. Lett. **B88**, 294 (1979).

[56] D. V. Nanopoulos and S. Weinberg, Phys. Rev. **D20**, 2484 (1979).

[57] H. Georgi and S. L. Glashow, Phys. Rev. Lett. **32**, 438 (1974).

[58] A. G. Cohen, D. B. Kaplan, and A. E. Nelson, Phys. Lett. **B245**, 561 (1990).

[59] A. G. Cohen, D. B. Kaplan, and A. E. Nelson, Nucl. Phys. **B349**, 727 (1991).

[60] I. Affleck and M. Dine, Nucl. Phys. **B249**, 361 (1985).

[61] S. L. Adler, Phys. Rev. **177**, 2426 (1969).

[62] J. S. Bell and R. Jackiw, Nuovo Cim. **A60**, 47 (1969).

[63] N. S. Manton, Phys. Rev. **D28**, 2019 (1983).

[64] V. A. Kuzmin, V. A. Rubakov, and M. E. Shaposhnikov, Phys. Lett. **B191**, 171 (1987).

[65] P. Arnold and L. D. McLerran, Phys. Rev. **D36**, 581 (1987).

[66] P. Arnold, D. Son, and L. G. Yaffe, Phys. Rev. **D55**, 6264 (1997), hep-ph/9609481.

[67] P. Arnold, D. T. Son, and L. G. Yaffe, Phys. Rev. **D59**, 105020 (1999), hep-ph/9810216.

[68] D. Bodeker, Phys. Lett. **B426**, 351 (1998), hep-ph/9801430.

[69] D. Bodeker, Nucl. Phys. **B559**, 502 (1999), hep-ph/9905239.

[70] R. N. Mohapatra and X.-m. Zhang, Phys. Rev. **D45**, 2699 (1992).

[71] S. Blanchet and P. Di Bari, JCAP **0606**, 023 (2006), hep-ph/0603107.

[72] G. Engelhard, Y. Grossman, E. Nardi, and Y. Nir (2006), hep-ph/0612187.

[73] R. Barbieri, P. Creminelli, A. Strumia, and N. Tetradis, Nucl. Phys. **B575**, 61 (2000), hep-ph/9911315.

[74] A. Abada *et al.*, JHEP **09**, 010 (2006), hep-ph/0605281.

[75] A. Abada, S. Davidson, F.-X. Josse-Michaux, M. Losada, and A. Riotto, JCAP **0604**, 004 (2006), hep-ph/0601083.

[76] H. Murayama and A. Pierce, Phys. Rev. Lett. **89**, 271601 (2002), hep-ph/0206177.

[77] M. Y. Khlopov and A. D. Linde, Phys. Lett. **B138**, 265 (1984).

[78] B. A. Campbell, S. Davidson, and K. A. Olive, Nucl. Phys. **B399**, 111 (1993), hep-ph/9302223.

[79] S. Sarkar (1995), hep-ph/9510369.

[80] G. G. Ross and S. Sarkar, Nucl. Phys. **B461**, 597 (1996), hep-ph/9506283.

[81] M. Y. Khlopov Singapore, Singapore: World Scientific (1999) 577 p.

[82] G. F. Giudice, A. Riotto, and I. Tkachev, JHEP **11**, 036 (1999), hep-ph/9911302.

[83] W. Buchmuller, R. D. Peccei, and T. Yanagida, Ann. Rev. Nucl. Part. Sci. **55**, 311 (2005), hep-ph/0502169.

[84] S. Davidson and A. Ibarra, Phys. Lett. **B535**, 25 (2002), hep-ph/0202239.

[85] A. Pilaftsis, Phys. Rev. **D56**, 5431 (1997), hep-ph/9707235.

[86] Y. Grossman, T. Kashti, Y. Nir, and E. Roulet, Phys. Rev. Lett. **91**, 251801 (2003), hep-ph/0307081.

[87] L. Boubekeur (2002), hep-ph/0208003.

[88] L. Boubekeur, T. Hambye, and G. Senjanovic, PHys. Rev. Lett. **93**, 111601 (2004), hep-ph/0404038.

[89] Y. Grossman, T. Kashti, Y. Nir, and E. Roulet, JHEP **11**, 080 (2004), hep-ph/0407063.

[90] G. D'Ambrosio, G. F. Giudice, and M. Raidal, Phys. Lett. **B575**, 75 (2003), hep-ph/0308031.

[91] L. Covi, N. Rius, E. Roulet, and F. Vissani, Phys. Rev. **D57**, 93 (1998), hep-ph/9704366.

[92] Y. Nir (2001), hep-ph/0109090.

[93] M. Fujii, K. Hamaguchi, and T. Yanagida, Phys. Rev. **D65**, 115012 (2002), hep-ph/0202210.

[94] P. H. Frampton, S. L. Glashow, and T. Yanagida, Phys. Lett. **B548**, 119 (2002), hep-ph/0208157.

[95] M.-C. Chen and K. T. Mahanthappa, Phys. Rev. **D71**, 035001 (2005), hep-ph/0411158.

[96] M. B. Green, J. H. Schwarz, and E. Witten Cambridge, Uk: Univ. Pr. (1987) 469 P. (Cambridge Monographs On Mathematical Physics).

[97] M. B. Green, J. H. Schwarz, and E. Witten Cambridge, Uk: Univ. Pr. (1987) 596 P. (Cambridge Monographs On Mathematical Physics).

[98] R. N. Mohapatra Berlin, Germany: Springer (1986) 309 P. (Contemporary Physics).

[99] O. W. Greenberg and J. Sucher, Phys. Lett. **B99**, 339 (1981).

[100] R. Barbieri, R. N. Mohapatra, and A. Masiero, Phys. Lett. **B105**, 369 (1981).

[101] J. F. Gunion, J. Grifols, A. Mendez, B. Kayser, and F. I. Olness, Phys. Rev. **D40**, 1546 (1989).

[102] J. F. Gunion, A. Mendez, and F. I. Olness, Int. J. Mod. Phys. **A2**, 1085 (1987).

[103] G. Gabadadze (2003), hep-ph/0308112.

[104] C. Csaki (2004), hep-ph/0404096.

[105] R. Sundrum (2005), hep-th/0508134.

[106] T. Kaluza, Sitzungsber. Preuss. Akad. Wiss. Berlin (Math. Phys.) **1921**, 966 (1921).

[107] O. Klein, Z. Phys. **37**, 895 (1926).

[108] N. Arkani-Hamed, S. Dimopoulos, and G. R. Dvali, Phys. Lett. **B429**, 263 (1998), hep-ph/9803315.

[109] I. Antoniadis, N. Arkani-Hamed, S. Dimopoulos, and G. R. Dvali, Phys. Lett. **B436**, 257 (1998), hep-ph/9804398.

[110] N. Arkani-Hamed, S. Dimopoulos, and G. R. Dvali, Phys. Rev. **D59**, 086004 (1999), hep-ph/9807344.

[111] L. Randall and R. Sundrum, Phys. Rev. Lett. **83**, 3370 (1999), hep-ph/9905221.

[112] L. Randall and R. Sundrum, Phys. Rev. Lett. **83**, 4690 (1999), hep-th/9906064.

[113] Y. Kawamura, Prog. Theor. Phys. **105**, 999 (2001), hep-ph/0012125.

[114] G. Altarelli and F. Feruglio, Phys. Lett. **B511**, 257 (2001), hep-ph/0102301.

[115] L. J. Hall and Y. Nomura, Phys. Rev. **D64**, 055003 (2001), hep-ph/0103125.

[116] G. Servant and T. M. P. Tait, Nucl. Phys. **B650**, 391 (2003), hep-ph/0206071.

[117] H.-C. Cheng, J. L. Feng, and K. T. Matchev, Phys. Rev. Lett. **89**, 211301 (2002), hep-ph/0207125.

[118] K. Agashe and G. Servant, Phys. Rev. Lett. **93**, 231805 (2004), hep-ph/0403143.

[119] N. S. Manton, Nucl. Phys. **B158**, 141 (1979).

[120] I. Antoniadis, K. Benakli, and M. Quiros, New J. Phys. **3**, 20 (2001), hep-th/0108005.

[121] C. Csaki, C. Grojean, and H. Murayama, Phys. Rev. **D67**, 085012 (2003), hep-ph/0210133.

[122] C. A. Scrucca, M. Serone, and L. Silvestrini, Nucl. Phys. **B669**, 128 (2003), hep-ph/0304220.

[123] C. Csaki, C. Grojean, H. Murayama, L. Pilo, and J. Terning, Phys. Rev. **D69**, 055006 (2004), hep-ph/0305237.

[124] C. Csaki, C. Grojean, L. Pilo, and J. Terning, Phys. Rev. Lett. **92**, 101802 (2004), hep-ph/0308038.

[125] G. Cacciapaglia, C. Csaki, C. Grojean, and J. Terning, Phys. Rev. **D74**, 045019 (2006), hep-ph/0604218.

[126] P. Candelas, G. T. Horowitz, A. Strominger, and E. Witten, Nucl. Phys. **B258**, 46 (1985).

[127] S. Dimopoulos, S. Kachru, N. Kaloper, A. E. Lawrence, and E. Silverstein, Phys. Rev. **D64**, 121702 (2001), hep-th/0104239.

[128] S. Dimopoulos, S. Kachru, N. Kaloper, A. E. Lawrence, and E. Silverstein, Int. J. Mod. Phys. **A19**, 2657 (2004), hep-th/0106128.

[129] B. Thomas and M. Toharia, Phys. Rev. **D73**, 063512 (2006), hep-ph/0511206.

[130] B. Thomas and M. Toharia (2006), hep-ph/0607285.

[131] J. Liu and G. Segre, Phys. Rev. **D48**, 4609 (1993), hep-ph/9304241.

[132] W. A. Bardeen, A. J. Buras, D. W. Duke, and T. Muta, Phys. Rev. **D18**, 3998 (1978).

[133] A. Pilaftsis and T. E. J. Underwood, Nucl. Phys. **B692**, 303 (2004), hep-ph/0309342.

[134] A. Pilaftsis and T. E. J. Underwood, Phys. Rev. **D72**, 113001 (2005), hep-ph/0506107.

[135] A. Anisimov, A. Broncano, and M. Plumacher, Nucl. Phys. **B737**, 176 (2006), hep-ph/0511248.

[136] M. E. Peskin and D. V. Schroeder Reading, USA: Addison-Wesley (1995) 842 p.

[137] E. Schrodinger, Ann. d. Phys. **80**, 437 (1926).

[138] K. Agashe, A. Delgado, M. J. May, and R. Sundrum, JHEP **08**, 050 (2003), hep-ph/0308036.

[139] A. Pilaftsis, Phys. Rev. **D60**, 105023 (1999), hep-ph/9906265.

[140] J. A. Harvey and M. S. Turner, Phys. Rev. **D42**, 3344 (1990).